THESIS FOR THE DEGREE OF DOCTOR OF PHILOSOPHY

Occupant Neck Muscle Modelling in Rear-End Crashes

I PUTU ALIT PUTRA

Department of Mechanics and Maritime Sciences
Division of Vehicle Safety – Injury Prevention Unit

CHALMERS UNIVERSITY OF TECHNOLOGY

Gothenburg, Sweden 2022

Occupant Neck Muscle Modelling in Rear-End Crashes

I PUTU ALIT PUTRA
ISBN: 978-91-7905-754-1
Series number: 5220
in the series Doktorsavhandlingar vid Chalmers tekniska högskola.
Ny serie (ISSN 0346-718X)

Department of Mechanics and Maritime Sciences
Chalmers University of Technology
SE-412 96 Gothenburg
Sweden
Telephone + 46 (0)31-772 1000

Printed by Chalmers Reproservice
Gothenburg, Sweden 2022

Dedicated to my wife and son
my companions during this journey

Abstract

The ultimate goal of the present research is to incorporate active and passive neck muscle effects in a female Finite Element (FE) Human Body Model (HBM). The application of interest is Whiplash Associated Disorders (WAD), which can occur in a low-speed rear-end impact. Two reflex mechanisms, the Vestibulocollic reflex (VCR) and the Cervicocollic reflex (CCR), are integral to maintaining head orientation. Therefore, active muscle modelling in HBMs should address the behaviour of these reflex mechanisms. Female FE HBMs are the focus of the present thesis because of their higher risk of sustaining WAD than males. This model should reproduce kinematics that can be used for global and local tissue injury prediction of WAD.

The present thesis was arranged to address the main objective systematically and consists of six studies addressing five research questions. Two human body models representing the 50th percentile population, the VIVA OpenHBM and VIVA+ HBM, were used. The model was developed with and benchmarked against volunteer test data.

Based on the collective studies in this thesis, the isolated head-neck model can be used to develop an active muscle controller. A simple, single-link approach was used to design a Proportional-Derivative (PD) controller called Angular Positioned Feedback (APF). This simple controller was convenient to implement and calibrate with available experimental data. Furthermore, reliable parameter identification, such as active muscle controller gains, were obtained via optimization using both head and cervical vertebral kinematics as objectives. A parameter study of different control strategies confirmed that the APF control strategy, combined with parallel damping elements (PDE), was the most effective for recreating volunteer kinematic responses compared to the model with only passive elements, particularly when impact severity was varied.

Real-world collision data was used to evaluate the model's usefulness using injury outcome data for known collision severities. The inclusion of neck muscle responses considerably influenced the cervical vertebral kinematics but only slightly influenced head kinematics before the rebound phase, depending on the head-to-headrest offset. Consequently, a slight difference in global kinematic-based injury criteria such as Neck Injury Criteria (NIC) was observed between a model with and without neck muscle responses. In contrast, significant differences between the two groups were observed for local, tissue-based, whiplash injury prediction. Hypotheses, such as Aldman pressure, require cervical spine kinematics and place higher requirements on the model's performance. This analysis revealed the need for both global-based injury criteria and local, tissue level analysis to understand how WAD occur. Therefore, whiplash injury prediction would be more reliable using a model with the APF control strategy combined with PDE developed herein, than a model without active neck muscle responses.

The FE HBMs with neck muscle responses have been developed and validated for low-speed rear-end impact and WAD analyses. The models have been shown to be robust and able to replicate volunteer head-neck kinematics.

Keywords: *Finite Element; Female; Human Body Model; Active Neck Muscle Responses;* Whiplash Associated Disorders

Acknowledgments

As I started this very last section of my dissertation, my mind wandered to five years back when I had just arrived in Gothenburg after long-haul flights from my hometown in Bali. What I brought to Gothenburg at that time was only one piece of luggage and one backpack. But I did bring an unlimited amount of curiosity and courage, my parents' infinite prayers, and my girlfriend's love in which they believed that I would be doing just fine and able to finish this "marathon" in that I decided to participate. Five years later, I presented this thesis.

Even though I come from an island, I have always believed that no one is an island. Even an island needs an ocean around it to be considered an island. It is exactly the same with my journey as a Ph.D. student and the thesis that you are reading right now. It would not have been possible to finish my Ph.D. study and complete my Ph.D. thesis without the guidance and helps of many people who, in one way or another, contributed and extended their valuable assistance.

First of all, I particularly want to thank my main supervisor, Professor Robert Thomson. Rob, thank you for everything. You are not just my supervisor, but I also consider you as my mentor, and I could ask for any suggestions about almost anything in research and private life. Thank you for giving me the opportunity to do a Ph.D. at Chalmers and teaching me to do proper research and providing me with courage when I feel down. Surely, I will miss have progress meeting with you. If I could repeat doing Ph.D., I will definitely want to do it again under your supervision.

I am very grateful to my co-supervisor, Dr. Johan Iraeus. Johan, thank you for all the advice and for helping me be more detailed and reminding me to reflect more on my research results. I have been inspired by your impressive technical and engineering abilities. If anyone ever asks me who is my role model as a CAE engineer, without a doubt, I will mention your name. Thank you also for our used-to-be "bi-weekly routine" of eating lunch at the Thai buffet. I will miss eating two plates and having a food coma in the afternoon.

I also want to thank Professor Mats Svensson as my examiner and manager. Mats, thank you for your feedback, guidance, and advice. Thank you for sharing your extensive knowledge of whiplash injury, you are more than an examiner for me. I still remember when I came to Gothenburg for an interview and arrived late at night. You were standing in front of the airport's luggage area, holding a paper with my name on it just to pick me up and drop me at the hotel. Despite your well-known name in whiplash injury research, you are always kind and low-profile. I have learned a lot from you.

I would like to thank my former co-supervisor, Dr. Jason Fice. Although he had only supervised me for around one year, he provided tremendous support in helping me to understand more about muscular neurophysiology. Jason, you're a co-supervisor that almost like a friend to me. Hope to discuss muscle with you again someday.

I would also like to thank all the VIVA II and VIRTUAL Project Partners for their support, especially Professor Astrid Linder (VTI), Adj. Prof. Anders Kullgren (Folksam Research), Adj. Prof. Lotta Jakobsson (Volvo Cars), Dr. Jobin John (Chalmers), Jonny Genzel (VTI) and Anders Flogård (Crash Scene Investigation). Also, people that had supported me during the beginning of the VIVA II project: Prof. Karin Brolin, Prof Johan Davidsson, Dr. Fusako Sato, Dr. Jonas Östh, and Dr. Jona Olafsdottir.

I want to thank all my colleagues and fellow Ph.D. students at the vehicle safety division, Chalmers, for the friendly atmosphere at work and also for helping me with many issues. Special thanks to Emma Larsson, Karl-Johan Larsson, Linda Pipkorn, Hosein Naseri, Alexandros Leledakis, Erik Brynskog, Petra Gustafsson and family, Dr. Selpi and family, and Sonja Laakso Gustafsson. Nevertheless, I also want

to thank my master's thesis students, Josefine Berntsson and Sarah El-Mobader, who indirectly helped me become a better person in teaching and supervising.

Furthermore, I would like to thank all of my former supervisors and teachers that inspired me to continue my formal education to the highest possible; I would especially like to thank Professor Nandy Putra and Professor Idrus Al-Hamid (Universitas Indonesia), Assoc.Prof Julaluk Carmai and Assoc.Prof Saiprasit Koetniyom (KMUTNB Thailand) and Professor Bernd Markert (RWTH Aachen University).

I also would like to thank all my Indonesian and Balinese friends in Sweden, the Indonesian Student Association in Gothenburg (PPI Gothenburg), the Indonesian Student Association in Sweden (PPI Swedia), and Indonesiska Kulturföreningen that helped my family and me and so that we feel like a second home here. Special thanks to Indra Wibawa and his family, that always have their house open for us.

I would also like to thank my parents and my family in Bali. I know my words will never be enough to thank my parents for everything they have done for me. My beloved father who has always inspired me and taught me from a very young age to never give up and let me become what I want in life. Endless love from my beloved mother, who taught me about the importance of working hard and basic survival skills. I know I have been roaming around from home for more than a decade, but you are always be my home, that I can come back whenever I want.

My brothers and sisters, in which as the youngest sibling, I have always had the privileged to be helped in many things by all of you. I hope with this thesis, you are more than proud as my brothers and sisters. My parents-in-law and my sister-in-law, thank you for everything. I am grateful to be part of your family.

Last but not least, I would like to thank my wife and life companion, Ayuwidia, and my son, Harsakanaka. Widia, thank you for your endless love, care, support, and understanding. Life has peaks and downs, but you are always there for me. Life is a journey, and I hope you enjoy this adventure with me. Thank you also for helping and drawing some of this thesis's illustrations. Harsa, thank you for choosing me as your father. I hope you know that, for me playing with you is always more fun than doing research. I hope someday, when you read this thesis, you could understand why sometimes we could not play together. And lastly, I dedicated this thesis for both of you.

”Eda ngaden awak bisa, depang anake ngadanin, geginane buka nyampat, anak sai tumbuh luhu, ilang luhu ebuke katah, yadin ririh, liu enu plajahin” Pupuh Ginada

Gothenburg, 2022

Funding Acknowledgements:

I would like to thank the funders of my Ph.D. research since without their supports, this thesis work would not have been possible. Throughout my Ph.D. research I had received fundings from the Swedish Governmental Agency for Innovation Systems (VINNOVA) under project titled Virtual Vehicle Safety Assessment Step 2: Open-Source Human Body Models and Crash Testing (VIVA II) as well as from the European Union's Horizon 2020 research and innovation programme under project titled Open access virtual testing protocols for enhanced road user safety (VIRTUAL) with Grant agreement No. 768960. Most of the simulations were performed on resources at Chalmers Center for Computational Science and Engineering (C3SE) provided by the Swedish National Infrastructure for Computing (SNIC) and partly carried out at Vehicle and Traffic Safety Research Center at Chalmers (SAFER).

List of Appended Papers

This thesis is based on the work reported and presented in the following publications:

Paper A	**I Putu A. Putra**, J. Iraeus, M.Y. Svensson, R. Thomson **"Comparison of Head-Neck Kinematics between Isolated Finite Element (FE) Head-Neck Model and Full-Body Model"** *Accepted to the 27th International Technical Conference on The Enhanced Safety of Vehicles (ESV), Yokohama, Japan.*
	Author's contribution*: Conceptualization**,** Formal analysis, Investigation, Methodology, Software, Validation, Visualization, Writing – original draft.
Paper B	**I Putu A. Putra**, J. Iraeus, R. Thomson, M.Y. Svensson, A. Linder, F. Sato. **"Comparison of Control Strategies for the Cervical Muscles of an Average Female Head-Neck Finite Element Model."** *Traffic Injury Prevention. 2019, Vol. 20, No. S2, S116–S122* https://doi.org/10.1080/15389588.2019.1670818
	Author's contribution: Methodology, Software, Formal analysis, Investigation, Writing – original draft, Visualization.
Paper C	**I Putu A. Putra**, J. Iraeus, F. Sato, M.Y. Svensson, A. Linder and R. Thomson. **"Optimization of Female Head-Neck Model with Active Reflexive Cervical Muscles in Low Severity Rear Impact Collisions."** *Annals of Biomedical Engineering.Vol. 49, No. 1, January 2021 pp. 115-128* *https://doi.org/10.1007/s10439-020-02512-1*
	Author's contribution: Conceptualization**,** Methodology, Software, Formal analysis, Investigation, Writing – original draft, Visualization.

Paper D	**I Putu A. Putra** and R. Thomson **"Analysis of Control Strategies for VIVA OpenHBM with Active Reflexive Neck Muscles"** *Biomechanics and Modeling in Mechanobiology. 2022* *https://doi.org/10.1007/s10237-022-01616-y*
	Author's contribution: Conceptualization**,** Formal analysis, Investigation, Methodology, Software, Validation, Visualization, Writing – original draft.
Paper E	**I Putu A. Putra**, J. Iraeus, F. Sato, M.Y. Svheheensson, R. Thomson **"Finite Element Human Body Models with Active Reflexive Muscles Suitable for Gender based Whiplash Injury Prediction"** *Frontiers in Bioengineering and Biotechnology. 2022* *https://doi.org/10.3389/fbioe.2022.968939*
	Author's contribution*: Conceptualization**,** Formal analysis, Investigation, Methodology, Software, Validation, Visualization, Writing – original draft.
Paper F	**I Putu A. Putra**, J. Iraeus, H. Yao, M.Y. Svensson, A. Kullgren, R. Thomson **"The Role of Neck Muscle Responses to the Whiplash Injuries based on Accident Reconstruction Simulation using Real-World Accident Pulses"** *Manuscript to be submitted to a Journal*
	Author's contribution: Conceptualization**,** Formal analysis, Investigation, Methodology, Software, Validation, Visualization, Writing – original draft.

* Contributor Roles Taxonomy (CrediT) (Brand et al., 2015) was used to recognize author's contribution.

Additional Publications not Included in the Thesis

I Putu A. Putra, Johan Iraeus, Robert Thomson, **Implementation and Calibration of the LS-DYNA PID Controller for Female Cervical Muscles**, Nordic LS-DYNA User Conference 2018, Gothenburg, Sweden. October 18-19, 2018.

I Putu A. Putra, Johan Iraeus, Robert Thomson, Mats Y. Svensson. **Implementation and Calibration of Active Reflexive Cervical Muscles on Female Head-Neck Model**. The 15th Annual Injury Biomechanics Symposium the Ohio State University, Ohio – United States, May 19-21, 2019.

I Putu A. Putra, Johan Iraeus, Robert Thomson, Mats Y. Svensson, Astrid Linder, Fusako, Sato, **Comparison of Control Strategies for the Cervical Muscles of an Average Female Head-Neck Finite Element Model**. The 63rd Annual Scientific Conference for the Association for the Advancement of Automotive Medicine. Madrid, Spain. October 15-18, 2019.

I Putu A. Putra, J. Iraeus, J.B. Fice, M.Y. Svensson, A. Linder, R. Thomson, **Kinematics Evaluation of Female Head-Neck Model with Reflexive Neck Muscles in Low-Speed Rear Impact.** The 6th SIMBIO-M Conference 2020 Virtual Conference, June 18-19, 2020.

Jobin John, **I Putu A. Putra** and Johan Iraeus. **Finite Element Human Body Models to Study Sex-Differences in Whiplash: Validation Of VIVA+ Passive Responses in Rear-Impact**. International Research Council on Biomechanics of Injury (IRCOBI) Conference, Porto, Portugal. September 14-16, 2022

Wim Wijnen, David Bützer, Rune Elvik, Petr Pokorny, **I Putu A. Putra**. **Calculating The Socio-Economic Costs and Benefits of Vehicle Safety Systems.** Transportation Research Procedia 00 (2022) 000–000 / Transport Research Area (TRA) Conference, Lisbon, Portugal. November 14-17, 2022

Corina Klug, Johan Iraeus, Jobin John, Arne Keller, Michal Kowalik, Christoph Leo, Ines Levallois, Felix Ressi, **I Putu A. Putra**, Mats Svensson, Linus Trummler, Astrid Linder. **Comparison of injury predictors and kinematics of Human Body Models representing average female and male road users in car crashes.** Submitted to Traffic Injury Prevention. 2022

List of Abbreviations

APF	Angular-positioned feedback
C.G.	Center of gravity
CCo	Co-Contraction
CCR	Cervicocollic reflex
CORA	Correlation Analysis
EMG	Electromyography
FE	Finite element
HBM	Human body model
MLF	Muscle-length feedback
NIC	Neck Injury Criteria
PDE	Parallel Damping Element
PHMS	Post mortem human subject
PID	Proportional integral derivative
PSV	Passive
VCR	Vestibulocollic reflex
VIVA OpenHBM	Virtual Vehicle Safety Assessment: Open-source Human Body Model
VIVA+	Virtual Vehicle Safety Assessment
WAD	Whiplash associated disorders

Table of Contents

Appended Papers

List of Figures

List of Tables

Chapter 1 Introduction

1.1 Whiplash Associated Disorders (WAD)

Whiplash Associated Disorders (WAD) or whiplash injuries are prevalent around the world (Table 1.1). For example, up to 235 people per hundred thousand in Europe suffered WAD (Björnstig et al., 1990, Jörg & Menger., 1998, Partheni et al., 2000, Martin et al., 2008, Styrke et al., 2012). Similarly, the incidence rates of WAD were also very high on the American continent (Cassidy et al., 2000, Quinlan et al., 2004). In addition, high incidences of WAD were reported in Asian countries such as Japan (Oka et al., 2017) and Korea (Korea Insurance Development Institute., 2002). Another ten-year study in Australia concluded that more than fifty thousand traffic accident compensation claims were for whiplash injury (Gisolf et al., 2013). Despite the high incidences of WAD worldwide, whiplash injury aetiology remains unclear and not fully understood.

Table 1.1 Comparison of Whiplash Associated Disorders (WAD) incidence rate

Rate of Incidence per Hundred Thousand Population	Country	Source
100	Sweden	Björnstig et al., 1990
235	Sweden	Styrke et al., 2012
200	Germany	Jörg & Menger, 1998
328	United States	Quinlan et al., 2004
417	Canada	Cassidy et al., 2000

Epidemiological data reviewed and summarized by Carlsson A. (2012) showed that females have a higher risk (up to three times) of experiencing WAD than males. Another study by Kullgren et al. (2013) also concluded that the whiplash protection seats found on the Swedish market were less effective for females than males.

Several common symptoms have been observed in the patients that sustain WAD. Based on literature reviews (McClune et al., 2002, Sterner and Gerdle, 2004, Yadla et al., 2008, Sterling, M. 2011) the symptoms experienced by the whiplash patients were neck pain and stiffness, pain in the arm, headache, numbness or paresthesia, dizziness, visual and auditory problems, problems with memory and concentration as well as psychological issues such as anxiety.

The injury mechanism of WAD is still poorly understood. Despite that, several hypotheses have been proposed. Aldman's (1986) hypothesis was based on the commonly observed symptoms of WAD, such as neck pain, headache, vertigo, vision and neurological problems. The injury was proposed to occur during the rapid and sudden changes in the inner volume of the spinal neck canal during extension-flexion motions that could cause transient pressure changes in the central nervous system (CNS). These hydrodynamic effects can mechanically load the nerve roots and cause damage to the tissues. The

hypothesis was supported using animal experiments (Svensson et al., 1993, 1998) and Örtengren et al. (1996). Apart from the previously mentioned hypothesis by Aldman (1986), several other hypotheses (summarized by Siegmund et al., 2009) have been proposed, resulting in five potential anatomical sites of the WAD such as facet joint and capsular ligaments, intervertebral disc and ligaments, vertebral artery, and neck muscles. Related to facet joint and capsular ligaments injuries, two mechanisms such as pinching of the synovial fold (Ono et al., 1997; Kaneoka et al., 1999) and excessive strain in the capsule (Luan et al., 2000; Pearson et al., 2004; Yang & King, 2003; Yoganandan et al., 2002) have been proposed and demonstrated. Studies involving in vivo animal models, such as the goat model (Lu et al., 2005) and the rat model (Dong et al., 2008; Lee et al., 2004; Quinn et al., 2007), supported the hypothesis of excessive strain in the capsule. In those studies, persistent pain symptoms were observed during capsular joint distraction. Partial or complete rupture of the spinal ligaments and intervertebral disc's annular fibres has been postulated as the injury mechanism related to spinal ligaments and intervertebral disc. This hypothesis was supported by cadaveric studies reported by Ivancic et al. (2004) and Panjabi et al. (2004). Muscle pain is a common symptom in patients suffering from WAD. However, direct muscle injury might not be responsible for WAD (Siegmund et al., 2009). Due to its significant volume relative to other structures in the neck, neck muscle forces could influence the risk of WAD by affecting other anatomical structures (Siegmund et al., 2009).

Table. 1.2 Whiplash Associated Disorder (WAD) level based on The Quebec Task Force

Grade	Whiplash Associated Disorder (WAD) Explanation
Grade 0:	No complaints about the neck. No physical sign(s).
Grade I:	Neck complaint of pain, stiffness or tenderness only. No physical sign(s).
Grade II:	Neck complaint AND musculoskeletal sign(s). Musculoskeletal signs include decreased range of motion and point tenderness.
Grade III:	Neck complaint AND neurological sign(s). Neurological signs include decreased range of motion and point tenderness.
Grade IV:	Neck complaint AND fracture or dislocation.

Based on the previously mentioned proposed mechanisms, several injury criteria for evaluating the risk of WAD have been proposed. A theoretical model was developed based on the transient pressure changes observed in animal experiments (Svensson et al., 1993, 1998, Örtengren et al., 1996) and used to develop a whiplash injury criterion called the Neck Injury Criterion (NIC, Boström et al., 2000). The NIC is based on the relative horizontal x-acceleration between the occipital condyles and the first thoracic vertebra (T1) and is the most prevalent and is now applied in EuroNCAP. The Nij Criterion (Eppinger et al., 2000), the Nkm Criterion (Schmitt et al., 2002), the Intervertebral Neck Injury Criterion (IV-NIC, Panjabi et al., 1999), the Neck Displacement Criterion (NDC, Viano & Davidsson, 2001), and The Lower Neck Load Index (LNL, Heitplatz et al., 2003) are other proposed criteria. The Nkm Criterion was derived based on Nij Criterion and combines moments and shear forces. An evaluation of the other injury criteria conducted by Kullgren et al. (2003), which combined crash pulses data from real-world accident data and simulations of a mathematical model (MADYMO), found that the NICmax (the

maximum value of the NIC that was calculated from the beginning of impact just until the head is not in contact with head restraint anymore) and the Nkm were most applicable for predicting whiplash injury.

In summary, high incidences of WAD are found on almost all continents. However, how WAD manifest in the body is still unclear, although several hypotheses and injury criteria have been proposed. Furthermore, when victims of WAD are classified by sex, females suffer WAD more than males. Therefore, further studies are needed to understand whiplash injuries, especially to shed some light on how the injury occurs and why females have a higher susceptibility to sustaining WAD.

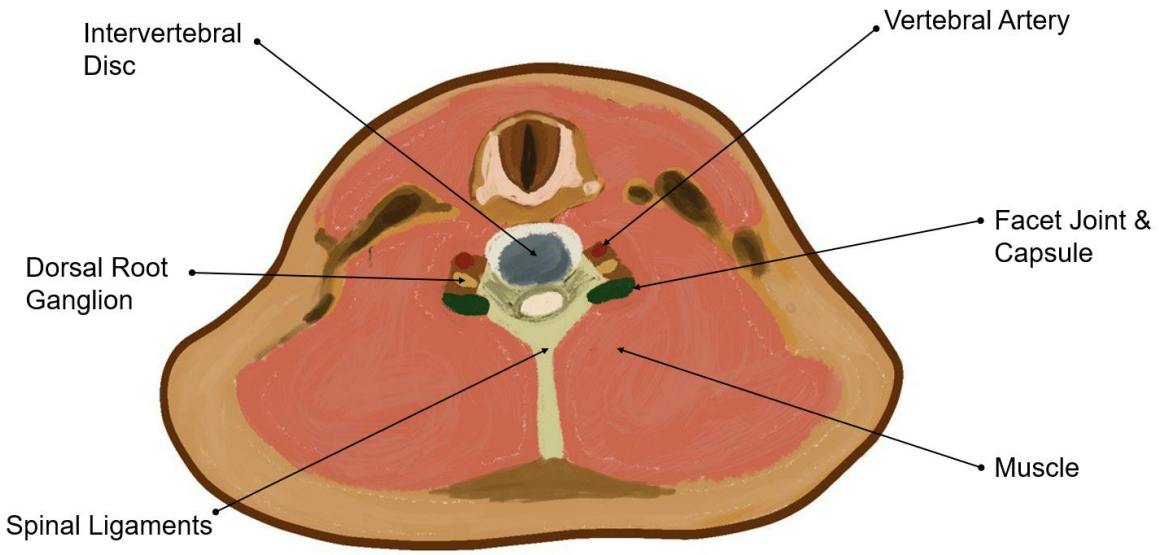

Figure 1.1 Illustration of neck cross-section showing the anatomical arrangement of whiplash injury's proposed sites based on Siegmund et al., (2009).

1.2 Head-Neck Kinematics during WAD-induced Rear-Impact

WAD have been found to be associated in motor vehicle accidents with different crash directions. Most WAD are associated with rear-impact collisions (Krafft et al., 2002, Stigson et al., 2015). To understand how WAD develop during rear-impact, an understanding of occupant head-neck kinematics is essential. The neck kinematics can be divided into several phases during a rear-impact collision (Svensson et al., 1993, Linder, A. 2001, Linder et al., 2002). The first phase is called the retraction phase, caused by the relative motion of the head and torso producing an S-liked shape in the cervical spine. The relative motion between the head and trunk occurs because the occupant's torso moves forward when the car is hit from behind. However, the occupant's head remains in the same position because of inertia. The second phase, called the extension phase, occurs until the head usually contacts the head restraint. After this contact, the third phase, called the flexion (or rebound) phase, occurs as the head and torso rebound from the vehicle seat head restraint and seatback cushion.

Many of the current WAD hypotheses, mentioned previously, are connected to the retraction phase of the neck (Aldman, 1986, Svensson et al., 1993, Grauer et al., 1997, Yang et al., 1997, Ono et al., 1997,2006, Yoganandan et al., 1998, 2000, 2001, and Deng et al., 2000). Therefore, any surrogate tools (for example, crash test dummy or human body finite element model) used to study the kinematics of WAD should be able to replicate the occupant's retraction motion.

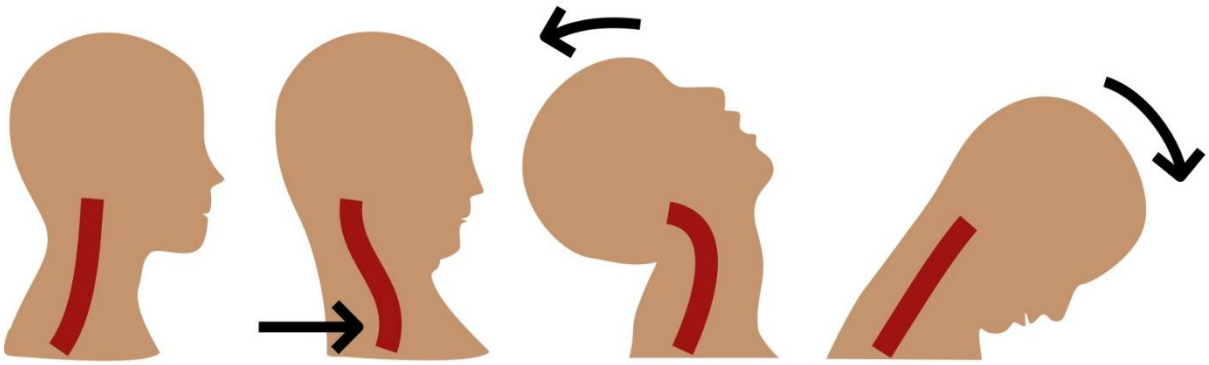

Figure 1.2 Occupant Motion during WAD Induced Rear Impact. The second figure illustrates the retraction phase with the neck S-shape.

1.3 Role of Neck Muscle Activity in Head-Neck Kinematics

Besides vehicle and crash-related factors, such as head restraint design and impact severity (summarized by Carlsson, A. 2012), the head-neck kinematics of the occupant during low-speed rear-impacts are also influenced by cervical muscle activity (Brault et al., 2000, Siegmund et al., 2003, Blouin et al., 2006, Dehner et al., 2013, Mang et al., 2015). In terms of volume, cervical muscles are a significant part of the neck structure. It is also postulated that neck muscles could influence the whiplash injury risk by affecting other anatomical structures of the neck, for example the dorsal root ganglion and facet capsular ligaments (Siegmund et al., 2009).

Several studies have documented the influence of the neck muscle activity on the head-neck kinematics during whiplash-like rear-impact volunteer tests (Brault et al., 2000, Siegmund et al., 2003, Blouin et al., 2006, Dehner et al., 2013, Mang et al., 2015). Siegmund et al., (2003) conducted a volunteer study to analyze the effects of awareness on the subject muscles and kinematics responses during the whiplash-like perturbations and found that the Sternocleidomastoid (SCM) muscle activated earlier in aware volunteers. Unaware male subjects had higher head accelerations. Meanwhile, the unaware female subjects had larger head retractions compared to alerted subjects. Blouin et al., (2006) conducted a test with 65 volunteers that were exposed to a perturbation with and without a startle stimulus (the startle stimulus was induced by 124dB sound). They found that the startled subjects had earlier muscle activation and more substantial peak head accelerations with smaller peak displacements. A rear-end impact test with eight female subjects conducted by Dehner et al., (2013) found that the higher activity of sternocleidomastoid muscle contributed to the reduction of head acceleration. Another study (Mang

et al., 2015) found that subjects who experienced a loud sound pre-impact inhibited the impact-related startle response and reduced cervical muscle activity (C6 multifidus and C4 PARAspinal muscles) and decreased peak head kinematic responses. In summary, muscle activities in the neck influence the head-neck kinematics during rear impacts. Therefore, it is necessary to include the neck muscle responses when conducting a study of head-neck kinematics in a whiplash inducing rear-impact condition.

1.4 Head-Neck Postural Control Reflexes

A detailed description of the human head-neck reflexes is beyond the scope of this thesis, but two main components, the Vestibulocollic reflex (VCR) and the Cervicocolic reflex (CCR) are presented (Armstrong et al., 2008., Cullen and Goldberg, 2014., Cullen, K.E., 2012. Keshner, E.A., 2003).

The VCR activates neck muscles to maintain the head position and responds to head motion (rotational and translational) detected by the vestibular system. The human vestibular system can be categorized by two main components, the peripheral and central parts. The detection of head position is conducted by the peripheral components, consisting of the semicircular canals and the otolithic organs (called saccule and utricle). The semicircular canals detect the head angular or rotational acceleration. The otolithic organs detect the head in space by responding to gravitational acceleration, linear acceleration, and tilting of the head. The information gathered by the vestibular components is used as input to the vestibular nuclei in the brain (medulla). The Central Nervous System (CNS) will process this input (along with other information from the eyes and cervical spine receptors) and then output different reflex mechanisms, one being the VCR. The reflex mechanisms then control the activation of the cervical spine muscles.

The CCR activates neck muscles to reduce the motion of the head relative to the trunk and responds to changes in muscle length detected by muscle spindles. Muscle spindles, which can be found within the muscle belly, are observed in higher concentrations in the deep cervical muscles (Amonoo-Kuofi, 1983, Liu et al., 2003). They detect the muscle's length changes. The information is transmitted to the CNS via the afferent nerve fibers. The CNS then processes the information and triggers the CCR. The CCR will activate the cervical muscles to maintain the head-on-trunk orientation.

Head and neck posture is also maintained though the combination of several input receptors such as the vestibular system, cervical muscle spindles, and joint articular receptors (Armstrong et al., 2008). All information is processed in the Central Nervous System (CNS) to activate different reflex mechanisms and triggering the corresponding muscles.

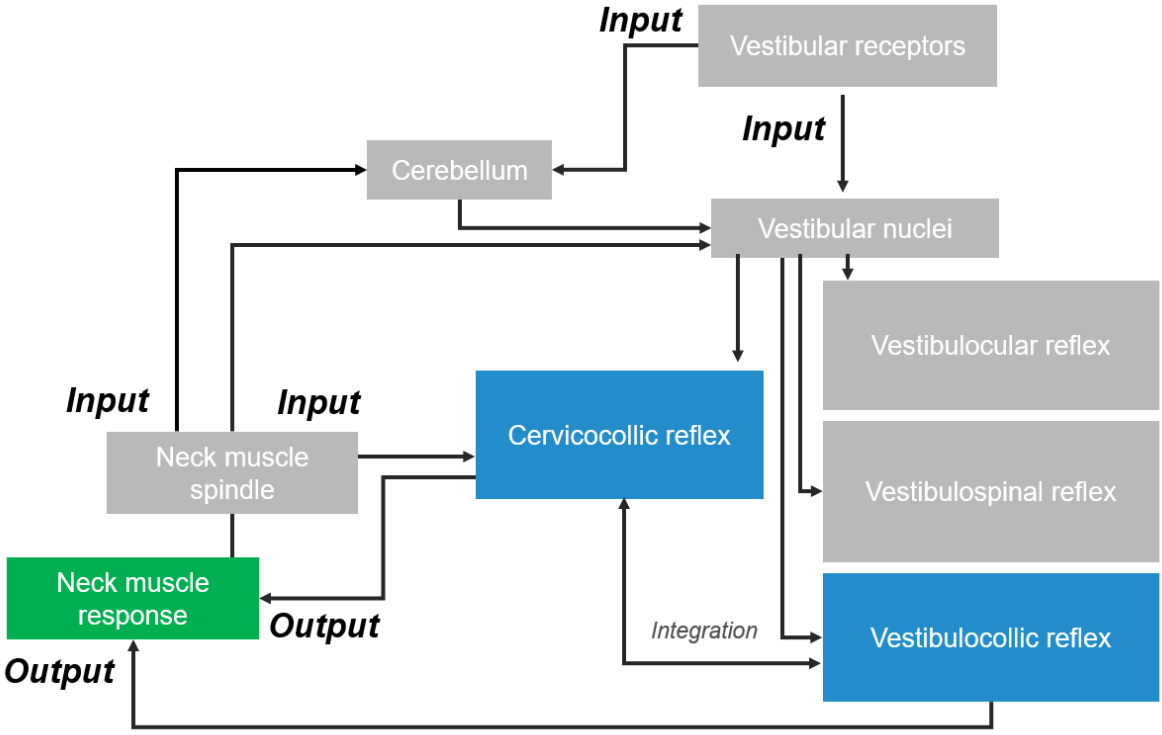

Figure 1.3 Simplified schematic of the neural connections in head and neck position sense adapted based on Armstrong et al., (2008).

1.5 Finite Element Human Body Model with Neck Muscles Reflexes

Several models have been developed with active neck muscle controllers to simulate muscular reflexes. This thesis focuses on finite element (FE) models, so the present review has excluded muscle control efforts on multibody dynamics (MB) models. Primarily, there are no substantial differences regarding the type of active muscle controller implemented between MB models or in FE models, as most of those models implement PID controllers (Östh et al., 2015). Recently, various MB models have implemented more advanced controllers, such as reinforced learning-based controllers or machine learning-based controllers (among others Amezquita-Garcia et al., 2022; Nowakowski et. al., 2021) which can possibly be also implemented in FE models in the near future but are not currently available in the FE simulation environment.

In most of the current active HBMs, modeling muscular reflexes loops has been accomplished using proportional, integral, and derivative (PID) controllers. In general, the PID controller (Åström and Murray, 2008) calculates an error value e(t) as the difference between the reference, r(t), and the current state, y(t) of the system (1) continuously. Corrections are applied simultaneously based on the proportional, integral, and derivative terms (2). The calculated control signal u(t) is proportional to the error value and reflected in the proportional term. The integral term integrates and reckons the past values and the derivative term calculates and estimates the future trends.

$$e(t) = r(t) - y(t) \tag{1}$$

$$u(t) = k_p \cdot e(t) + k_i \cdot \int_0^t e(\tau)d\tau + k_d \cdot \frac{de(t)}{dt}. \tag{2}$$

The PID feedback control can be used to model human postural responses with the proportional and derivative feedback used to model the reflexes responses from the muscle spindle and vestibular system. The steady-state error due to constant loads (such as gravity acceleration) can be removed using integrative feedback (Östh et al., 2015).

Several models called SAFER A-HBM (Östh et al., 2012, 2014a, 2014b, Ölafsdottir et al., 2019, Larsson et al., 2019), THUMS version 5 (Iwamoto & Nakahira, 2015), VIVA OpenHBM (Kleinbach, C.G. 2019), and GHBMC (Correia et al., 2021) have been used to model human reflex mechanisms for controlling the neck muscle activation.

Östh et al., (2012, 2014a, 2014b) developed a model called SAFER A-HBM to simulate car passengers during braking. The model included active neck, lumbar, upper, and lower extremity muscles. To control the activation of the muscles, the authors implemented Proportional Integral Derivative (PID) controllers. For the head-neck complex, the controller error signals were based on the head link angle and neck link angle. They grouped the neck muscles into flexion or extension groups based on the anatomical description of muscle function. The model was compared against volunteer responses with 10m/s^2 deceleration over 0.2s and autonomous braking with peak deceleration of 6.7m/s^2. From those studies, they concluded that the model with active muscles could capture the kinematic response of the volunteer's data used for the validation data.

More recently, Olafsdottir et al., (2019) developed a head-neck model based on SAFER A-HBM with active muscles representing both VCR and CCR mechanisms. They developed an omnidirectional controller based on the neck link angle using PID controllers. The muscle activity was determined by spatial tuning patterns, physiologically based muscle grouping that varied continuously depending on impact direction. The model was evaluated using 1G loading in multiple directions. They found that the model with active cervical muscles reduces the head and neck motions compared to the model without muscle activation.

Larsson et al., (2019) enhanced the neck and lumbar muscle controllers of the SAFER A-HBM. They compared the model's kinematics responses to volunteer responses in braking, lane-changing and combined maneuvers. The enhancements were conducted by updating the active muscle controller's reference coordinates to three coordinate systems (local reference, vehicle reference and gravity field reference). They concluded that the inclusion of active muscle responses improved the volunteers' kinematics predictions for combined lane change and braking scenarios with CORA scores ranged from 0.78 to 0.88.

Another FE HBM with active muscle reflexes called THUMS version 5 was developed by Iwamoto and Nakahira (2015). They implemented PID based active muscle controllers in all body regions, including the neck, and used a sigmoid function to model the firing rate. Their model was intended to study the head injury mechanism in lateral acceleration and was evaluated against volunteer data with sled acceleration of 4.0m/s^2 and 6.0m/s^2. They observed that the models with active muscle could capture the volunteer head kinematics better than the model without muscle activation (CORA Scores of 0.685 and 0.668).

Kleinbach, C.G (2019) enhanced an open-source FE HBM representing the 50th percentile female called VIVA OpenHBM. The author implemented an angle-based and length-based active muscle controller and validated the model using low-speed rear impact tests of volunteer. The author concluded that the active muscle controllers increased the model agreement when the head CG, T1, and pelvis kinematics were compared. The author also emphasized that the head-neck rotation agreement needs to be improved further. The author obtained promising results, although there was no evaluation for the intervertebral rotation in the cervical spine.

The head-neck of the 50th percentile male model called Global Human Body Models Consortium (GHBMC) was also enhanced by active neck muscle controllers (Correia et al., 2021). The model was evaluated against frontal, lateral and rear-end impacts. They implemented active muscle controllers based on the function of the VCR reflex and CCR reflex. Correia et al., (2021) used the IF function to activate the VCR-like controller if the head rotates more than 5 degrees, based on decerebrated cat experiments. The CCR-like controller was only implemented for the Trapezius and SCM muscle groups with a maximum activation of 10% of total muscle force. They concluded that robust performance for different impact directions and severities could be achieved with active neck muscle controllers.

Based on this summary, it was found that the most complex controller implemented a PID controller. Only one model by Kleinbach, C.G (2019), summarized in this section, focused on predicted kinematics during a low-speed rear impact. Also, only one similar model was found to represent the average size of females, which is a vulnerable occupant compared to males. However, cervical vertebral kinematics validation or comparison between the FE model and volunteers was not conducted in that study. Replicating cervical vertebral kinematics is vital if a model will be used to study kinematics that could influence the WAD.

The need for an HBM with active neck muscles that can offer better biofidelity than a passive muscle version is essential. This will ideally enable a better assessment of different potential injury mechanisms. With increased biofidelity, the ability to assess the protective performance of safety measures will be improved.

Access to both a female and a male HBM version allows for investigations influenced of sex on different responses and injury risk. It also allows for accident reconstruction studies that help evaluate the validity or correlation of various injury criteria and corresponding injury mechanisms (and injury sites). Ideally, this will make it possible to derive injury risk functions for valid injury criteria.

In order to achieve the best possible active muscle simulation, models of muscle properties and muscle controllers need to be developed with appropriate control strategies and integrated into a FE HBM.

Chapter 2 Objectives

The ultimate goal of the present research is to model neck muscle responses and corresponding head-neck kinematics during a low-speed rear-end impact in a female Finite Element (FE) Human Body Model (HBM). This model can facilitate the analysis of head-neck kinematics that may cause WAD. The work has been applied to the average size female HBM. This occupant size was selected since females have a higher risk of sustaining WAD than males and there was a lack of HBMs of this size. By implementing active neck muscles in the female HBM it becomes possible to study the effects of neck muscle action on the dynamic neck response and potential injury outcomes for females. In combination with a corresponding average male size HBM this also becomes a vital tool to better understand why females are more susceptible to WAD than males. To achieve the ultimate goal of the present thesis, several specific objectives were addressed by formulating the six research questions below:

- **Research Question (RQ) 1:** "How well can an isolated head-neck model replicate head-neck kinematics observed in a full-body model"?
- **Research Question (RQ) 2:** "Which active muscle controllers, angle-based or muscle-displacement based, can detect the head-neck motion and best simulate volunteer head displacement time histories?"
- **Research Question (RQ) 3:** "How well can different optimization schemes, targeting head and or vertebral volunteer kinematics responses, identify active muscle controller parameters to reproduce volunteer kinematics?"
- **Research Question (RQ) 4:** "What is the best configuration of an active neck muscle model to be used for whiplash injury assessment?" Several configurations or combinations of neck muscle representations were used to enhance the passive head-neck model with different sets of active muscle properties.
- **Research Question (RQ) 5:** "What is the influence of neck muscle responses on whiplash injury assessment in real life crashes of a modern vehicle?"

These research questions are specifically addressed by several studies presented in the following chapters of this thesis. Six papers were written to answer the questions within the scope of a four-year research period, relying on available experimental data.

Chapter 3 Methodology

The present work was arranged so that the research questions in Chapter 2 could be addressed systematically (Figure 3.1). The present thesis used two human body models representing the 50th percentile female called the VIVA OpenHBM (Östh et al., 2017a; 2017b) and VIVA+ HBM (John et al., 2022a; 2022b). VIVA+ HBM was developed as a successor and was a continuation from the VIVA OpenHBM (John et al., 2022a; 2022b). In addition, the 50th percentile male version of the VIVA+ HBM was also developed to allow direct comparison between two sexes (John et al., 2022a; 2022b). The first objective was to analyze whether the isolated head-neck model can replicate the full-body model head-neck kinematics and be used to develop an active muscle controller strategy. This first objective was addressed in Paper A. The second study (Paper B) was aimed to answer the second research question by comparing and understanding how different muscle controllers (angle-based and muscle-displacement based controllers) influence head kinematics of the model in a low-speed rear impact. In the third research question, the effects of different optimization objectives, were evaluated with the angle-based controller (Paper C). With a chosen muscle controller (based on Paper B and C), the head-neck kinematics of the model were improved over a passive neck model. However, there were undesirable oscillations and buckling observed in the lower cervical spine (C4 – C6) due to the active muscle controller. Therefore, Paper D and Paper E were designed to remove neck buckling and oscillations, improving the head-neck kinematics agreement of the model with volunteer responses. After successfully improving the head-neck kinematics agreement, further work was conducted to study different active muscle controller configurations and evaluate which configuration was the best model to be used for WAD assessment. These studies were also conducted as part of paper E. Finally, a study to evaluate the influence of neck muscle responses on head-neck kinematics, a local pressure transient phenomenon in the spinal canal, and whiplash global injury criteria using crash pulses based on real-world crashes (Paper F) was conducted.

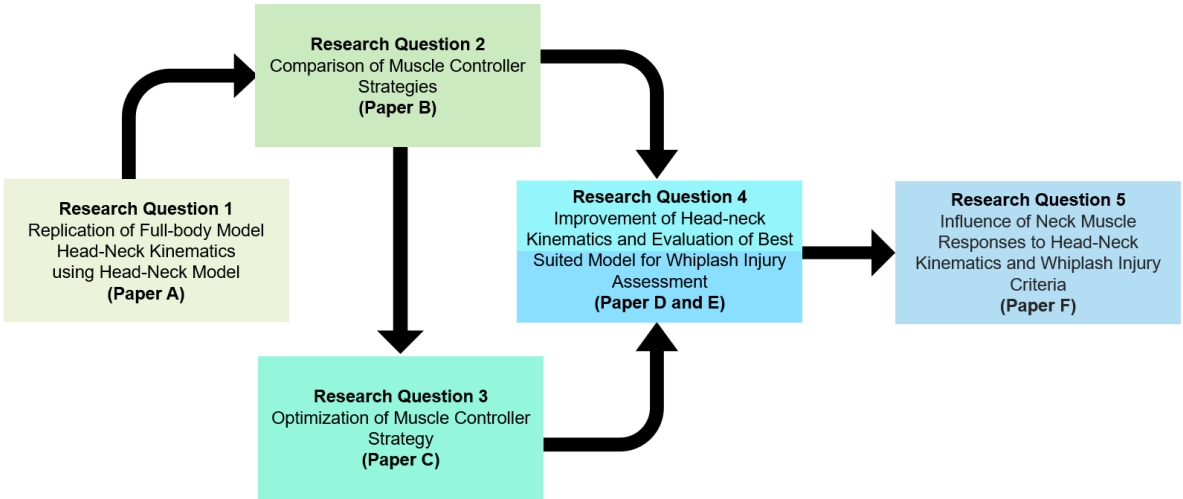

Figure. 3.1 Structure and relation between studies in the present thesis

3.1 Overview of VIVA Open Human Body Model I (VIVA OpenHBM I) (Paper B, C and D)

The original VIVA OpenHBM was originally created by Östh et al., (Östh et al., 2016, 2017a, 2017b). The model was developed to represent the stature and mass of a 50th percentile average female (Figure 3.2). The model development focused on the neck because the main intention was to study WAD in a low-speed rear-impact collision. Thus, the model has a detailed neck structure, while other body parts were simplified. The model was validated against quasi-static loading component tests and whole-body rear-impact tests (Östh et al., 2017a, 2017b). In addition to the detailed cervical spine, a simplified cervical spine model was also developed (Östh et al., 2017b). The simplified model was created by removing the non-muscular intervertebral soft tissues in the neck. To compensate for the soft tissue removal, compliant joints (translational, axial rotational, lateral bending and flexion-extension) were added with joint stiffnesses based on published human in-vitro tests (Panjabi, MM. et al., 1986,2001 and Nightingale RW, et al., 2002). Only small differences in kinematics, evaluated using an objective rating evaluation (CORA) method (Gehre et al., 2009), were found when the detailed and simplified cervical spine models were compared in dynamic rear-impact test conditions (Östh et al., 2017b).

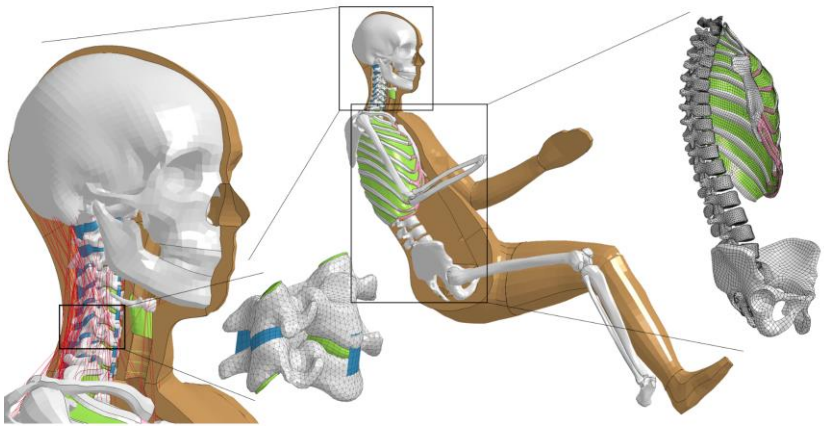

Figure. 3.2 VIVA I OpenHBM (Östh et al., 2017b). Source: Östh et al., VIVAOpenHBM I Project (Paper B, C and D).

3.2 Overview of VIVA+ Human Body Model (VIVA+ HBM) (Paper A, E and F)

VIVA+ FE HBMs representing the 50th percentile female (50F) and male (50M) occupants were also used in the present study (Figure 3.3). The 50th percentile female occupant model was initially developed and used as a baseline to create other models by conducting rescaling and morphing. The derivative models include the 50th percentile male occupant model. The morphed models have identical elements to the baseline model; however, the nodal coordinates were adjusted accordingly. The original geometry of the baseline model (including outer body shape, ribcage, femur, tibia and pelvis) was based

on physical statistical shape models (Reed and Ebert, 2013). Besides changes in geometry needed to derive average male from average female, several properties were also updated. These properties included head mass inertial properties, the soft tissues densities, knee ligaments and quadriceps muscles properties. Kinetic and kinematics responses of VIVA+ HBMs have been validated to blunt impacts in different directions (frontal, lateral and back). Specifically, for the rear-end impact collision, the kinematics responses of VIVA+ FE HBMs have been validated starting from the functional spinal unit (FSU) level, isolated head-neck level, and whole-body level. The details of VIVA+ HBMs developments and validation are described further in John et al., (2022a; 2022b).

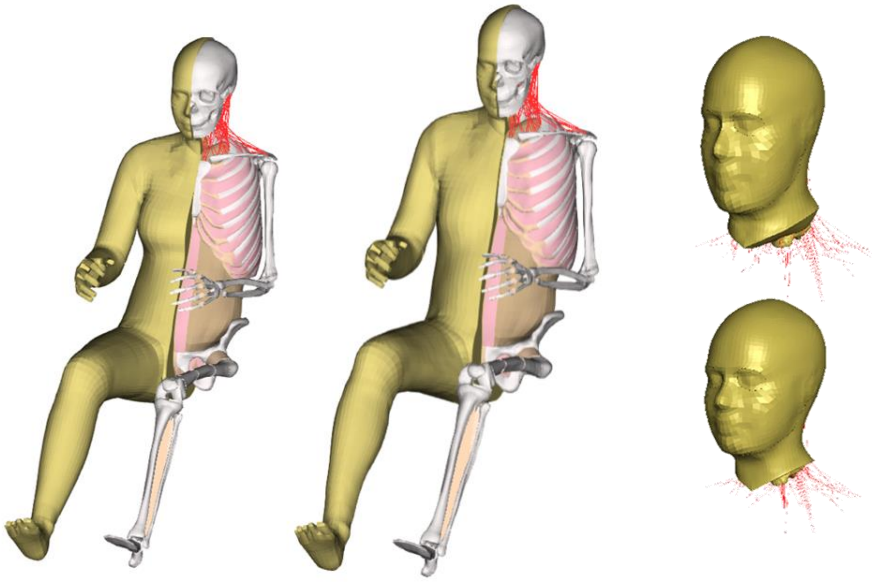

Figure. 3.3 VIVA+ finite element human body models and isolated viva+ head-neck models.

The soft tissue in the neck of VIVA OpenHBM and VIVA+ HBM (Figure 3.4) was modeled as hexahedral elements and lumped into one part to represent both adipose tissue and passive muscle tissue. The LS-DYNA *MAT_77/*OGDEN_RUBBER was used with material properties based on Engelbrektsson (2011) to model the VIVA OpenHBM neck's soft tissues (Östh et al., 2017a). Material properties based on Naseri (2022) were used for the soft tissue of the VIVA+ model. The VIVA OpenHBM and VIVA+ HBM neck's skin was modeled as quadrilateral shell elements with LS-DYNA *MAT_001/*LINEAR_ELASTIC and LS-DYNA *MAT_034/*FABRIC used as material model based on properties from Manschot and Brakke (1988), respectively.

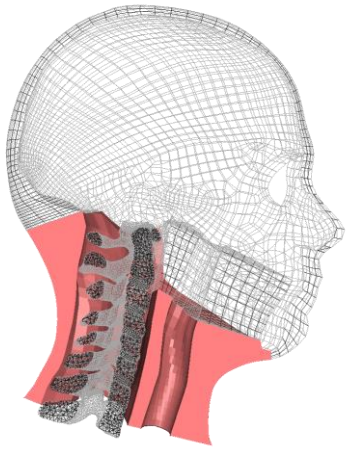

Figure. 3.4 Neck's soft tissue of VIVA+ HBM (showed in colour)

3.3 Volunteer Kinematics Data (All Papers)

The kinematics data from volunteer test based on Sato et al., (2014) were adopted to optimize the model head-neck kinematics responses in this thesis. Since detailed muscle response data was not available, the analysis was limited to the head and neck kinematics. The reference volunteer data of Sato et al., (2014) consisted of two sled test series. The first test series was conducted with twelve males and eight female volunteers seated in a rigid seat without a headrest. Rear-impact tests with delta velocity 8.1 km/h and 10km/h were conducted using an inclined sled rail with a 10-degree inclination from the horizontal line. The peak accelerations were 27m/s^2 and 37 m/s^2, respectively. The head C.G x-accelerations and T1 C.G displacements data (linear x- and z- displacements), as well as head C.G y-rotational displacement from first test series in Sato et al., (2014) were used in the present study.

The second volunteer test series of Sato et al., (2014) was based on a low-speed rear-impact test conducted using a mini sled test with a delta velocity of 5.8 km/h and peak acceleration of 42m/s^2. Four male volunteers and two female volunteers were seated in a rigid seat without a headrest. Head C.G displacements and accelerations, T1 C.G displacements and C1-C7 rotational displacement and velocity data in sled coordinate system from that test series were used in the present study to calibrate and compare the VIVA+ FE models kinematics.

The head-neck model was simulated by prescribing the volunteers' T1 (first thoracic spine) kinematics in the T1 of the model (Figure 3.5). In the head-neck model the lower nodes of the skin and several nodes of the soft tissues were constrained to move and rotate with the T1. Full model simulations of both female and male models were done following the Sato et al., (2014) setup (Figure 3.5). The two models were seated in a rigid seat with a 20-degree seatback angle from the vertical. Sled acceleration from the experiment was prescribed on the seat model.

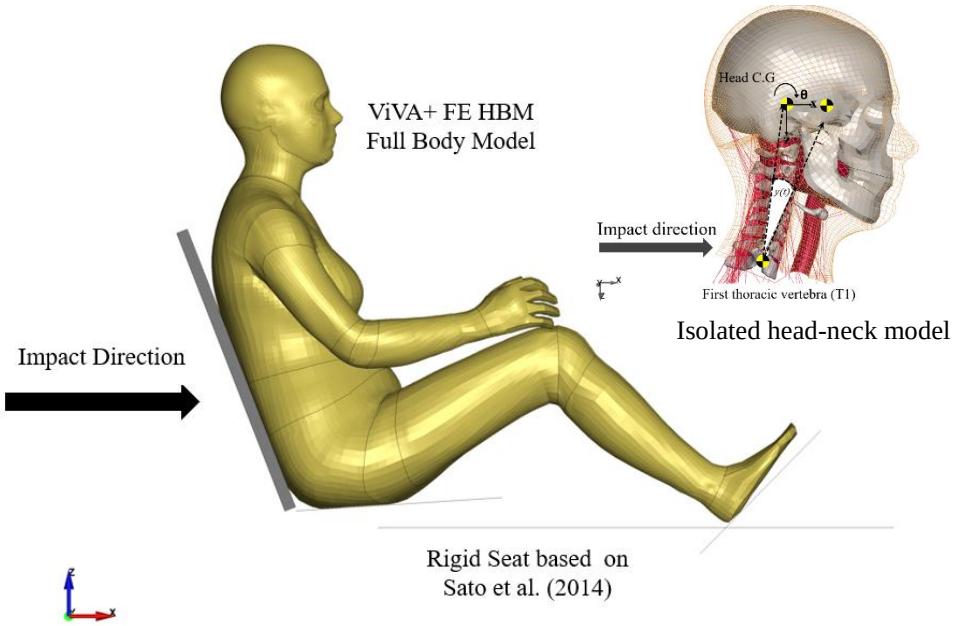

Figure. 3.5 Simulations Setup of Head-Neck and Full Body Model based on Sato et al., (2014).

3.4 Comparison of Head-Neck Kinematics between Isolated Finite Element (FE) Head-Neck Model and Full-Body Model (Paper A)

The objective of this section was to analyze whether the isolated head-neck model can replicate the full-body model head-neck kinematics and be used to develop an active muscle controller strategy (Paper A). First, the full-body passive model was run following the volunteers' test setup to generate the T1 linear and rotational accelerations. The generated T1 accelerations were then prescribed to the isolated passive VIVA+ head-neck models. This was conducted to ensure that both models had identical T1 accelerations. The head C.G. and cervical vertebra C.G. displacements and rotations from the full-body models and head-neck models were compared and analyzed.

3.5 Modelling Mechanical Properties of Neck Muscle (All Papers)

The passive neck muscle modeling of VIVA OpenHBM is described in Östh et al., (2017a). The neck muscles of the VIVA OpenHBM I model were implemented using the Hill muscle model (LS-DYNA *MAT_156/*MAT_MUSCLE) with PCSA from Borst et al., (2011). The origin and insertions of the muscles were based on anatomical descriptions from Standring (2008). There are 129 resultant truss elements to represent 34 muscles (Östh et al., 2017a) since muscles with larger volumes are represented with more than one truss element. Passive neck muscle modeling of VIVA OpenHBM was also adapted for the VIVA+ HBM.

The implementation of LS-DYNA Hill muscle model (Figure 3.6) was based on Hill's three element model from Hill (1938). The Hill's muscle model consists of Parallel Element (PE), Series Elastic Element (SEE) and Contractile Element (CE). The PE is modelled as non-linear spring in parallel with the CE and SEE.

The PE is responsible to model passive behaviour of muscle tissue such as viscoelastic properties. The SEE is modelled also as a non-linear spring but arranged in series with the CE. The SEE is usually modelled to represent the tendon structure and is often neglected when a series model of tendon compliance properties is included. The CE is used to model the active force produced by the muscle and can freely extend when the muscle is not producing active force. The muscle force generated by the CE is modelled as the function of activation level, muscle length and shortening velocity (Figure 3.7).

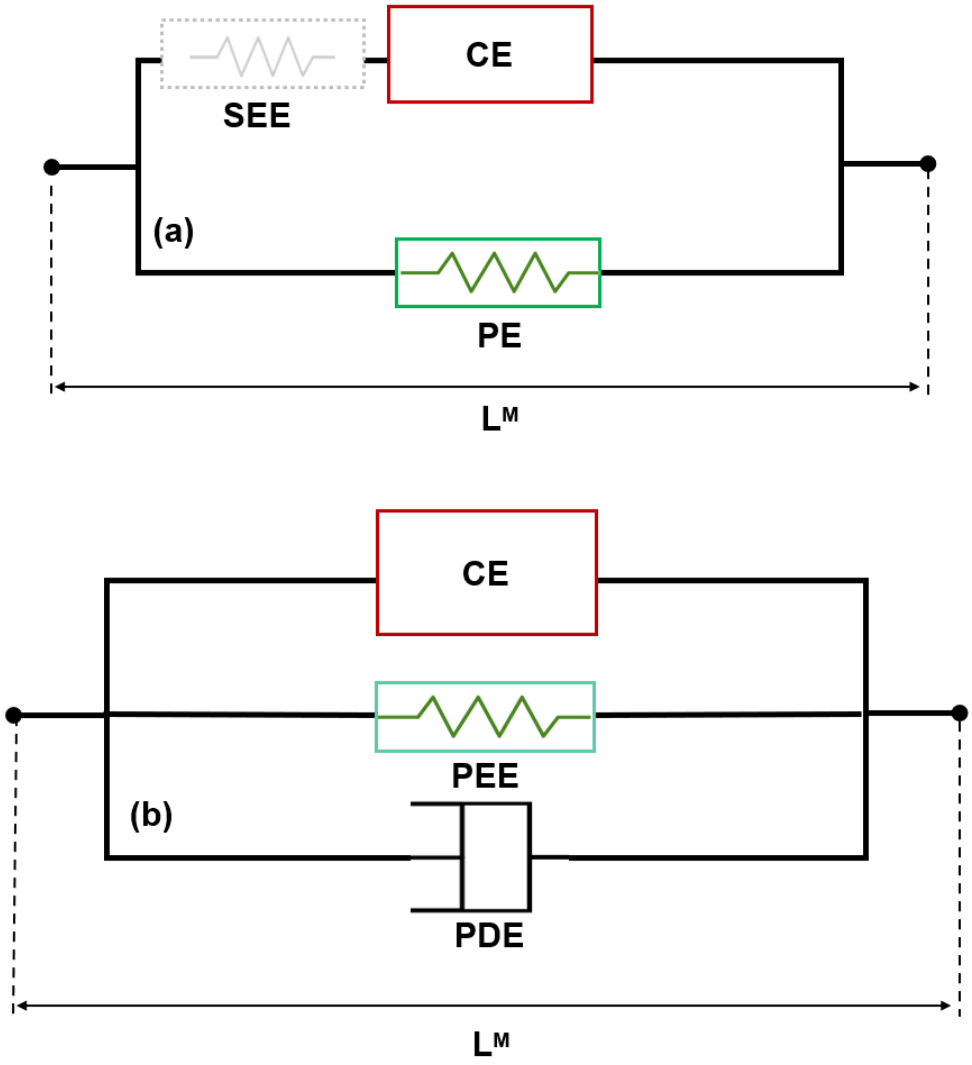

Figure. 3.6 Hill's three-element muscle model implemented in LS-DYNA as discrete element (a) and as a standard material (b). Adapted from LS-DYNA Manual (LST 2021) and Kleinbach et al., (2017)

Previously, Hill's muscle model was implemented as discrete elements in LS-DYNA by Dr. J.A. Weiss (Figure 3.6.a) and furthermore developed as standard material (*MAT_156/*MAT_MUSCLE) by replacing the force, relative length and shortening velocity as the stress, strain and strain rate (Figure 3.6.b). A parallel damping element was also added in the latest implementation. Consequently, the total muscle stress is equal to the sum of stress from the contractile element, the passive element and the damping element. See LS-DYNA Manual for the details (LST 2021).

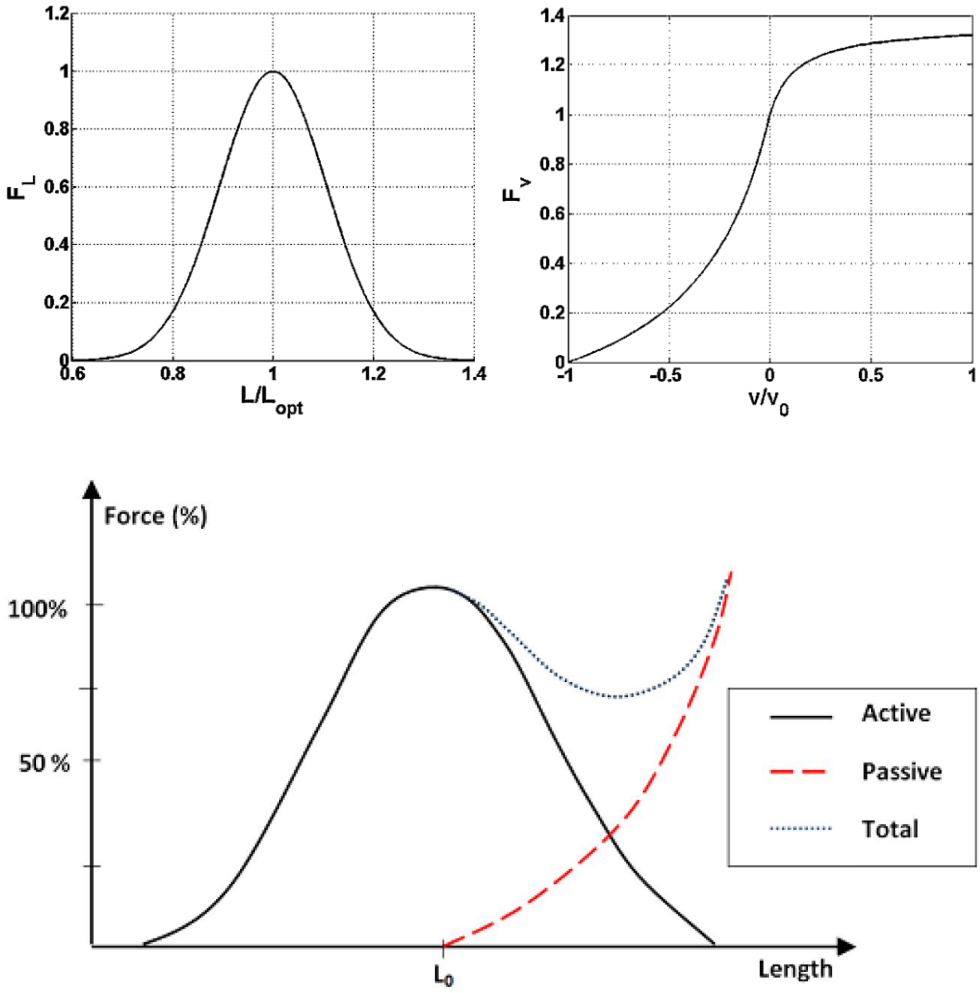

Figure. 3.7 Muscle force-length relationship, force-velocity relationship and relationship between active, passive and total muscle force.

3.6 Modelling Active Reflexive Neck Muscle Responses (Paper B to F)

The modelling of the active neck muscles used in the present thesis was built on earlier research conducted by Östh et al., (2012,2015) and Olafsdottir et al., (2017, 2019). The Proportional and Derivative (PD) controller, as defined by the PIDCTL function in LS-DYNA, was used to give activation signals to the neck muscles of the model.

In the present thesis, two forms of active neck muscle controllers are utilized. The first muscle controller is called the Angular-positioned Feedback (APF) Controller. The APF controller activates neck muscles to maintain the head orientation relative to the global reference system. In this way, it is a similar in function to the VCR in humans. The controller vector (Figure 3.8) is defined based on the coordinate of the model head center of gravity (C.G.) and the center of the first thoracic (T1) spine vertebral body. This controller vector is sampled at time zero (t_0). When the model head and neck move (due to impact loading), the new position of the head C.G. and T1 are sampled and used to update the controller vector.

An error angle, e(t), will be produced if there are any differences between the controller vector at t_0 (reference angle) and the current angle, y(t). The projection of the controller vector on the horizontal plane is also used as the input to the spatial tuning pattern which defines directionally specific muscle activations for each muscle group.

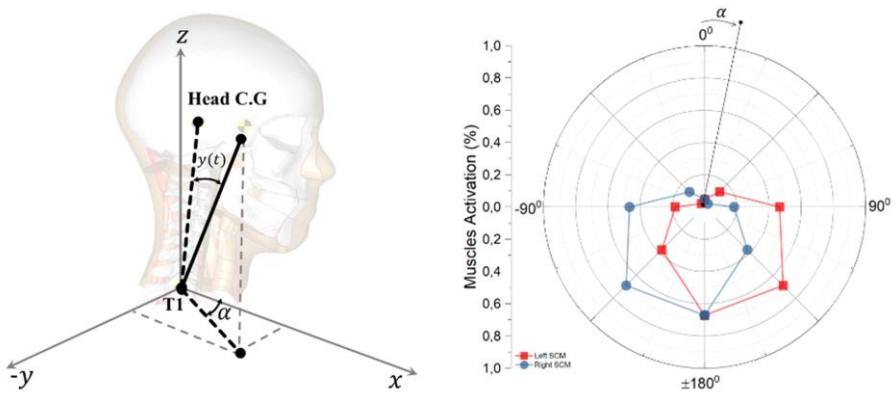

Figure 3.8 Controller Vector Calculation and Projection using Spatial Tuning Pattern

To mimic the neural processing delay, a delay was introduced in the error angle feedback signal, as presented in Figure 3.9. The delayed signal was then given to the PD controller. To define the muscle activation, the computed-control signal was then given to the spatial tuning pattern.

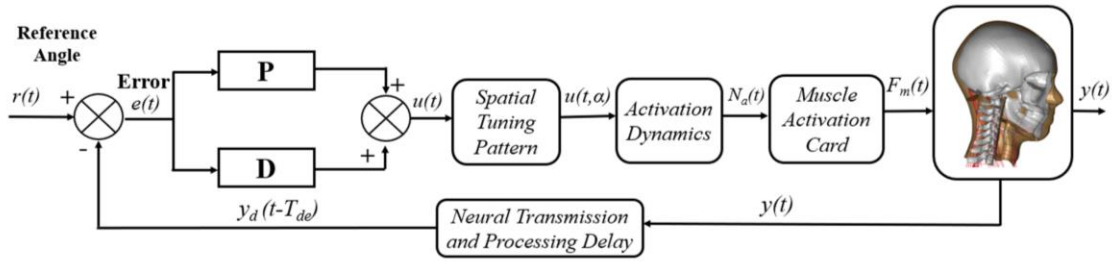

$r(t)$: Reference Angle calculated based on initial position of controller vector

$e(t)$: Error Angle defined by Reference Angle $r(t)$ subtracted with Current Angle $y(t)$

$y(t)$: Current Angle of the model calculated based on controller vector

$u(t)$: Excitation signal as output from PD Controller

$u(t,\alpha)$: Spatial Tuning Pattern-scaled PD Controller excitation signal

$N_a(t)$: Muscle activation level

$F_m(t)$: Muscle force generated by LS-Dyna Muscle Activation Card

$y_d(t\text{-}T_{de})$: Current Angle $y(t)$ delayed using Neural Transmission and Processing Delay (T_{de})

Figure 3.9 Controller Algorithm to Approximate the Feedback from Human Vestibular System.

The second type of controller used in this thesis is called the Muscle-length Feedback (MLF) controller. It was developed to have similar a function as the CCR, which is to maintain head posture relative to

body. The controller mechanism was similar to the APF controller, however instead of changes in angles, changes in muscle length were used to define the controller signal. As each muscle element has its own controller, there is no need for a muscle spatial tuning pattern in the MLF controller.

In the current study, each neck muscle element in the model has its own muscle length controller. At time zero, the length of each muscle element was calculated and used as the reference length and is unique for each muscle. The length of each muscle element was first calculated at a pre-defined time (set at time zero). Then, after a delay mimicking the neural processing delay, the muscle length was measured again. The error signal in the MLF is calculated by measuring the change in length of the muscle referred to t_0. When the length of the muscle changes due to a difference in length between the current and the reference length, the PD controller produces an activation signal. The signal will be given to the corresponding muscles after being filtered and scaled using the activation dynamics filter.

In the present thesis, the APF controller was used in all papers except the paper A and the MLF controller was used only in paper B and D.

3.7 Optimization-based Parameter Identification (Paper B to E)

Optimizations to determine muscle controller gains were conducted using LS-OPT (Stander et al., 2015) with objective to match volunteer head and cervical vertebral kinematics. In Papers B and D, the optimizations were designed to determine the values of the Proportional Gains (KP), Derivative Gains (KD), and Neural Transmission and Processing Delay (TND) for both APF and MLF controllers. For Paper C, the optimizations were extended to identify the time constants defining the muscle activation dynamics (TNA_a, TNA_d, TNE) in addition to KP, KD, and the TND. Correlation analysis between optimization parameters was also analyzed and presented in Paper C. In Paper E, an additional optimization to define the value of the parallel damping element (PDE) was also conducted. Metamodel-based optimization using Sequential Response Surface Method (SRSM) with Domain Reduction incorporated in LS-OPT (Stander et al., 2015) was the optimization method in all studies. The optimization algorithm was the Hybrid SA (Simulated Annealing + Leapfrog Optimizer for Constrained Minimization). A Linear Polynomial Metamodel with D-optimal point selection was used to define the metamodel of the optimizations. The preset maximum number of iterations was kept at ten for papers B to E. The reader is referred to Stander et al., (2015) for details on LS-OPT.

3.8 Developing a Head-Neck Model to Stay Upright under Gravitational Acceleration (Paper D)

A model that can stay upright under gravitational acceleration was achieved in Paper D by adjusting and optimizing the muscle co-contraction levels. Muscle co-contraction is defined as the simultaneous activation of agonistic and antagonistic muscles and has been known to contribute to maintaining spinal stability (Lee et al., 2006). The neck muscle co-contraction should keep the head in an upright position under gravitational acceleration. In the present thesis, the neck muscles of the VIVA OpenHBM model were divided into eight groups of muscles based on Ólafsdóttir et al., (2019b) before optimizing the co-contraction level.

3.9 Improving Head-Neck Kinematics Agreement (Paper D and E)

Two methods were tested to improve the head-neck kinematics agreement between the models developed in the previous studies and the volunteer reference data. The first method was conducted by combining the two active muscle controllers (Paper D). Two approaches were studied to combine the APF and MLF controller (Figure 3.10). The first approach assumed that both APF and MLF controllers were controlling the activation of all neck muscles (based on the review from Armstrong et al., 2008). Since only one activation card is available in LS-DYNA *MAT_156/*MAT_MUSCLE, therefore the stronger between APF and MLF controller output signal was selected using the Min-Max function at each time step. Consequently, for the impact duration of 300ms, the activation signal for each muscle element was based on the combination of APF and MLF signals. This first approach is called a Combined-Control approach (Figure 3.5a). In the second approach, the APF controller was used to regulate the activation of the superficial muscles. Meanwhile, the deep neck muscles were controlled by the MLF controller. The second approach was motivated by the higher densities of muscle spindles found in the deep cervical muscles (Amonoo-Kuofi 1983; Liu et al., 2003). The grouping of deep and superficial neck muscles was based on Borst et al., (2011). The second approach is denoted the Distributed-Control approach (Figure 3.10b).

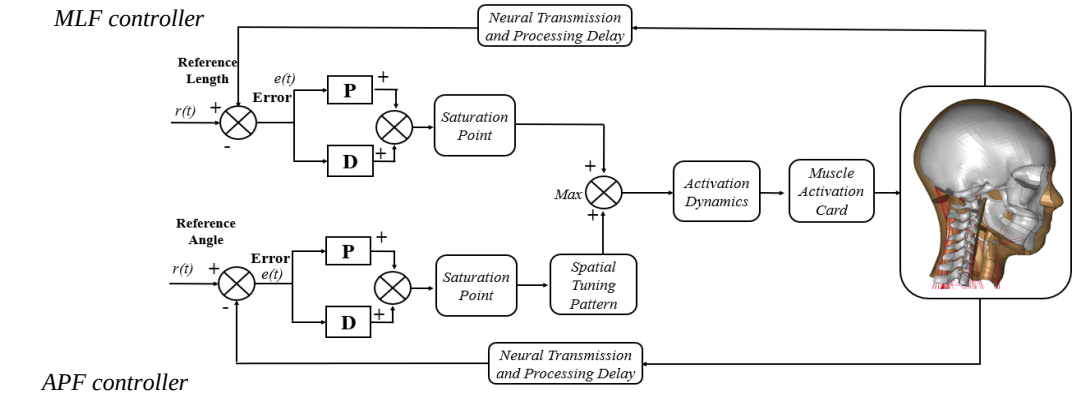

(a)

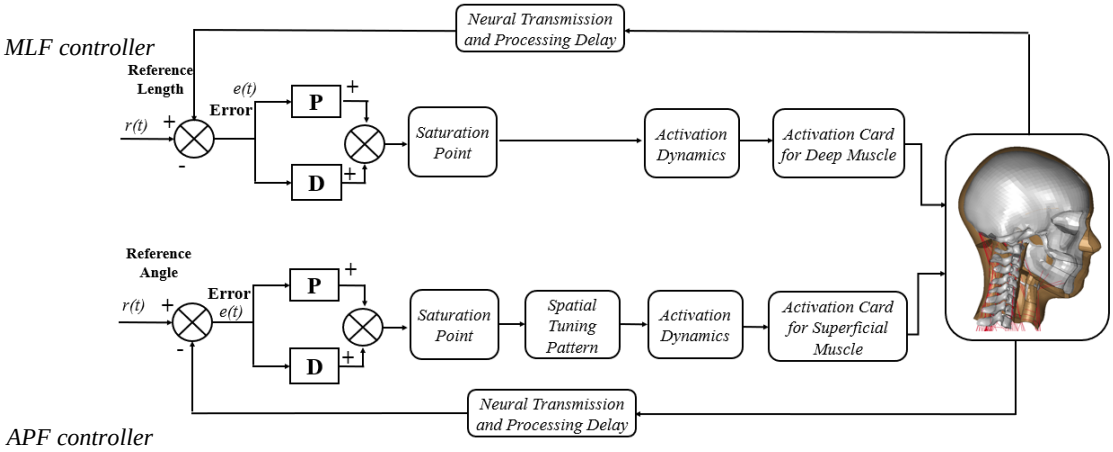

(b)

Figure 3.10 (a). Combined-Control Approach and (b). Distributed-Control Approach

The second method to improve the head-neck kinematics involved adding and optimizing a parallel damping element (PDE, paper E). It was hypothesized that this buckling could be due to the limitations of the current Hill muscle implementation in LS-DYNA itself. As mentioned in Kleinbach et al., (2017), the current implementation of LS-DYNA Hill muscle only includes a parallel damping element and neglected the serial elastic and damping elements to represent tendon structures. Subsequently, some limitations were observed, such as instabilities (oscillations and sudden drop in the active force generation) produced by the force-velocity or force-length relation formulation (Wittek et al., 2000), incorrect energy storage and release in the interaction with the environment (Siebert et al., 2008, Mörl et al., 2016), and unrealistic high-frequency oscillations (Günther et al., 2007). In addition, the muscle model in VIVA OpenHBM was modeled as 1D Truss elements and may not reproduce damping implicitly in a human neck with 3D muscles.

3.10 Parametric Simulations of Active Muscle Controller Configurations (Paper E)

Parametric simulations of muscle controller features were conducted (Paper E). The purpose of these parametric simulations was to evaluate each feature in the active head-neck models and determine the best configuration to match volunteer kinematics based on CORA score evaluation. The roles of each feature in the active muscle controller should be determined to identify their influence on head-neck kinematics. Head-neck kinematics such as head and T1 center of gravity (CG) x-acceleration and the cervical vertebral angular displacements will be used as input to the calculation of whiplash injury criteria. For example, the primary inputs for global injury criteria such as Neck Injury Criterion (NIC) (Boström et al., 2000) are head and T1 center of gravity (CG) x-acceleration. In addition, for indirect tissue-based injury assessment, such as simulating transient pressure gradients in the spinal canal (Svensson et al., 1998; Yao et al., 2016), vertebral angular displacements of the cervical spine are required.

3.11 Accident Reconstruction Simulation to Study the Influence of Active Reflexive Neck Muscle Responses (Paper F)

Accident reconstruction simulations based on real-world crash data were conducted to evaluate the influence of active neck muscle simulation on the head-neck kinematics. This was assessed both in the local anatomical site and with global kinematics-based injury criteria. In addition, the differences between females and males under identical crash conditions were analyzed. Furthermore, the differences between injured and uninjured occupants in head-neck kinematics were also analyzed (Paper F). Crash pulses recorded by Folksam Research from real-world accident data were implemented in the finite element (FE) simulation setup to simulate real-world crashes. The database contained 13 rear-impact cases where the struck car was a Toyota Auris. Toyota Auris was specifically chosen due to the availability of a finite element (FE) model of that specific car's seat. Selection criteria were defined, such as the occupant's position (driver or front seated occupant), and only cases with adult female occupants (18 years old or above) were selected. Those criteria yielded nine different crash pulses. The resultant delta velocity ranged from 9 km/h to 20.4 km/h, with mean accelerations from 2G to 5.3G and peak acceleration from 4.3G to 12.7G (Table 3.2) Additional information was collected by looking into the occupant data, such as the whiplash symptom duration and Whiplash Associated Disorder (WAD) level from those nine rear-end impact crashes. The occupants experiencing whiplash symptom durations of at least one month and a minimum WAD level grade 1 were classified as "Injured". The other cases were classified as "Uninjured" occupants. Three occupants were identified as "Injured" occupants (in which one occupant had permanent medical impairment-PMI) and six as "Uninjured".

Table. 3.1 Impact severity of the selected nine cases based on Folksam research database (Paper F)

Crash Pulse Name	Resultant of Delta Velocity (km/h)	Resultant of Mean Acceleration (G)	Resultant of Peak Acceleration (G)	Injured/ Uninjured
Injured-1	10.6	4.8	8.6	Injured
Injured-2	10.7	3.1	4.9	Injured (PMI)
Injured-3	15.9	4.8	11.6	Injured
Uninjured-1	9	2	4.9	Uninjured
Uninjured-2	9.4	2.3	4.3	Uninjured
Uninjured-3	11.2	2.4	5.6	Uninjured
Uninjured-4	11.5	4.8	11	Uninjured
Uninjured-5	14.4	5.3	12.7	Uninjured
Uninjured-6	20.4	4.6	11.1	Uninjured

The open-source seat FE model used in the current study was developed based on a Toyota Auris driver seat (model year 2010-2012). The model was developed and validated within the project VIRTUAL (EU-Project No. 768960) (Jakobsson et al. 2022). Reasonable agreement between the FE model and physical tests were achieved for the most measured location of the seat, such as seat cushion, backrest, and head-restraint. In the present study, the positioning procedure of the VIVA+ FE HBM for both female and male models was based on the setup proposed by Trummler et al., (2022). Trummler et al., (2022) adapted the statistical model based on Park et al., (2016) to define the seating posture. This method resulted in the head to a head-restraint distance of 56.3 mm.

Figure. 3.11 The VIVA+ female occupant model at the time 0 ms before the crash pulses were applied.

In total, 18 accident reconstruction simulations were conducted in the present study based on nine different crashes. The female occupant simulations were divided into two sets of simulations: 9 simulations with a VIVA+ female passive model and 9 with active neck muscles.

The tissue-based whiplash injury hypothesis, here denoted Aldman pressure (Svensson et al., 1993, 1998) and a global-based kinematics injury criteria denoted Neck Injury Criterion (NIC, Boström et al., 2000) were also calculated as additions to the head, neck and T1 kinematics. In the current study, the NIC was calculated following the calculation procedure from the EuroNCAP (2021) protocol and the Aldman pressure was calculated from a hydrodynamic modelling tool which was developed by Yao et al., (2016).

All response corridors presented in Paper F were defined by the average response ± 1 Standard Deviation (SD). Analysis of the NIC (max) and the negative Aldman pressure was limited to the first 100ms of input because almost all hypotheses related to WAD postulate that WAD are more likely to occur during the retraction phase. T-tests with a statistical significance level of 0.05 were conducted to evaluate whether the head-neck kinematics, head-to-headrest contact, and NIC and Aldman pressure were statistically significant between the two datasets following the corresponding two research questions.

3.12 Quantitative Ratings Evaluation

Throughout this thesis, the quantitative rating evaluation was conducted using CORA analysis (Gehre et a. 2009). The default corridor (5% inner limit and 50% outer limits) of CORAplus 3.6.1 and 4.0.5 was chosen.

3.13 Software and Computational Environment

The pre- and post-processing software of the simulation models were conducted using LS-PrePost version 4.5 -x64 to version 4.8 x-64 (LSTC 2012). ANSA v18.1.0 (64-bit), MATLAB R2019B and OriginPro 2019(64-bit). LS-DYNA binary version 9.2 and 9.3 MPP double precision (LSTC 2016) was used for all simulations.

Chapter 4 Results

Key results from the appended papers are provided in the following sections.

4.1 Replicating Head-Neck Kinematics of Full Body Model using Head-Neck Model (RQ 1 – Paper A)

The head-neck model could replicate the full-body model responses up to 200ms (Figure 4.1) except for head C.G. rotational displacements, which were in agreement up to 150ms. These responses were observed for both female and male models. Generally, with identical T1 kinematics, the head-neck model produced less stiff responses than the full-body model both for head and neck kinematics (see Paper A).

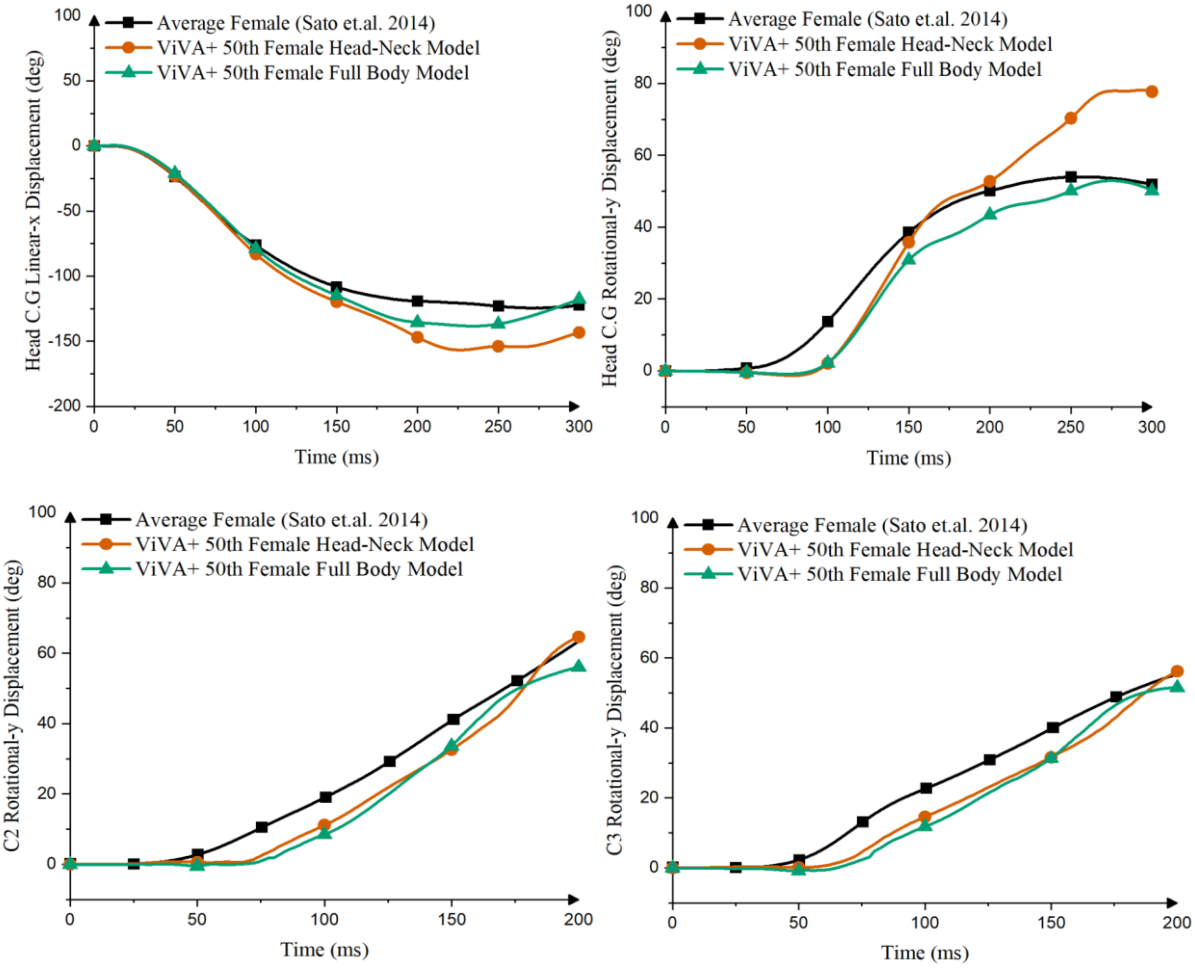

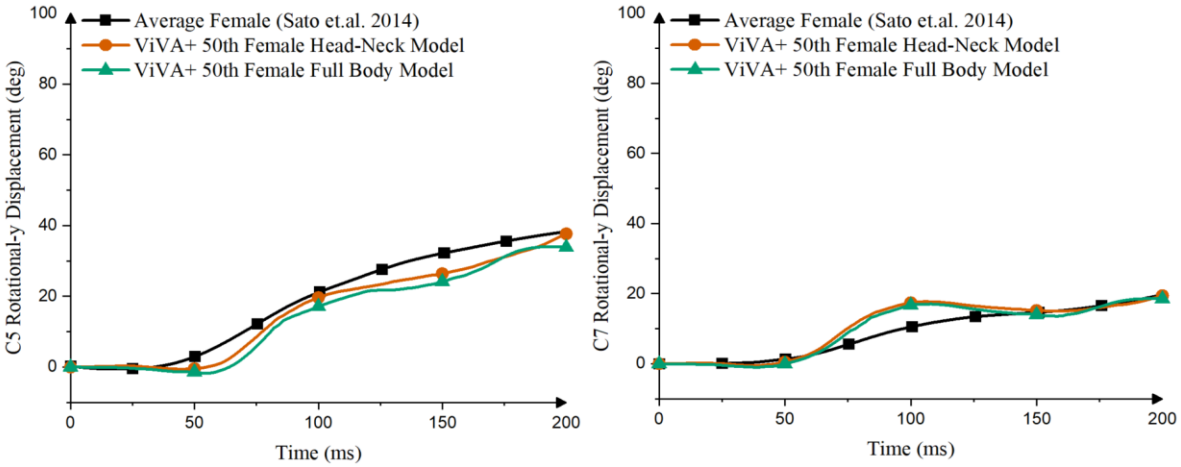

Figure 4.1 Comparison of Head-Neck Kinematics of VIVA+ Head-Neck Female Model and Full-Body Female Model with Similar T1 Displacement and Rotations as Input

4.2 Comparison of Neck Muscle Controller Strategies (RQ 2- Paper B)

The initial implementation of APF and MLF controller presented in Paper B were optimized to match the volunteer head C.G linear and rotational displacements. Both the APF and MLF controller changed the head kinematics (Figure 4.2) from the passive model. The model with the APF controller had the best agreement with volunteer data. In the vertical direction, active models could reduce the peak head displacements. However, no version of VIVA OpenHBM (active or passive) could capture the first 100ms of the volunteer motion in the vertical direction (Figure 4.2b). When the head rotational displacements were compared, only slight differences in head motion were observed in the APF and passive models until 100ms after the impact time. The model with a MLF controller had higher head rotations compared to other models (Figure 4.2c). The model with the MLF controller could slightly improve the head kinematics from the passive model but had non-realistic responses early in the simulation (Figure 4.2abc), which were not observed with the APF controller.

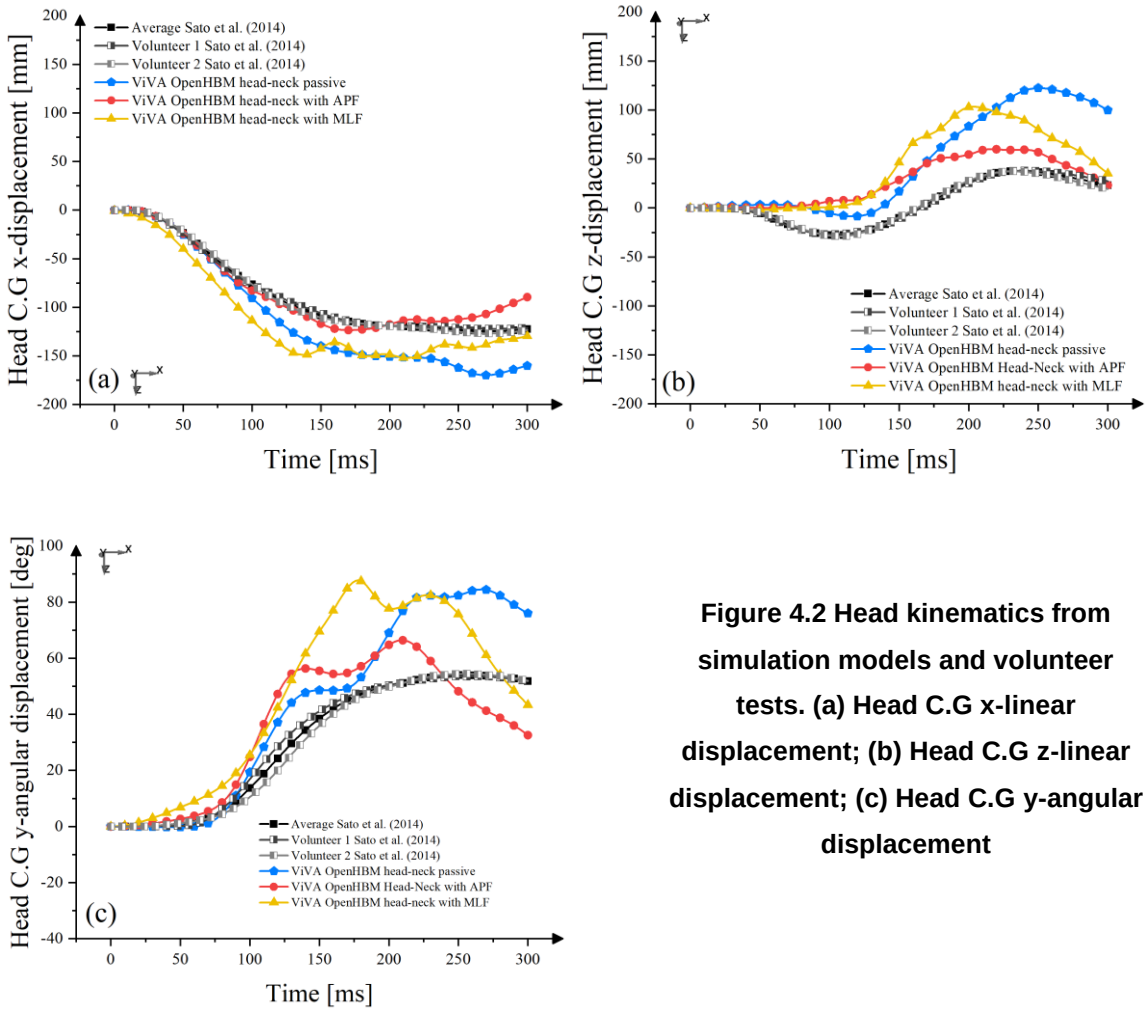

Figure 4.2 Head kinematics from simulation models and volunteer tests. (a) Head C.G x-linear displacement; (b) Head C.G z-linear displacement; (c) Head C.G y-angular displacement

4.3 Optimization of Neck Muscle Controller Strategies (RQ 3 – Paper C)

Only APF controller was implemented in Paper C. Four different sets of controller gains, resulting in four schemes, were optimized. The schemes were: Opt.1 model (optimized only for volunteer head kinematics), Opt.2 model (optimized only for cervical vertebral kinematics), Opt.3 model (optimized for both head and neck kinematics), and Opt.4 model (as Opt.3 but used one weighting factor for all cervical vertebral kinematics).

In general, all optimization simulations of these studies were numerically stable. The optimum value for KP tended towards the lower bound of permitted parameter identification range except for Opt. 2. For KD, the optimum values were at the lower boundary for most of the optimizations except for the Opt. 2 and the Cross-Validation optimization. The optimum values for the TND and the time constants describing the muscle activation dynamics were similar in all optimizations.

The controller parameter convergence and correlations were also analyzed in Paper C. An example of parameter optimization convergence is presented in Figure 4.3. From the parameter correlation

analysis, it was found that most of the parameters in all optimizations had weak inter-parameter correlations (≤ ±0.29). Although, several medium correlations (±0.30 - ±0.49) were observed between parameters in some optimizations and only one strong correlation (between TND and Tna_d) was found in Opt.2 (±0.50 - ±1.00). When the correlation between optimization parameters and objectives was analyzed, the KD and KP had the strongest correlation to the optimization objectives (Figure 4.4).

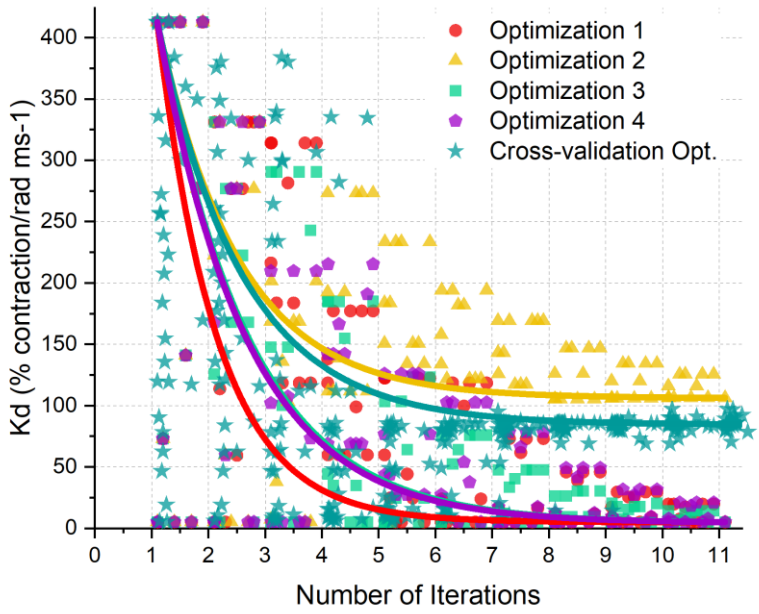

Figure 4.3 Parameter convergence plot

	Head C.G x-disp	Head C.G z-disp	Head C.G rot-y disp	C1 rot-y disp	C2 rot-y disp	C3 rot-y disp	C4 rot-y disp	C5 rot-y disp	C6 rot-y disp	C7 rot-y disp
Tnd	-0.01	-0.07	0.01	0.06	0.07	0.09	0.13	0.14	0.15	0.28
Kd	0.35	0.53	0.66	0.47	0.52	0.51	0.61	0.59	0.65	0.48
Kp	-0.15	0.07	0.28	0.84	0.85	0.87	0.55	0.40	0.38	0.15
Tna,a	-0.08	-0.04	-0.16	-0.08	-0.08	-0.10	0.07	0.02	-0.04	-0.08
Tna,d	-0.02	0.03	0.00	-0.14	-0.13	-0.15	0.01	0.09	0.06	0.01
Tne	-0.11	0.08	-0.14	-0.27	-0.24	-0.27	-0.05	0.01	-0.05	-0.01

Figure 4.4. Correlation matrix between parameters and optimization's objectives.

Generally, the active muscle controllers altered the head kinematics by reducing the head peak displacements in all displacement directions except in the Optimization 3 approach (Figure 4.5). Head x-displacement in the Opt. 1, Opt. 2 and Opt. 4 approaches closely replicate the volunteer head motion until 220ms after impact. Meanwhile, Opt. 3 and the passive model had almost identical head horizontal motion. In the vertical direction, no models could fully capture the volunteer kinematics between 50-100ms after impact. The Opt. 1, Opt. 2 and Opt. 4 cases generally followed the volunteer head z-

displacement trend, but with some discrepancies in the magnitudes. Comparison of head rotational y-displacement highlighted that no model could mimic the volunteer motions after 125ms after impact although some models (Opt. 1, Opt. 2 and Opt. 4) could limit the head rotational motion.

Some of the optimization schemes did not improve the intervertebral cervical spinal kinematics correlation to volunteer data (Figure 4.6). In the period 50-100ms after impact, all models over predicted the rotational motion of the C1. After that, two models (passive and Opt. 2 models) could replicate the volunteers' kinematics until 150ms after impact. Both active and passive models could match the volunteers' C3 rotations up until 100ms after impact. When the C4 rotations were compared, the Opt. 1 and Opt.3 models could mimic the volunteer motions up until 120ms after impact. This trend was also observed for the C5 and C6 rotational displacements. All models could reasonably follow the volunteers' C7 kinematics up until 140ms after impact. After this time, most of the models could still replicate the volunteers' C7 rotational y-displacement but not the Opt.1 model (optimized for head kinematics) and Opt. 4 model (optimized for head kinematics with weighting factor of 3 and neck kinematics with weighting factor of 1).

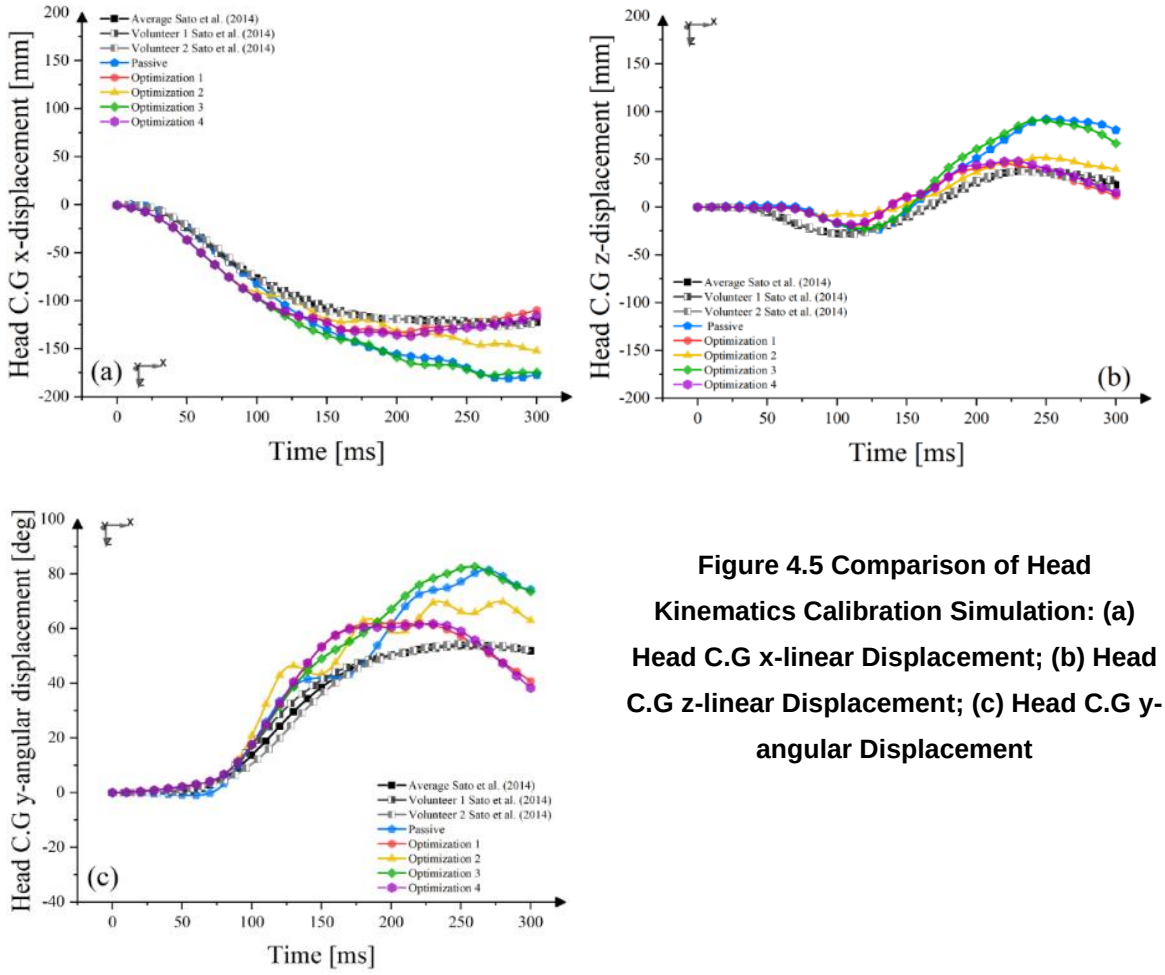

Figure 4.5 Comparison of Head Kinematics Calibration Simulation: (a) Head C.G x-linear Displacement; (b) Head C.G z-linear Displacement; (c) Head C.G y-angular Displacement

.

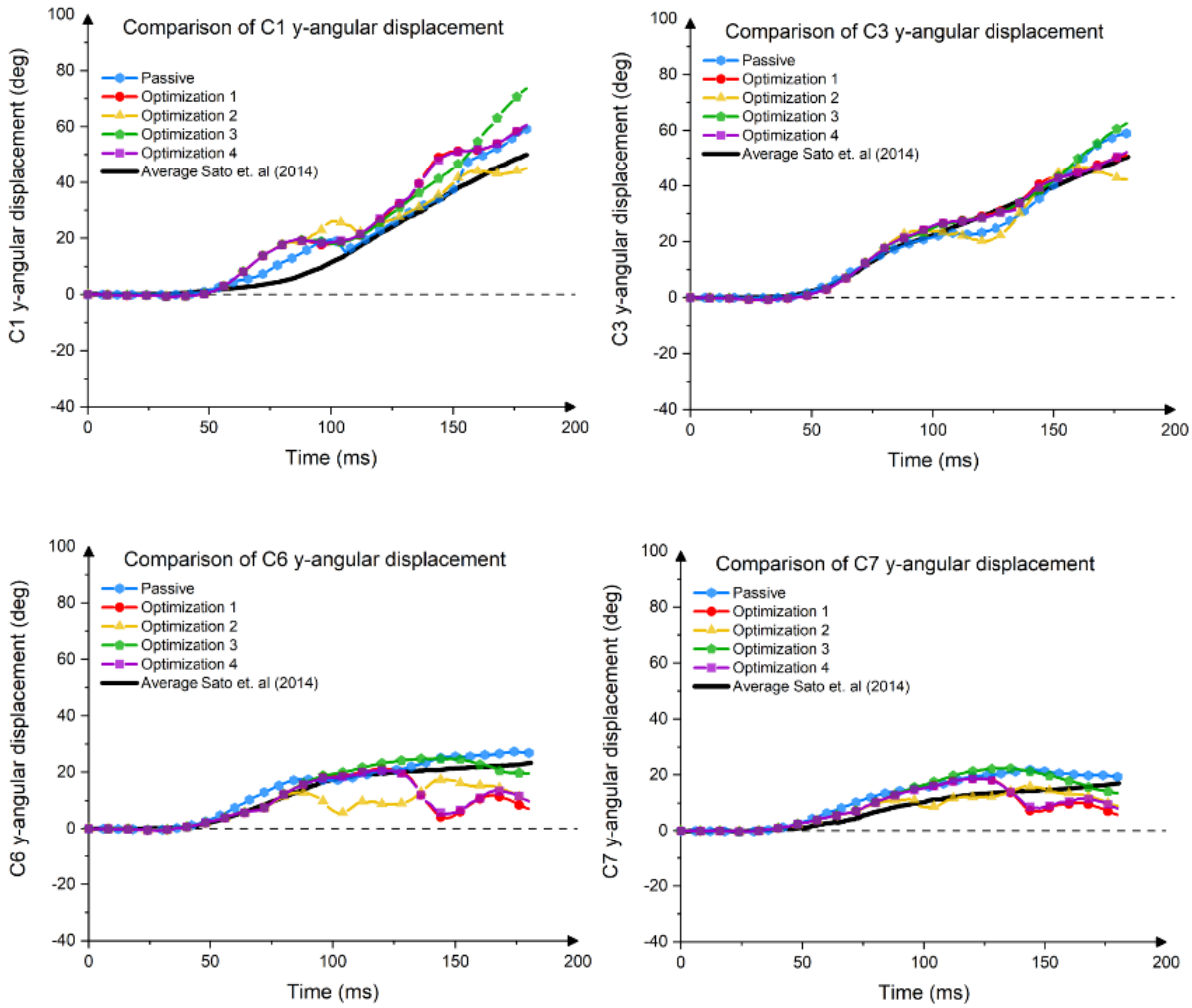

Figure 4.6. Comparison of Selected Cervical Spine Vertebral Rotational Displacement in Sled Coordinate System

4.4 Improving Head-Neck Kinematics Agreement and Evaluations of Model Best Suited for Whiplash Injury Assessment (RQ 4 - Paper D and E)

Based on co-contraction level optimization conducted in Paper D, it was found that Multifidus Cervicis, Obliqus Capitis Inferior, Rectus Capitis Lateralis (CM-C6 group) muscles had the highest co-contraction level (4.94%), meanwhile the lowest co-contraction level was assigned to Scap group (Semispinalis Capitis, Rectus Capitis Posterior Minor, Recturs Capitis Posterior Major, Obliqus Capitis Superior muscles). It was also observed that the model with optimized Co-contraction level neck muscle could maintain its posture under gravity loading after 200ms based on the head Centre of Gravity (C.G) rotational and vertical-z displacements.

4.4.1 Combination of Active Muscle Controllers (Paper D)

For head C.G x-displacements, models with only APF or MLF controllers could best follow the volunteer's head kinematics (Figure 4.7). Models with combined and distributed controllers over-predicted the displacements at 200ms (optimization reference period). Similar trends were also observed in the head vertical z-displacement. When the head C.G rotations were compared, more rebound was observed in the active models than the passive model. The model with Distributed-Control had the worst rebound performance. Figure. 4.7 also shows the comparison of cervical spine vertebral C.G rotational y-displacement. Overall, the cervical spine vertebral C.G rotations were better in the model without an active muscle controller, although oscillations were observed in C1-C5 without any muscle controller. Buckling (rapid changes in rotational velocites) was observed in C4 to C7 with all active muscle controllers except the Combined-Controller.

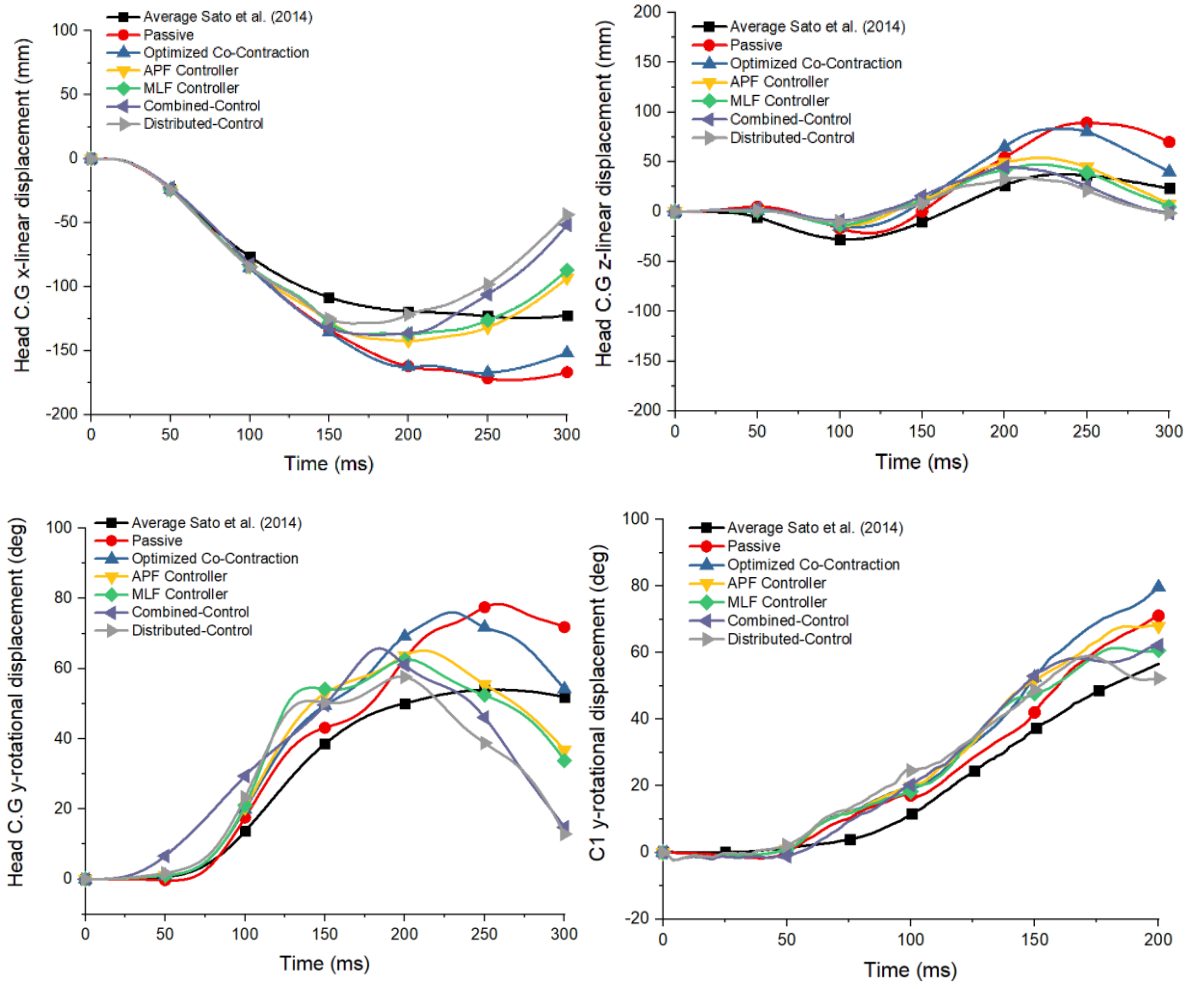

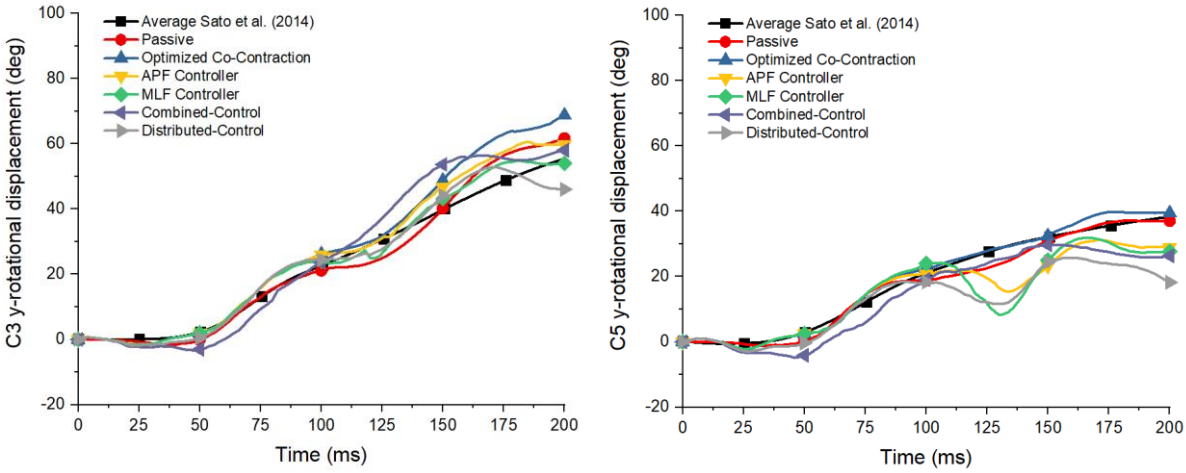

Figure. 4.7 Comparison of Head Displacements and Cervical Vertebral Rotational y-Displacement

4.4.2 Optimization of Parallel Damping Element (Paper E)

The model used as the baseline model was changed from VIVA OpenHBM to VIVA+ in Paper E. Two optimization runs using LS-OPT resulted in two sets of active muscle controller parameters (KPA, KDA, and TNDA) and parallel damping element (PDE), for the female and the male VIVA+ models (Table 4.1). Significant improvements of the model agreement to volunteer data from Sato et al., (2014) 5.8km/h were obtained in the Active Female VIVA+ model compared to the original passive Female VIVA+ model (Figure 4.8). The VIVA+ model with active muscle controllers also removed the oscillations observed in the original model, significantly improving the predicted cervical rotations compared to the volunteers. However, in the C1 C.G rotations, the active female model rotated more than the volunteer responses. The C3 to C7 rotations were underpredicted by the active model.

Table 4.1 Active Muscle Controller Parameter based on Optimization

Model	**Parameter**			
	Proportional gain / KPA (%contraction/rad)	Derivative gain / KDA (%contraction/rad ms^{-1})	Neural transmission and processing delay / TNDA (ms)	Parallel Damping Coefficient / PDE (kN.ms/mm^2)
Active VIVA+ Female	0.19	34.09	4.23	0.03
Active VIVA+ Male	0.01	93.48	19.66	0.02

The male version of the model exhibited similar characteristics as the female – the optimized controller produced almost identical responses for both head C.G. and cervical spine C.G. kinematics (Figure A3), better than the passive model. The Active VIVA+ male model also reduced the cervical vertebral

rotations, especially after 150ms, improving the overall cervical spine rotations when the responses were compared with volunteers. The original VIVA+ model was slightly better at mimicking the volunteers' rotational displacements of C1 and C4 than the active models.

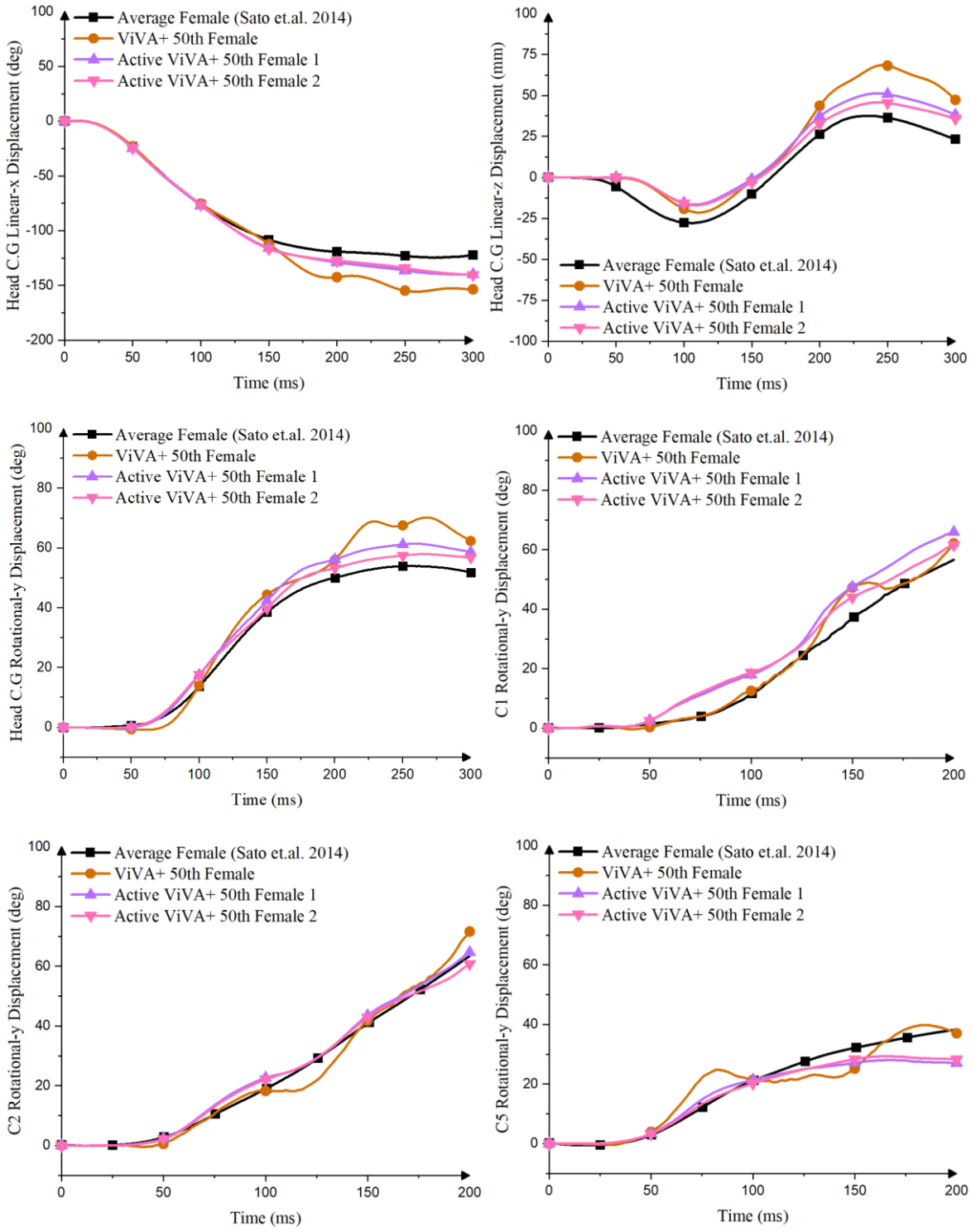

Figure. 4.8 Comparison of Head C.G and Cervical Vertebra C.G linear and rotational displacements between Original VIVA+ Female Model, Active Female VIVA+ Models and Volunteer Kinematics from Sato et al., (2014) 5.8km/h

To objectively compare the different types of models' formulations, Table 4.2 shows the CORA scores for all displacement data. For the female and male models, the Active VIVA+ Female and Male models had the highest total average scores of 0.869 and 0.824, respectively.

Table 4.2 CORA Score of Head and Cervical Spine Kinematics of Active VIVA+ Models

Kinematics	**VIVA+ Head-Neck Female Model**		**VIVA+ Head-Neck Male Model**	
	VIVA+ 50th Female	**Active VIVA+ 50th Female**	**VIVA+ 50th Male**	**Active VIVA+ 50th Male**
Average HCG	0.72	0.85	0.78	0.83
Average Cervical Spine	0.87	0.89	0.81	0.82
Total Average	**0.79**	**0.87***	**0.79**	**0.82***

Both active models also replicated the S-shaped cervical spine when the differences between two adjacent vertebras in extension and flexion were greatest and occurred approximately 75 to 100ms after the impact started (Figure 4.9).

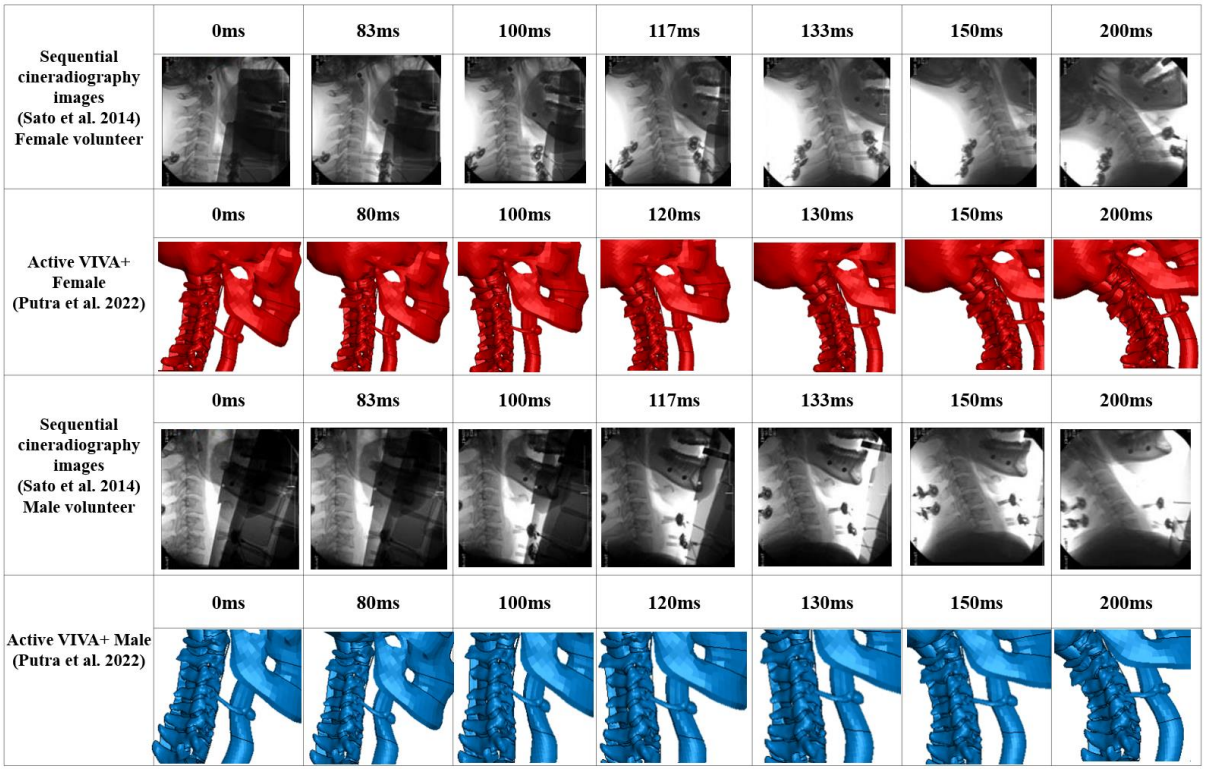

Figure 4.9. Neck kinematics comparison between active models (reported in Paper E) and volunteer neck kinematics from Sato et al., (2014).

4.4.3 Parametric Study of Active Neck Muscle Controller Configuration (Paper E)

Parametric simulations based on Table 4.3 were conducted to study different configurations of active neck muscle controllers and neck muscle properties for both female and male models. The head-neck kinematics of all models were affected by the parallel damping elements (PDE). Four models without PDE (Passive, PSV+CCo, PSV+APF, and PSV+CCo+APF) produced noticeably higher head displacements compared to the models with PDE. More pronounced differences were observed in vertebral rotations. Oscillations in the cervical spine occurred in the four models without PDE. However, the oscillations were significantly reduced in the four models with PDE.

CORA scores of female models with various complexities are presented in Tables 4.4. When the average CORA scores of head kinematics and cervical vertebral kinematics were averaged in the female model, the four models with the highest scores were the models with PDE. The highest average scores were obtained by the PSV+PDE+APF. For the male models the best configurations were the PSV+PDE, followed by the PSV+PDE+APF. Refer to paper E for the CORA scores of male models.

Table 4.3 Parametric Simulations to Reduce Model Configuration

Name of Simulation	Co-Contraction	Parallel Damping Element	APF Controller	Notes
PSV+PDE+CCo+APF	yes	yes	yes	The same model as in previous step
PSV+PDE+APF	no	yes	yes	
PSV+CCo+APF	yes	no	yes	
PSV+CCo+PDE	yes	yes	no	
PSV+APF	no	no	yes	
PSV+PDE	no	yes	no	
PSV+CCo	yes	no	no	
Passive	no	no	no	Original model

Table 4.4. CORA Score of Female Head-Neck Model with Various Complexities

Kinematics	PSV	PSV+ CCo	PSV+ PDE	PSV+ APF	PSV+ CCo+ PDE	PSV+ CCo+ APF	PSV+ PDE+ APF	PSV+ CCo+ PDE+ APF
HCG-x	0.83	0.79	0.96	0.87	0.88	0.83	0.99	0.94
HCG-z	0.52	0.43	0.81	0.51	0.58	0.43	0.80	0.64
HCG-ry	0.82	0.73	0.99	0.82	0.93	0.73	0.99	0.96
Average HCG	**0.72**	**0.65**	**0.92**	**0.73**	**0.79**	**0.66**	**0.93**	**0.85**
C1-ry	0.94	0.79	0.95	0.92	0.90	0.78	0.97	0.88
C2-ry	0.97	0.85	0.94	0.98	0.99	0.86	0.92	0.99
C3-ry	0.94	0.88	0.87	0.93	0.98	0.91	0.85	0.94
C4-ry	0.90	0.92	0.85	0.86	0.94	0.90	0.82	0.88
C5-ry	0.88	0.90	0.90	0.82	0.96	0.83	0.85	0.89
C6-ry	0.78	0.80	0.91	0.78	0.85	0.82	0.97	0.91
C7 -ry	0.70	0.69	0.69	0.75	0.69	0.75	0.70	0.71
Average Cervical Spine	**0.87**	**0.83**	**0.87**	**0.86**	**0.90**	**0.84**	**0.87**	**0.89**
Total Average	**0.80**	**0.74**	**0.89****	**0.80**	**0.85******	**0.75**	**0.90***	**0.87*****

4.4.4 Evaluations of Model Best Suited for Whiplash Injury Assessment (Paper E)

Evaluation in Head-Neck Model

Comparison of head C.G x-acceleration and cervical spine rotational y-velocity were conducted to evaluate the performance of VIVA+ models for quantifying WAD criteria (NIC and Pressure transient in vertebral canal) (Figure 4.10 and 4.11). Four models with parallel damping elements had similar responses. Reasonable agreement can be observed for three different test severities.

A comparison of cervical vertebral rotational velocities (Figure 4.11) revealed high gradients in the angular velocities in the VIVA+ female models C1, C2, and C3 than in the volunteers. However, in the lower cervical spine (C4-C7), the VIVA+ rotational velocities response better follow the results in Sato et al., (2014) 5.8 km/h. No significant differences between the four different models were observed.

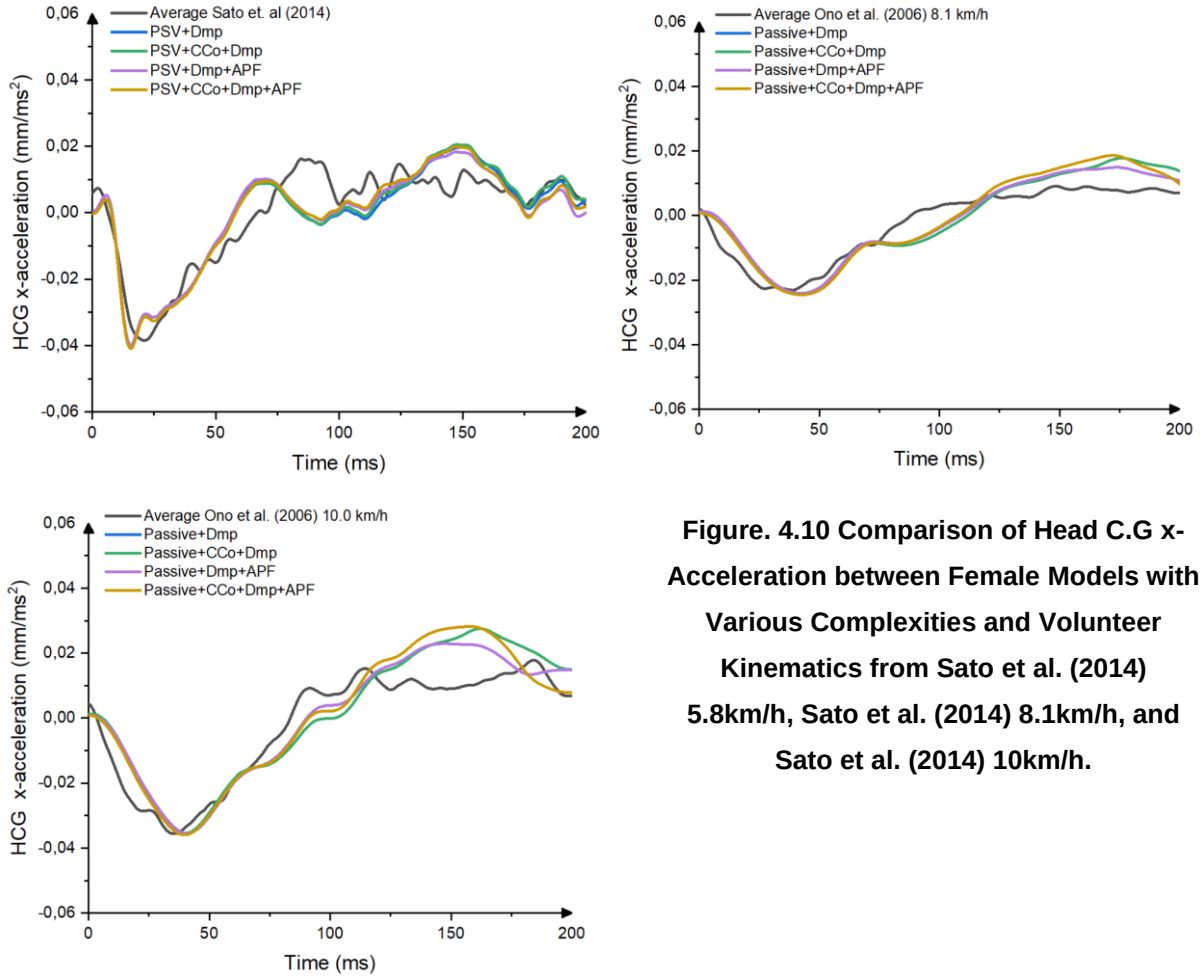

Figure. 4.10 Comparison of Head C.G x-Acceleration between Female Models with Various Complexities and Volunteer Kinematics from Sato et al. (2014) 5.8km/h, Sato et al. (2014) 8.1km/h, and Sato et al. (2014) 10km/h.

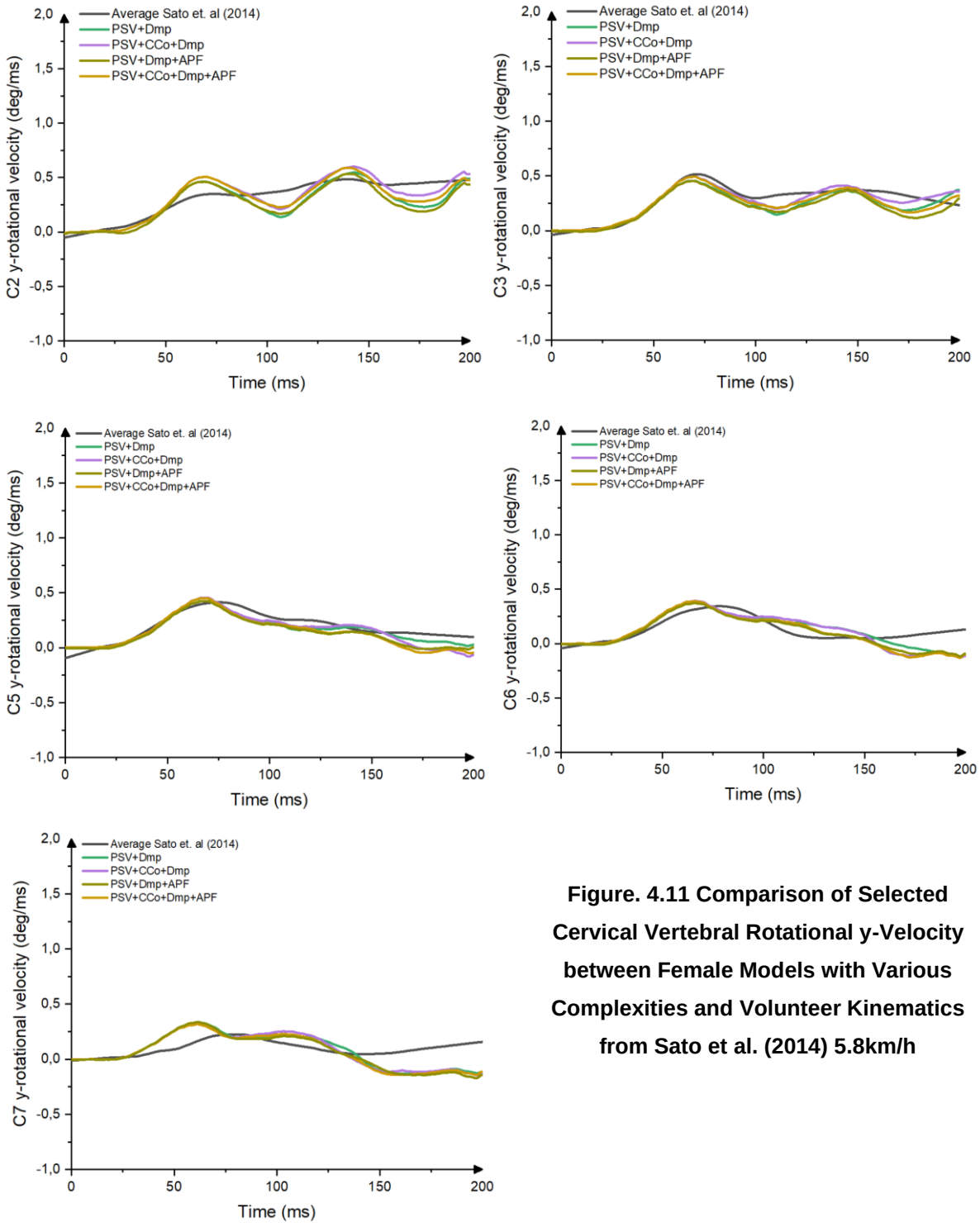

Figure. 4.11 Comparison of Selected Cervical Vertebral Rotational y-Velocity between Female Models with Various Complexities and Volunteer Kinematics from Sato et al. (2014) 5.8km/h

CORA scores evaluation showed similar results between female and male models when the models' head C.G x-acceleration and cervical vertebral rotational y-velocities were compared to the volunteer responses (Paper E). In both models, the closest model that replicates the volunteers was the model with parallel damping element and APF controller (PSV+PDE+APF). However, the exact CORA scores

itself was slightly different between the female and male model, with the female and male model obtaining CORA score of 0.667 and 0.653, respectively. Note that the CORA score of males were lower than females in the earlier comparison of the head-neck displacements.

Evaluation in Full-Body Model

No notable differences between the models with PDE+APF and PDE+CCo+APF were observed in female and male VIVA+ full-body head and neck responses, only a slight offset in magnitudes (Paper E). It was observed that the VIVA+ model with PDE+APF controller best matched volunteer kinematics. The models' head C.G x-acceleration followed the volunteers' acceleration closely. In comparison, the model T1 C.G x-acceleration lagged behind the volunteers' T1 acceleration. Comparison of cervical spine rotational velocities showed that the model followed the reference's velocities profiles but did not fully match their peaks.

Objective rating evaluation using CORA (Table 4.5) showed that female and male VIVA+ full-body models had different scores when the models were compared with Sato et al., (2014) 5.8 km/h volunteer data. The best model based on the CORA score was achieved by the PSV+PDE+APF model for the female VIVA+ model. However, the best agreement with volunteers' kinematics for the male VIVA+ model was the PSV+CCo+PDE+APF model. The difference between this model and the PSV+PDE+APF model was not as pronounced as in the female VIVA+ models.

Table 4.5 CORA Score of Female and Male Full-Body Model with Various Configurations and Sato et al., (2014) 5.8km/h

Kinematics	**VIVA+ Female Full-Body Model**		**VIVA+ Male Full-Body Model**	
	PSV+PDE +APF	**PSV+CCo+ PDE+APF**	**PSV+PDE +APF**	**PSV+CCo+ PDE+APF**
HCG x-acceleration	**0.75**	**0.66**	**0.73**	**0.76**
C1-ry velocity	0.77	0.76	0.79	0.78
C2-ry velocity	0.63	0.63	0.77	0.80
C3-ry velocity	0.76	0.74	0.66	0.69
C4-ry velocity	0.73	0.65	0.67	0.67
C5-ry velocity	0.69	0.61	0.74	0.73
C6-ry velocity	0.67	0.68	0.75	0.81
C7-ry velocity	0.46	0.48	0.64	0.67
Average Cervical Spine	**0.67**	**0.65**	**0.72**	**0.74**
T1-x acceleration	0.52	0.50	0.57	0.56
Total Average	**0.65***	**0.60**	**0.67**	**0.69***

Furthermore, analyzing the muscle forces of the relevant muscle groups, such as SCM and STH, revealed that the main contributor to total muscle forces produced by these muscle groups came from

the active forces. The viscous force generated from the PDE produced significantly lower forces than the muscle forces produced by the CE or active element (Figure 4.12).

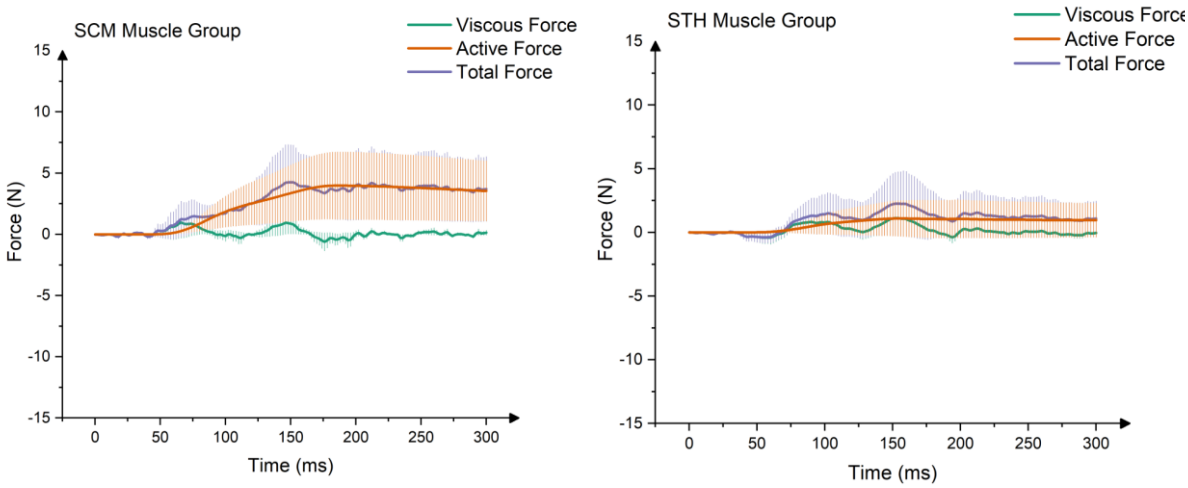

Sternocleidomastoid (SCM), Scalenus Posterior, Scalenus Medius, Scalenus Anterior,Rectus Capitis Anterior

Sternohyoid (STH), Sternothyroid, Omohyoid, Longus Colli Superior Oblique, LongusColli Vertical, Longus Colli Inferior Oblique, Longus Capitis

Figure 4.12. Muscle forces comparison (Viscous force, Active force and Total force) of SCM muscle group and STH muscle group from VIVA+ female model with APF controller and PDE.

4.5 Influences of Neck Muscle Responses to the Head-Neck Kinematics, Spinal Canal Pressure Transients and Global Kinematics Based-Injury Criteria (RQ 5 – Paper F)

4.5.1 Comparison between Female Models with and without Active Neck Muscle Responses

A comparison between a model with and without neck active muscle responses was conducted in accident reconstruction simulations based on real-world accident pulses. Neck muscle activity only slightly reduced the peak head rotations (Figure 4.13). The differences between female VIVA+ models with and without neck muscles were more pronounced in the rebound phase. The rebound phase happened after the last contact between head and headrest (starting at 142ms).

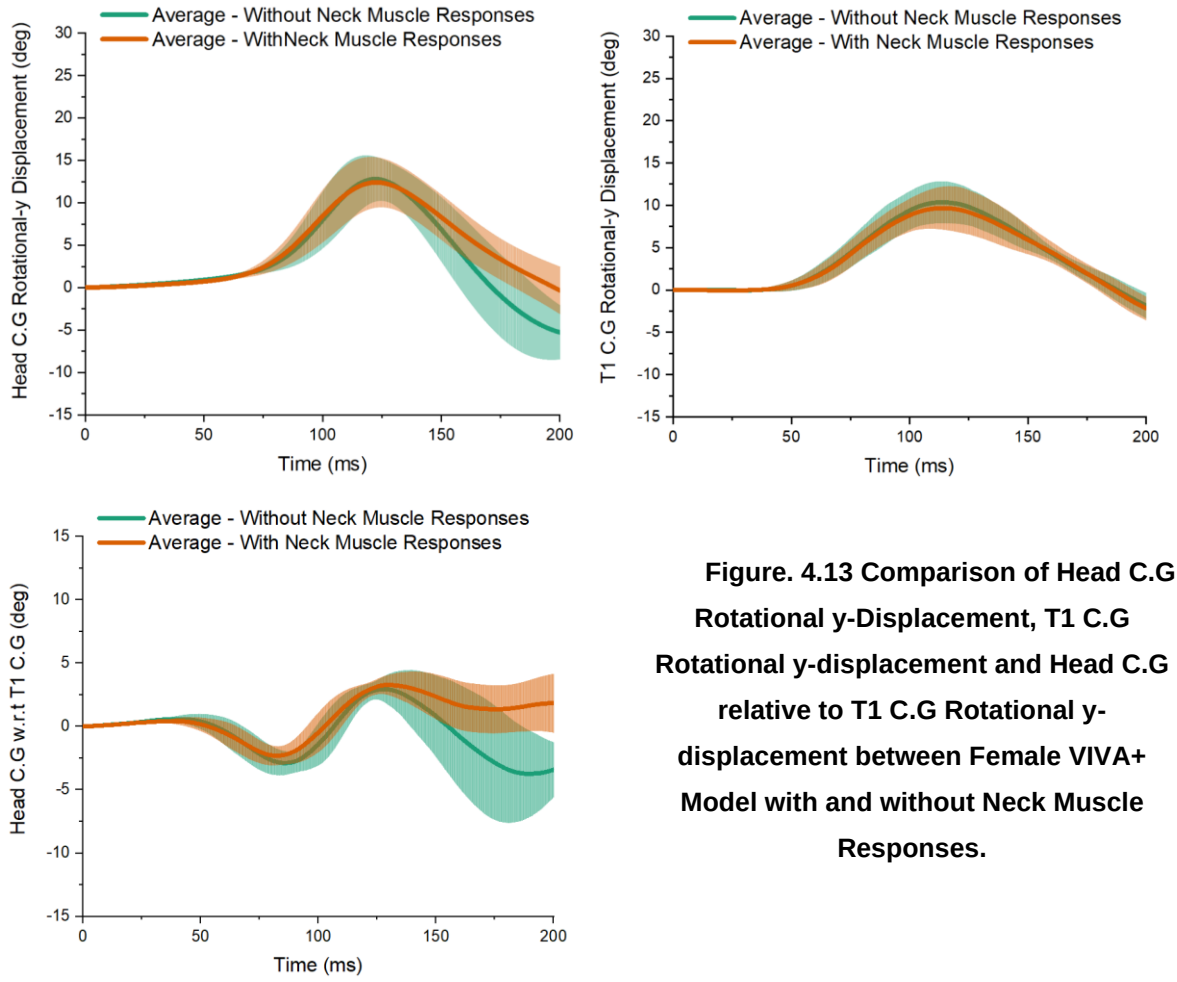

Figure. 4.13 Comparison of Head C.G Rotational y-Displacement, T1 C.G Rotational y-displacement and Head C.G relative to T1 C.G Rotational y-displacement between Female VIVA+ Model with and without Neck Muscle Responses.

Almost identical head C.G horizontal acceleration responses were observed for the model with and without neck muscle activity. The average maximum head horizontal acceleration was only slightly reduced, from 121.14 m/s^2 to 116.67 m/s^2. The maximum head C.G horizontal acceleration was statistically different between the model with and without neck muscle responses, however not for the maximum motions to T1 (P=0.12 and P=0.16 respectively).

More pronounced relative rotations in the model without neck muscle activity were observed when the cervical spine rotations relative to T1 rotations were compared (Figure 4.14). The differences between the two models were more notable in the lower cervical spine (C4 to C7). The maximum relative rotations were also reduced when neck muscle responses were added to the model, with the lowest reduction observed in the C2-T1 rotations (0.31 degrees) and the highest reduction found in the C6-T1 (4.79 degrees).

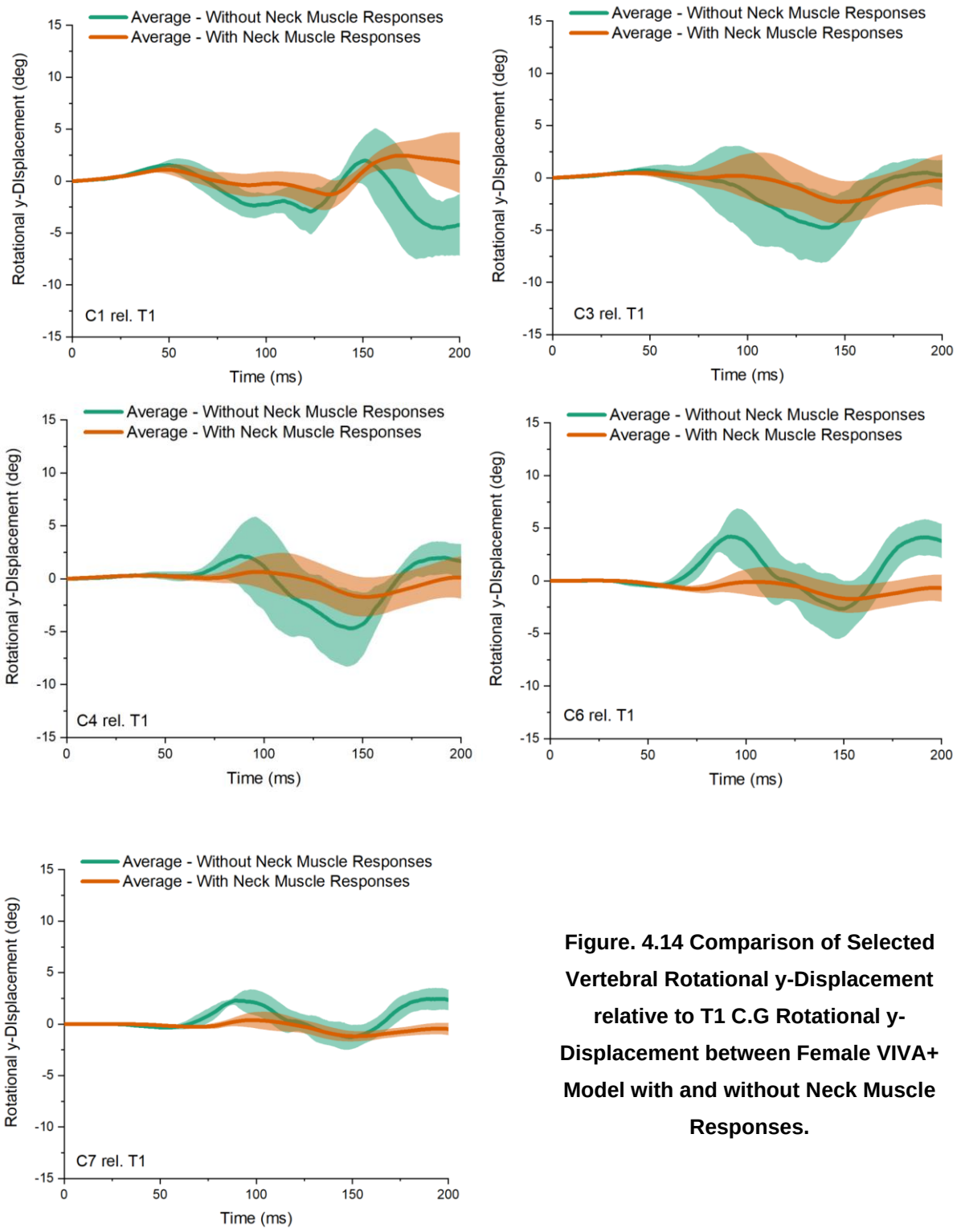

Figure. 4.14 Comparison of Selected Vertebral Rotational y-Displacement relative to T1 C.G Rotational y-Displacement between Female VIVA+ Model with and without Neck Muscle Responses.

Significant differences in pressure magnitude and pressure profile were seen when the pressure transient in the spinal canal was compared between the model with and without neck muscle responses. The average negative pressure in the first canal was equal to -1704.04 Pa when no muscle responses were included in the model. However, when the neck muscle responses were added, the negative pressure was equal to -319.30 Pa. A similar trend was observed throughout all canals, with the highest differences observed in canal 6.

The maximum NIC (NIC Max) occurred almost at the same time between models with and without neck muscle responses. The average value of the NIC Max was equal to 7.86 m^2/s^2 for the model without neck muscle responses and was equal to 7.24 m^2/s^2 when the neck muscle responses were added to the VIVA+ female model (Figure 4.13). For reference a NIC value of 15 m^2/s^2 is usually used as the injury threshold value.

The average initial head-to-head restraint contact was 71ms, with the earliest initial contact at 59ms and the latest contact equal to 81ms in the passive model. With active neck muscles, the average value was reduced slightly to 70.67ms, although the maximum time for the head to headrest contact remained the same. Neck muscle responses only slightly reduced the head contact duration with the head restraint (0.78ms).

4.5.2 Comparison of Female Models with Active Muscle Responses between Injured and Uninjured Occupants

The average responses between injured and uninjured cases in the model with active neck muscle responses were further evaluated using accident reconstructions. The average maximum head rotations were slightly higher in the uninjured cases (13.16 degrees) compared to the injured cases (11.56 degrees). A similar trend was observed in the average maximum T1 rotations (10.06 degrees for the injured cases and 9.24 for the uninjured cases). When the head to T1 relative rotations were compared, the injured cases had higher maximum rotations than the uninjured ones (3.72 and 3.64 degrees, respectively). In addition, higher average maximum head, T1, and head relative to T1 horizontal x-acceleration were seen in the injured cases compared to the uninjured cases. In the injured cases, the maximum head, T1 and head relative to T1 horizontal x-accelerations were122 m/s^2, 93 m/s^2, and 37 m/s^2, respectively. For the uninjured cases, the values were 144.0 m/s^2, 86 m/s^2, and 34 m/s^2 for the head horizontal x-acceleration, T1 horizontal x-acceleration and the head relative to T1 x-acceleration.

Comparison of cervical spine C.G rotations relative to T1 C.G rotations showed that, on average, the uninjured cases produced higher maximum rotations than the injured cases except for the C1 relative to the T1, where the injured cases had higher maximum rotation. A similar trend was also observed when the average of minimum rotations between two groups was compared (injured and uninjured cases). Except for the C1-T1 level, the injured cases had more negative rotations than the uninjured ones. Different kinematics trends were observed when two adjacent vertebras' rotations were compared between injured and uninjured cases. The average of maximum rotations was higher in the injured cases for the C1-C2 and C2-C3 than in the uninjured cases. However, it was lower in the C3-C4 to C6-C7.
A consistent trend was observed when the pressure transients in the spinal canal were compared between the injured and uninjured cases when neck muscle activity was included (Figure 4.15). The average negative pressures from 0 to 100ms were always higher for the injured crash pulses (Table 4.6). For example, the average negative pressure in the first Canal was about 100 Pa lower for the injured cases, about 1/3 lower than the uninjured cases. The greatest difference between the two groups was seen in Canal 5 and the lowest difference was observed in Canal 8.

Table 4.6 Comparison of Negative Pressure during 0-100ms between Injured and Uninjured Cases

Canal	Injured – Average of Negative Pressure (Pa)	Uninjured – Average of Negative Pressure (Pa)	Average Pressure Difference (Pa)	P-values from t-test
1	-383,5	-287,2	-96,2	0.17
2	-1055,7	-757,7	-298,0	0.01
3	-1219,2	-902,1	-317,1	0.07
4	-1517,6	-1024,6	-493,0	0.09
5	-1689,4	-1066,7	-622,7	0.05
6	-1698,4	-1163,1	-535,3	0.03
7	-1275,3	-993,0	-282,3	0.02
8	-359,6	-286,0	-73,6	0.02

The model with the injured pulses had later peak than the uninjured pulses. The average of NIC max was higher in the injured cases (7.66 m^2/s^2) compared to the uninjured cases (7.03 m^2/s^2) (Figure 4.16).

On average head-to-head restraint contact and shorter contact durations were calculated when the injured pulses were used as input to the model. The average initial contact between head to head restraint was equal to 72ms and 70ms for the injured and uninjured cases. In addition, the average head-to-head restraint contact duration was equal to 75ms for the injured pulses and 80ms for the uninjured pulses, respectively.

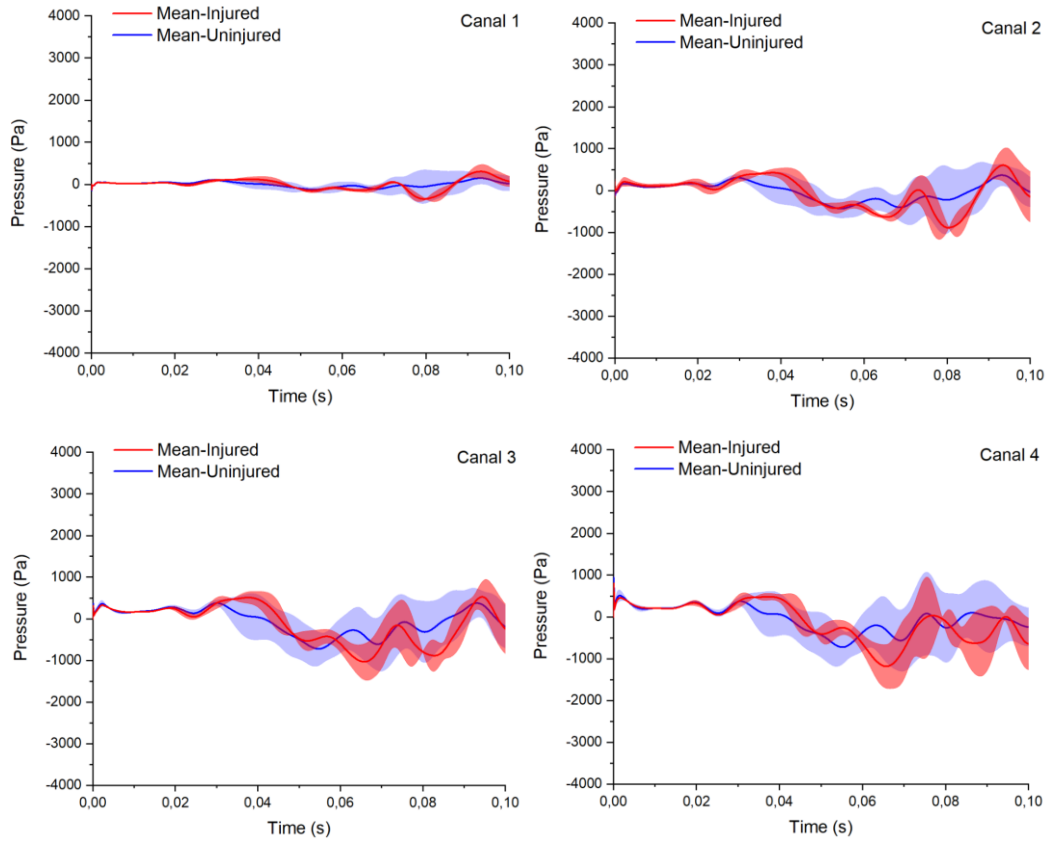

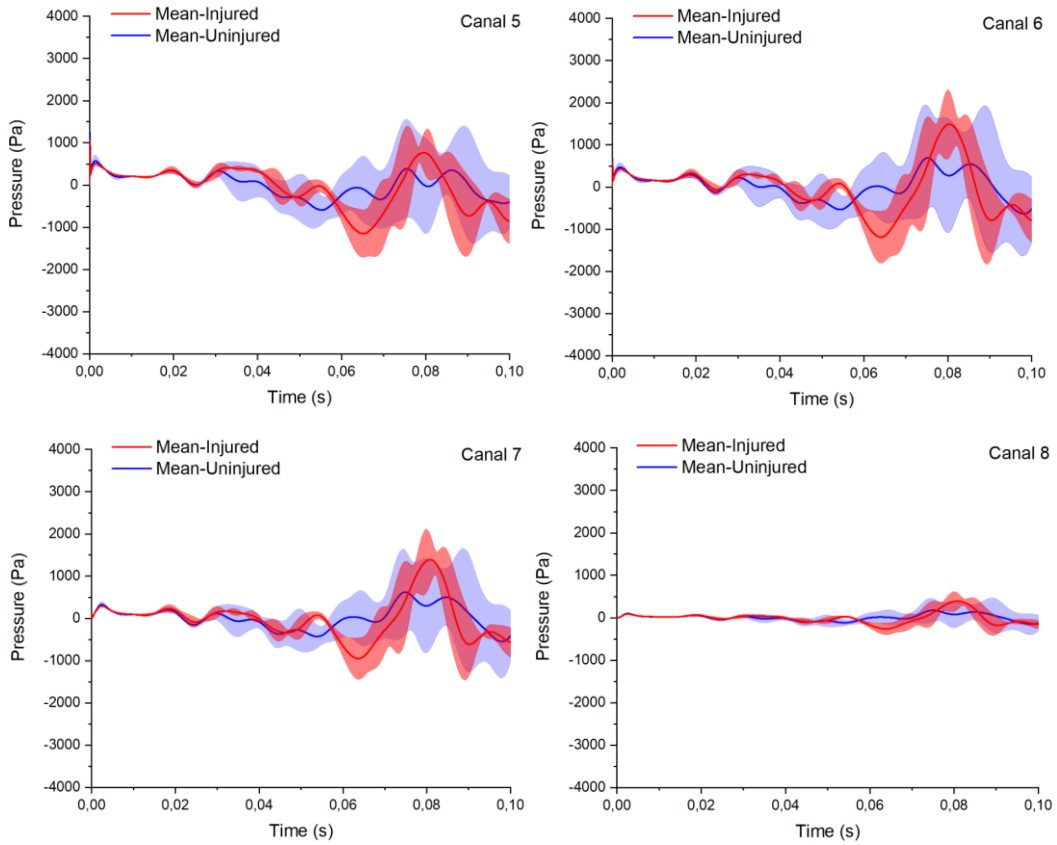

Figure. 4.15 Comparison of the Pressure Transient at the Spinal Canal (Canal 1 to Canal 8) between Uninjured and Injured Female VIVA+ Model with Neck Muscle Responses.

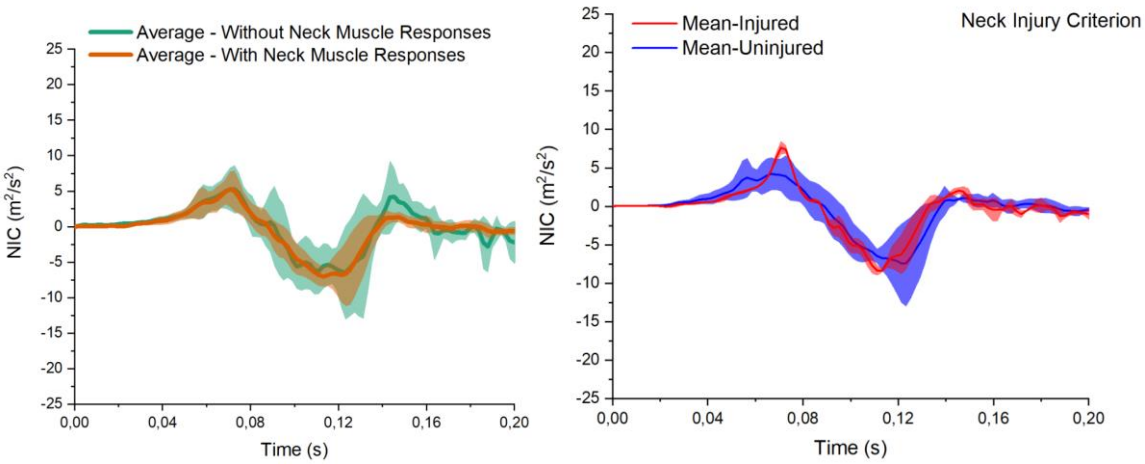

Figure. 4.16 Comparison of the Neck Injury Criteria (NIC) between Female VIVA+ Model with and without Neck Muscle Responses (a) and between Uninjured and Injured of Female VIVA+ Model with Neck Muscle Responses (b).

Chapter 5 Discussion

Previous studies using human volunteers have documented the influence of neck muscle activity on head-neck kinematics during low-speed rear-impact volunteer tests (Brault et al., 2000, Siegmund et al., 2003, Blouin et al., 2006, Dehner et al., 2013, Mang et al., 2015). The human reflex mechanism triggers muscle activity in the neck during a rear impact (summarized by Siegmund, G.P. 2011). Even though human feedback and reflex mechanism are not completely understood, it has been highlighted that two reflex mechanisms called the VCR and the CCR are integral to maintaining head orientation (Armstrong et al., 2008., Cullen and Goldberg, 2014., Cullen, K.E., 2012. Keshner, E.A., 2003). Therefore, active muscle modeling in HBMs should address the behavior of these reflex mechanisms. To answer this challenge, reflex mechanisms were investigated in the present thesis based on the neck muscle responses in low-speed rear-impacts. Hence, the present thesis contributes to the state of the art for modeling reflex mechanisms in whiplash-type motion and their influence on head-neck kinematics. This knowledge will also help future research on potential whiplash injury mechanisms.

The ultimate goal of the present research is to model neck muscle responses in low-speed rear-end impacts. This would enhance a whole-body, female Finite Element (FE) Human Body Model (HBM) for the head-neck kinematics and WAD analysis. Female FE HBMs have been specifically used as the focus of the present thesis because females have a higher risk of sustaining WAD than males (Carlsson A., 2012). Furthermore, female FE HBMs have been specifically used as the focus of the present thesis because of the lack of female FE HBMs and, in particular, active neck muscle activity. By developing the FE HBM with neck muscle responses, the dynamic responses and injury outcomes for females can be studied with improved confidence. Besides enhancing the female model to include active reflexive neck muscle responses, a muscle controller was also added to the male counterpart of VIVA+ female HBM. This allows for a more direct comparison between female and male for future analysis. Consequently, this could provide clues to solve the enigma of the whiplash injury mechanism and acute injury site.

The thesis addresses five research questions and consists of six papers (studies) and. It was arranged to systematically address the main objective. Two human body models called the VIVA OpenHBM (Östh et al., 2017a, 2017b) and VIVA+ HBM John et al., (2022a; 2022b) were used. The VIVA OpenHBM represents the 50th percentile female population and the two sizes of the VIVA+ HBM represent the 50th percentile female and male populations.

Development activities to model neck muscle responses in a FE HBM could be very expensive in terms of computational costs. Therefore, an isolated head-neck FE model was used extensively throughout this thesis to reduce the computational cost. This allowed more rapid optimization iterations which were needed to define both passive and active characteristics of human neck muscle responses during low speed rear-end impact. However, before using the isolated head-neck model, an investigation was conducted to ensure that the isolated model could replicate the head-neck kinematics from the full-body

model with sufficient accuracy. The first study in this thesis (Paper A) was designed to address this objective.

The results from Paper A revealed that the head-neck model could replicate the head-neck kinematics of the full-body model for the duration of motions when WAD are proposed to occur. Currently, most of the WAD hypotheses suggest that WAD are more likely to occur during the retraction phase or in the first 150ms after impact (Svensson et al., 1993, Grauer et al., 1997, Ono et al., 1997, Yoganandan et al., 2002, Ono et al., 2006). Therefore, by connecting the current whiplash injury hypotheses and the results from Paper A, it was determined that the isolated head-neck model could be used to calibrate the active muscle controller parameters. Running an isolated head-neck model under similar loading conditions to the full-human body model reduced computational time by almost 75%. This allows for extensive optimization and parameter studies that can be used to define active neck muscle parameters.

The differences observed between the isolated head-neck model and full-body model after the primary period of interest for WAD were likely caused by the boundary conditions defined for the head-neck model. These were constraints for the neck skin, lower neck soft tissues and neck muscles. Specifically, the origins of neck muscles were constrained to move rigidly with the T1. While, the lower part of the neck skin and soft tissues were partially constrained to move with T1 (refer to Paper A, Figure 4). The assumption of constraining the origin of neck muscles to move with the T1 might not capture the interactions of neck muscles with other structures in the upper body such as upper rib cage and the shoulder. If identical head-neck kinematics between isolated head-neck and full-body models are needed for the entire duration of the impact, future studies should investigate the assumptions of these boundary conditions. Boundary conditions showed in Correia et al. (2021), where the muscle attachment points to the upper thorax were represented, could be adapted. Nevertheless, the head and cervical spine kinematics of the isolated head neck model produced similar kinematics to the full-body model. Therefore, the isolated head-neck model was an efficient approach for developing an active HBM with neck muscle responses.

The studies described in Papers B, C, D, and E focused on how to model neck muscle responses to study WAD in low-speed rear impacts. The main goal was to develop a simple and robust representation of human neck muscle responses during low speed rear-end impact, not an exact duplicate of the human reflex system that cannot be fully validated due to the lack of validation data. Availability of published volunteer data to be used to validate the neck muscle responses motivated the main goal.

To begin the development of a model with neck muscle responses, a strategy to control neck muscles using a simulated reflex feedback loop was needed. An angle-based muscle controller (APF controller) representing the VCR reflex and a displacement-based muscle controller (MLF controller) capturing the CCR reflex were implemented and optimized (Paper B). The APF controller demonstrated better performance in low-speed rear-impacts as it could simulate the head C.G displacement time histories better than the MLF controller. A drawback of the APF controller was buckling in the model's cervical spine (Paper B, Figure A1), which resulted in a poor agreement of vertebral rotations with the volunteers. The MLF controller could limit the APF controller's pulling force to an expected biomechanical range

and, consequently, prevents nonphysical motions. Happee et al., (2017) and Olafsdottir et al., (2017) studied muscle length feedback control that could reduce cervical spine buckling. However, their models were evaluated with a lower delta velocity than Sato et al., (2014).

In Paper C, optimization methods used to derive muscle controller parameters were explored. Cervical spine vertebral rotations from volunteer responses were added as optimization objectives in addition to global head kinematics. The addition of cervical spine kinematics as performance objectives in optimization is novel since no previous studies were found to consider these when deriving parameters for active neck muscle controllers. This study found that the method of approximating the VCR reflex by sampling a vector between the head C.G and the T1 center of the vertebral body was robust and could detect the changes in head motion well. When the cervical spine kinematics were added as the optimization objective, much less cervical spine buckling was found than in the previous active model (Paper B). An extended version of the implemented APF controller can be created by adding additional position vectors to better capture the neck kinematics (representing the neck as a multi-link system instead of a single link). However, as the complexity of the model increases, more data are needed to optimize and validate the controller's parameters.

Based on the results of Paper C, optimization-based parameter identifications were conducted extensively in the subsequent studies (Paper D and E). As discussed previously, the head-neck kinematics of the full-body model could best replicate the volunteer head-neck motions during the proposed period of interest for whiplash injury motions, not the entire impact event. The proposed optimization setup can be used and improved for future studies. Furthermore, more optimization iterations and more studies can be conducted by reducing computational costs when running optimization simulations to derive active muscle controller parameters.

The initial cervical spine alignment of the model in Paper C was adjusted to represent the average cervical spine alignment based on female volunteers (Sato et al., 2016). The new cervical spine alignment was more kyphotic than the original VIVA Model, which was more straight. The updated passive model demonstrated better agreement (in particular head C.G vertical displacement) with reference data. This result indicates that the cervical spine alignment is vital to get fully biofidelic head and neck kinematics and is an important issue when differences in male and female responses are studied. Unfortunately, adjusting spinal alignment required extensive volunteer data that are not publicly available. Also, the seat properties highly influence the cervical spine alignment; therefore, only cervical spine alignment measured for boundary conditions similar to Sato et al., (2014) were used.

Combining the APF and MLF controllers to improve the head-neck responses was investigated in Paper D. This was studied using the optimization objective functions and adjusted cervical spine alignment results from Paper C. Combining APF and MLF controllers using the combined-control or distributed approach presented in Paper D (Section 2.4 and 3.3), could not improve the head and neck kinematics agreement, at least as implemented. When the activation signals of each controller were compared (Paper D), the combined control always had the highest magnitude and was active earlier than other

strategies. This high magnitude could be due to the fact that combining two different controllers maybe unsuitable with a minimum and maximum function.

The simplified methods to combine the APF and MLF controllers can be considered pragmatic approaches. Several studies have implemented and combined VCR-like and CCR-like controllers under various loading conditions (Ólafsdóttir et al., 2019b, Kleinbach 2019, Correia et al., 2021, Larsson et al., 2019). Ólafsdóttir et al., (2019b), (Kleinbach 2019), and Larsson et al., (2019) assumed simple addition of the VCR-like and CCR-like controllers meanwhile (Correia et al., 2021) assumed a limited combination between VCR-like and CCR-like controller using the IF function. The present study did not include a simple APF and MLF controller summation because simple addition could request muscle forces exceeding biomechanical limits.

The CCR-like controller was found to request 100% of the muscle forces (Paper D, Supplementary Material). These differences might be due to controller-specific behavior, which is the case for most existing muscle control strategies. Each specific muscle controller may have multiple admissible solutions to achieve a target. However, no experimental studies using animals or normal human subjects reported full activation of CCR alone without any contribution from VCR.

Correia et al., (2021) used the "IF" function to activate the VCR-like controller if the head rotates more than 5 degrees, based on decerebrated cats' experiments (Peterson et al., 1985). However, it is unclear which degree of head rotation the VCR reflex is active for the human head. Therefore, the VCR-like controller was kept active during the whole duration of the simulation based on the well-known function of the VCR reflex itself, which is to maintain and stabilize head motion in space. Furthermore, an experimental study by Forbes et al., (2014) showed that VCR in the neck muscle is active even during conditions where there is no requirement to balance the head. Small VCR activity was also observed during neck muscle co-contraction relative to isometric neck muscle contractions. This probably can be seen as an indication that the VCR reflex is always active in humans despite the fact that it might be in a very small magnitude. Nevertheless, it is essential to remember that the actual parameters when the VCR-like controller is active may vary and will likely have some degree of model specificity. For future studies, it would be interesting to understand the sensitivity of models to variations of different VCR-like controller activities. This study would be important to be conducted as long as it is specified within known physiological limits and the models' assumptions.

Another important difference between the present study and previous studies (Ólafsdóttir et al., 2019b, Kleinbach 2019, Correia et al., 2021, Larsson et al., 2019) was that previous studies did not conduct any evaluations of intervertebral rotations of the cervical spine or use the intervertebral rotations as objectives in the optimization process to derive controller gains. The correct prediction of intervertebral rotation in the cervical spine is vital if a model will be used to study head-neck kinematics in whiplash-type motions.

Another hypothesis why the combined model implementations had no notable improvements over a single active controller could be due to the limitations of the current Hill muscle implementation in LS-

DYNA itself. As described in Kleinbach et al., (2017), the current implementation of LS-DYNA Hill muscle only includes a parallel damping element and neglects serial elastic and serial damping elements representing tendon structures.

Although the combination of controllers representing VCR and CCR reflexes did not produce improvements in head-neck kinematics, the numerical methods to combine the two controllers are considered novel and contributes to an understanding of how both controllers can be implemented in a single head-neck model. The proposed methods can be further studied, for example, by including an optimized parallel damping element until knowledge of how human reflex systems becomes better established.

The need for additional damping for the APF controller was highlighted by the much higher derivative controller gains (KD) when compared to the MLF-based control. MLF seems to control buckling behavior in the neck, but the controller could not produce acceptable human-like responses. Another study found that the 3D muscle could stiffen the neck model response compared to the 1D muscle (Hedenstierna & Halldin, 2008). These hypotheses led to the method presented in Paper E.

The parallel damping element (PDE) and APF controller were refined to improve the model's head and cervical spine kinematic agreement with volunteer neck muscle responses (Paper E). The damping value of 0.004 kN.ms/mm^2 was initially used to define parallel damping elements for the VIVA OpenHBM and was based on approximation simulation conducted by Östh et al., (2012). To derive the PDE value, Östh et al., (2012) conducted simulation of human arm to match the angular kinematics of Hayes and Hatze's (1977) experimental studies. However, this value may not be suitable for the present model as the study conducted by Östh et al., (2012) was based on simulations of a human arm. The new results in Paper E found that the suitable range was 5 to 10 times higher than previously used. With the new value of the PDE, the oscillations and buckling on the cervical spine rotational displacements were minimized or even removed.

When the muscle forces of the relevant muscle groups, such as SCM and STH muscle groups, were analyzed, the main contributor of total muscle forces produced by these muscle groups came from the active forces. The viscous force generated from the PDE produced significantly lower forces than the muscle forces produced by the CE or active element. This comparison suggested that the value of PDE derived in this study is likely within a realistic range, but no experimental study was available to confirm this assumption.

The tuning of the APF controller by including the new damping values produced a much better performance for the models. It was found that a lower PDE damping coefficient was needed for the male model compared to the female model. The main reason why the male model needed less damping than the female model could be because the male's neck's larger anatomical structures (see Figure 1.1) particularly the muscle and soft tissues, provides more damping properties than the female's leading to less oscillations. With higher passive dampening effects in the neck, the male model needed less explicitly modeled damping in the muscle elements than the female model, as observed in the lower

PDE coefficient. The additional PDE may be attributed to the incomplete representation of the neck muscles as purely linear actuators without any of the 3D interactions with the spine.

Based on the head-neck kinematics and CORA score evaluations, the active models for female and male models produced better head-neck kinematics agreement with the volunteers than the original passive models. Furthermore, the active models have more representative cervical spine rotations as measured by the Sato et al., (2014) 5.8km/h volunteer test without any oscillations or buckling. Furthermore, the active models could replicate the S-shaped cervical spine kinematics, which happened during the retraction phase, as shown in volunteer neck kinematics analysis (Sato et al., 2014). These results are very important if the model from the current study is used for the whiplash injury prediction. Apart from a good prediction of head C.G and T1 C.G horizontal acceleration, the correct prediction of the cervical vertebral sagittal rotations is necessary for analyzing proposed injury mechanism hypotheses based on cervical spine motion, such as a transient pressure at the spinal root ganglion (Yao et al., 2016). Compared to previous results in Paper B, C and D, the models from Paper E produced much better agreement with volunteer kinematics and show the importance of PDE in the model with APF controllers. Hessel et al., (2017) showed an almost instant muscle force build up as the muscle is exposed to sudden rapid involuntary eccentric elongation. This phenomenon was shown to be independent of the muscle EMG activity. The neck muscle would probably experience a similar type of involuntary eccentric elongation in the typical rear-end impact that could lead to WAD.

Throughout this thesis, cervical spine kinematics based on volunteer response have been considered important parameters that should be replicated in the head-neck model of this thesis. No previous research was found that optimized and compared model performance to neck kinematics for studying WAD. Even though the aetiology of WAD is not fully understood, WAD still occurs in the neck. Therefore, the model developed for WAD should be able to replicate the volunteer cervical spine kinematics in addition to global head and T1 kinematics. It was also observed that a model could produce good head kinematics agreement with the volunteer data but sacrificed representative cervical spine rotations. Furthermore, it is more straightforward to achieve head kinematics, but vertebral kinematics are more challenging and more relevant to injury. Also, if the vertebral kinematics are incorrect, this may affect the values measured for some injury criteria.

Suppose the cervical spine kinematics from such a model were used as input to calculate local tissue-based WAD prediction. In that case, the analysis results more likely could not be trusted. Based on Paper E, a model with good agreement with volunteer head and cervical spine kinematics has successfully been developed. Global kinematics-based whiplash injury criteria and local tissue injuries analysis can be assessed with the same model.

It was also observed when co-contraction (CCo) was included in the passive model without PDE, objective rating scores were below the original passive model. In parallel, when all models with PDE were compared, lower average CORA scores were observed when CCo was included. This result implies that the CCo level based on one model (VIVA OpenHBM) was not appropriate for another model (VIVA+). The difference in model behaviour after gravity settling could be the main reason. Thus, it might

be that some models only need co-contraction level during gravity settling to maintain a stable initial position before the pulse is applied.

Benchmarking of the model with neck muscle responses and input data that are valid for whiplash injury prediction in higher delta velocities was conducted in Paper E. Head C.G x-acceleration and cervical spine rotational velocities were the key kinematic parameters. The reason was that the primary input for Neck Injury Criteria (NIC) (Boström et al., 2000) is head and T1 C.G x-acceleration. For the indirect tissue-based injury assessment, such as the analysis of pressure gradients in the spinal canal (Svensson et al., 1998; Yao et al., 2016), the cervical vertebral rotational velocities are input into the calculation. Therefore, it is crucial to have the head C.G x-acceleration and cervical vertebral rotational velocities as close as possible to volunteer kinematics responses. In addition, evaluating models at higher delta velocities is vital because whiplash injury cases have been reported to occur at delta velocities up to 25 km/h (Kullgren et al., 2003).

The model with APF controller and PDE proved to have good head kinematics agreement with volunteer data at higher test severities after optimizing for the head and neck kinematics at one test speed. However, only head kinematics between the volunteer and models were compared at higher severities as cervical spine vertebral rotational velocity data were unavailable in those datasets. This data requires high speed X-Ray recordings which only have been reported in Sato et al., (2014). Although there is no guarantee, the neck rotations calibrated at one test speed should lead to good agreement at higher speeds given that the head kinematics are replicated at the higher test case. Thus, the current model should produce reasonable cervical spine kinematics at higher delta velocities but requires additional test data to confirm this.

The final study of the present thesis consisted of accident reconstruction simulations based on real-world crashes. The aim of the Paper F was to study active and passive neck muscle models in accident reconstruction simulations to observe the influence of neck muscle models. It was also motivated by the fact that no studies involving a FE HBM with active reflexive neck muscles were used to assess WAD based on real-world accidents. Simulating crash pulses from real-world accidents provides a realistic scenario to study the influence of neck muscle responses on occupant kinematics during low-speed rear-end impact.

The positioning procedure proposed by Trummler et al., (2022) was adopted and resulted in head to head restraint distance of 56.3mm. The reason for using the positioning procedure proposed by Trummler et al., (2022) was that no data on how the occupants were seated before the crash was available. Therefore, the main focus was to use a repeatable and reproducible positioning method.

With a head-to-head restraint distance of 56.3 mm, the inclusion of neck muscle responses influenced the cervical vertebral kinematics considerably but only slightly affected head kinematics. More oscillations and greater relative rotations of cervical vertebral were observed in the passive model without neck muscle activity. Verifying which cervical spine rotations correctly represent the human cervical spine kinematics for the present boundary conditions was challenging. Some indications can

be found by comparing the volunteer tests conducted by Ono et al., (1999) and Sato et al., (2014) and PHMS tests by Kang et al., (2015). These indicate that the cervical spine rotations in the model with neck muscle activity are closer to the measured human and PMHS responses. No high-frequency oscillations were observed in any tests that measured cervical spine rotations (Ono et al., 1999, Sato et al., 2014, Kang et al., 2015). The test conducted by Kang et al., (2015) used a commercial car seat, which had similar features to the present study's seat model. These results highlighted the importance of including active neck muscle to study head neck kinematics for whiplash injury assessment. Fairly similar head kinematics for active and passive models were observed despite the fact that cervical spine kinematics are totally different.

Comparing the pressure transient changes in the spinal canal (Aldman pressure) also revealed a significantly different trend between the active and passive models. It was found that the magnitude of the Aldman pressure was significantly reduced (with a smoother pressure response over time) when the neck muscle activity was included in the model. The trend observed in the Aldman pressure was reflected by the cervical spine rotations relative to T1 rotations. Very high and noisy pressure transients in the spinal canal were observed in the model without active neck muscle. It is difficult to confirm which pressure magnitude is more representative for humans as the only available data from in vivo conditions comes from animal tests conducted by Örtengren et al.,1996; and Svensson et al., 1998 and PHMS rear-end impact test based on Eichberger et al., (2000). Based on the profile of the pressure transient changes observed in Svensson et al., (1998) and Eichberger et al., (2000), the pressure transient responses for the model with active neck muscles were more representative of the experimental animal tests. Thus, if the profile of Aldman pressure in humans and animals are similar, the model with active neck muscle responses would be a better tool to analyze the difference in Aldman pressure in occupants with and without WAD.

As previously mentioned, with a head-to-head restraint distance of 56.3 mm, the relative head-torso kinematics was not significantly different between a model with and without neck muscle responses before the rebound phase. These results were reflected in the slight difference in NIC(max) value when the two groups were compared. Therefore, if the WAD criteria based on NIC(max) were used to evaluate WAD (such as proposed by Ono et al., 2009), they were more likely to give a similar outcome with or without neck muscle responses. However, local whiplash injury prediction, such as Aldman pressure based on the cervical spine kinematics, resulted in significant differences between the two groups. This specific analysis revealed the need for both global-based injury criteria and local indirect tissue analysis to understand how WAD occur. Similar results of NIC can be obtained despite the fact that the cervical spine rotations were different. Therefore, evaluating global kinematics-based injury criteria such as NIC(max) and local kinematics-based injury prediction such as Aldman pressure would be more reliable using an active model, such as that presented in the current thesis, than a passive model.

No clear distinctions were observed in head-neck kinematics between the injured and uninjured cases. The kinematic responses of injured cases were within the kinematics response corridors of the uninjured cases. This could be due to the small sample size of injured cases. The simulations all had the same original boundary conditions (statures, age, posture, seatback adjustment) that are not likely

representative of the actual case. Therefore, more simulations of injured cases are needed. The first limitation to conducting more simulations would be the availability of seat models that correspond with the car seat brand found in any accident pulse data. Presently, only three injured females were found in the Folksam database for the Toyota Auris. Furthermore, another limitation would be knowing how the occupant was sitting just before the crash. It is worth noting that the model used in the final study was calibrated and validated against volunteer data without any head restraint. Therefore, the model would be better suited if used to simulate rear impact crash simulation with a larger head-to-head restraint distance until more calibrations are conducted.

Trends observed in the Aldman pressure profile were plotted and compared between the injured and uninjured group. During the neck retraction phase, the injured cases always had more negative pressure on all eight spinal canals than the uninjured ones. This also reflected in the cervical vertebra relative to the T1 rotation. In addition, the lower half of the spinal canal (except Canal 8) had more significant pressure differences than the other upper half. The magnitude of the negative pressures observed in the spinal canal were similar to those found in animal tests (Svensson et al., 1993) which resulted in injuries to the spinal ganglia. These lesions may explain the symptom of WAD. However, it is still unclear which pressure magnitudes cause spinal ganglia injuries in humans. The cervical spine anatomy in pigs and humans are similar to a great extent, but the dimensions and detailed shape of the cervical tissues are different (Svensson et al., 1993). Therefore, it is impossible to know whether the negative pressure magnitudes observed in the injured cases correlates to a risk of sustaining ganglion injuries. The simulations suggested that the Aldman pressure could discriminate the accident cases with and without WAD. More simulation results with a larger sample size are needed to positively confirm if Aldman pressures are correlated with a higher risk of WAD.

In the present thesis, kinematics data of two female volunteers seated in rigid seats (Sato et al., 2014) were used to derive the optimum muscle controller parameters. The reason to focus on the data from Sato et al., (2014) was because it is the most comprehensive published data that included cervical spine kinematics. Since the kinematic responses were only based on two female volunteers, the data might not be representative of the average female population responses. In addition, the volunteers were also seated in a rigid seat, which might not be representative of a real-life scenario in which the occupant is sitting in an automotive seat with a head-restraint. It is important to use data from tests where volunteers are seated in an automotive seat to derive the optimum parameters for the muscle controllers.

A separate MLF controller was implemented to control each muscle element in the present thesis producing 258 MLF controllers. However, only one global gain was assigned to those controllers. This may be a limitation of the MLF controller in the present work. It is likely necessary to group the muscles into several groups with different controller gains. Another potential limitation may be related to muscle routing. The location of muscle origin and insertions were based on anatomical descriptions, but the muscle lines of action were assumed to be straight. This approach may miss relevant complexities in the human muscle response and be responsible for some of the additional damping in the PDE to better represent volunteers.

Nominal posture was selected to represent the occupant's posture in the accident reconstruction simulations. It was selected because no study was found to quantify how usually the occupants were seated just before the crash happened. This can be considered a pragmatic approach as it could miss any relevant factors that should be considered during the analysis of whiplash injury.

Several contributions to the state of the art in neck muscle modelling have been produced in this thesis. These contribute directly and indirectly to the ultimate goal of how to model active reflexive neck muscle responses in a low-speed rear-end impact. The first research contribution of the present thesis is to develop FE HBMs with active neck muscle responses that produce and replicate volunteer head and cervical spine kinematics. The present thesis provided further understanding of how to approximate the reflex input from the human VCR and CCR and which human reflex mechanism is more relevant in rear-end impact simulations. The proposed numerical methods to combine the two controllers are considered novel and contributed to the new methods of implementing both controllers in a single head-neck model. The fourth research contribution shows the isolated head-neck FE model can derive muscle controller parameters and is valid for volunteer data in both a full body body or isolated representation, at least for the response interval deemed applicable for WAD. Analysis of the response kinematics with and without active neck muscle responses shows how occupant kinematics, global injury criteria, and proposed indirect tissue injury mechanisms are affected by the presence of neck muscle forces. The collective understanding and knowledge from the accident reconstruction study conducted in the present thesis is a fifth research contribution. All research contributions highlighted in the present thesis are believed to expand the boundary of current knowledge of how to model active, reflexive neck muscle responses in a low-speed rear-end impact.

Chapter 6 Conclusions and Future Directions

6.1 Conclusions

The FE HBMs with neck muscle responses have been developed and validated to be used for low-speed rear-end impact and WAD analysis. The models have been proven to be robust and able to replicate volunteer head-neck kinematics.

RQ 1: "How well can an isolated head-neck model replicate head-neck kinematics observed in a full-body model?"

The isolated head-neck model could be used to develop an active muscle controller. Furthermore, the isolated head-neck model produces similar head-neck kinematics responses as in the full-body model up to 200ms capturing the time interval relevant for studying WAD. With identical T1 kinematics, the head-neck model produced less stiff responses than the full-body model both for head and neck kinematics.

RQ 2: "Which active muscle controllers, angle-based or muscle-displacement based, can detect the head-neck motion and best simulate volunteer head displacement time histories?"

The angle-based input is the most effective and straightforward input to detect the head motion in a low-speed rear-impact collision. The single angular input is convenient to implement in a controller that could be defined with available experimental data. The results of the active models were comparable to the volunteer responses. The model with the APF controller could replicate the volunteer head displacement time histories better than the MLF.

RQ 3: "How well can different optimization schemes, targeting head and or vertebral volunteer kinematics outputs, identify active muscle controller parameters to reproduce volunteer kinematics?"

Reliable parameter identification such as active muscle controller gains (for example: proportional and derivative gains) can be obtained via optimization. The optimization using the published volunteers head kinematics as the objective showed the best agreement in head kinematics.

RQ 4: "What is the best configuration of an active neck muscle to used for whiplash injury assessment?"

It can be concluded that including and optimizing the parallel damping element (PDE) and the APF controller improved the model's head kinematics agreement with volunteer responses over the passive model. Meanwhile, combining active muscle controller types could not improve the model's kinematics agreement. Therefore, the importance of the parallel damping element (PDE) was identified since it was observed that any model that included PDE improved head and neck kinematics compared to the original passive model. Furthermore, based on the evaluation conducted in Paper E, a model with a parallel damping element and APF controller is most suitable for injury prediction studies. Since that model, based on the configurations that were investigated, most closely matches the experimental data

RQ 5: "What is the influence of neck muscle responses on whiplash injury assessment?"

The inclusion of neck muscle responses considerably influenced the cervical vertebral kinematics but only slightly influenced head kinematics before the rebound phase depending on the head to headrest offset. More oscillations and more significant relative rotations were observed in the passive model without neck muscle activity. When the neck muscle activity was included in the model, the magnitude of the Aldman pressure was significantly reduced with a smoother pressure response over time. Active neck muscle responses slightly reduced the Neck Injury Criteria (NIC) value. The injured cases always had more negative pressure on all eight spinal canals than the uninjured ones when the transient pressure observed in the spinal canal was compared between the injured and injured groups.

6.2 Future Directions

To fulfil the goal of understanding why females have a higher risk of sustaining WAD and how muscle activity influences the injury risk, a future study that involves both female and male models should be conducted. Accident reconstruction simulations based on real-world accident data could be conducted using the female and male active HBMs developed in this thesis. The whiplash injury outcomes using global injury criteria (such as Neck Injury Criteria, NIC) and proposed tissue-based local injury criteria (for example, transient pressure in spinal root ganglion, facet joint capsular ligament strains) can be analyzed. Finally, based on the knowledge gained from the accident reconstruction study, design principles to develop a gender-equivalent whiplash protection seat design can be identified. Ultimately, it will contribute to reducing the incidence of WAD. The models developed herein are not limited to studying WAD using NIC and Aldman pressure. A more biofidelic head and neck response will benefit other WAD injury criteria investigations.

References

Aldman, B. 1986. An analytical approach to the impact biomechanics of head and neck injury. in Proceedings of the 39th American Association for Automotive Medicine Conference; October 6-8, 1986, Montreal, QC, 439–461.

Amezquita-Garcia, J., Bravo-Zanoguera, M., Gonzalez-Navarro, F. F., Lopez-Avitia, R., & Reyna, M. A. 2022. Applying Machine Learning to Finger Movements Using Electromyography and Visualization in Opensim. Sensors (Basel, Switzerland), 22(10), 3737. https://doi.org/10.3390/s22103737

Amonoo-Kuofi, H.S., 1983. The density of muscle spindles in the medial, intermediate and lateral columns of human intrinsic postvertebral muscles. J. Anat. 136 Pt 3 , 509–19.

Armstrong, B., McNair, P., Taylor, D., 2008. Head and Neck Position Sense. Sport. Med. 38 2 , 101–117. doi:10.2165/00007256-200838020-00002

Åström, K.J. and Murray, R.M., 2008. Feedback systems. Princeton University

Björnstig, U., Hildingsson, C., Toolanen, G., 1990. Soft–Tissue injury of the neck in a hospital based material. Scand. J. Public Health 18 4 , 263–267. doi:10.1177/140349489001800405

Blouin, J.S., Inglis, J.T., Siegmund, G.P., 2006. Auditory startle alters the response of human subjects exposed to a single whiplash-like perturbation. Spine (Phila. Pa. 1976). 31 2. 146–154. doi:10.1097/01.brs.0000195157.75056.pdf

Blouin, J.-S., Siegmund, G.P., Carpenter, M.G., Inglis, J.T., 2007. Neural Control of Superficial and Deep Neck Muscles in Humans. J. Neurophysiol. 98 2 , 920–928. doi:10.1152/jn.00183.2007

Borst, J., Forbes, P.A., Happee, R., Veeger, D., 2011. Muscle parameters for musculoskeletal modelling of the human neck. Clin. Biomech. 26 4 , 343–351. doi:10.1016/j.clinbiomech.2010.11.019

Boström, O., Fredriksson, R., Håland, Y., Jakobsson, L., Krafft, M., Lövsund, P., et al., 2000. Comparison of car seats in low speed rear-end impacts using the BioRID dummy and the new neck injury criterion (NIC). Accid. Anal. Prev. 32, 321–328. doi: 10.1016/S0001-4575(99)00105-0.

Brault, J.R., Siegmund, G.P., Wheeler, J.B., 2000. Cervical muscle response during whiplash: evidence of a lengthening muscle contraction. Clin. Biomech. 15 6 , 426–435. doi:10.1016/s0268-0033(99)00097-2

Carlsson, A., 2012. Addressing Female Whiplash Injury Protection - A Step Towards 50th Percentile Female Rear Impact Occupant Models, PhD Thesis - Chalmers University of Technology, Goeteburg (Sweden).

Cassidy, J.D., Linda, J.C., Coté, P., Lemstra, M., Berglund, A., Nygren, Å., 2000. Effect of eliminating compensation for pain and suffering on the outcome of insurance claims for whiplash injury. N. Engl. J. Med. 342 16 , 1179–1186. doi:10.1056/NEJM200004203421606

Correia MA, McLachlin SD, Cronin DS. 2020. Optimization of muscle activation schemes in a finite element neck model simulating volunteer frontal impact scenarios. J Biomech 104:. https://doi.org/10.1016/J.JBIOMECH.2020.109754

Correia MA, McLachlin SD, Cronin DS. 2021.Vestibulocollic and Cervicocollic Muscle Reflexes in a Finite Element Neck Model During Multidirectional Impacts. Ann Biomed Eng 49:1645–1656. https://doi.org/10.1007/s10439-021-02783-2

Cullen, K.E., 2012. The vestibular system: Multimodal integration and encoding of self-motion for motor control. Trends Neurosci. 35 3 , 185–196. doi:10.1016/j.tins.2011.12.001

Cullen, K.E., Jay M. Goldberg, 2014. Vestibular control of the head: possible functions of the vestibulocollic reflex. Exp Brain Res 210 0 , 331–345. doi:10.1007/s00221-011-2611-5.Vestibular

Dehner, C., Schick, S., Kraus, M., Hell, W., Kramer, M., 2013. Muscle Activity Influence on the Kinematics of the Cervical Spine in Rear-End Sled Tests in Female Volunteers. Traffic Inj. Prev. 14 4 , 369–377. doi:10.1080/15389588.2012.714018

Deng, B., Begeman, P. C., Yang, K. H., Tashman, S., and King, A. I. 2000. Kinematics of Human Cadaver Cervical Spine during Low Speed Rear-End Impacts. SAE Tech. Pap. 2000-Novem. doi: 10.4271/2000-01-SC13.

Dong, L., Odeleye, A. O., Jordan-Sciutto, K. L., & Winkelstein, B. A. 2008. Painful facet joint injury induces neuronal stress activation in the DRG: implications for cellular mechanisms of pain. Neuroscience letters, 443(2), 90–94. https://doi.org/10.1016/j.neulet.2008.07.059

Eichberger, A., Steffan, H., Geigl, B., Svensson, M., Boström, O., Leinzinger, P.E. and Darok, M., 1998. Evaluation of the applicability of the neck injury criterion (NIC) in rear end impacts on the basis of human subject tests. In Proceedings of the International Research Council on the Biomechanics of Injury conference (Vol. 26, pp. 321-333). International Research Council on Biomechanics of Injury.

Engelbrektsson, K., 2011. Evaluation of material models in LS-DYNA for impact simulation of white adipose tissue. Master Thesis. Chalmers University of Technology, Gothenburg, Sweden.

Eppinger, R., Kuppa, S., Saul, R. and Sun, E., 2000. Supplement: development of improved injury criteria for the assessment of advanced automotive restraint systems: II.

EuroNCAP (2021). The dynamic assessment of car seats for neck injury protection: Testing protocol. Version 4.1.1. https://cdn.euroncap.com/media/67263/euro-ncap-whiplash-test-protocol-v411.pdf

Forbes, P.A., Siegmund, G.P., Happee, R., Schouten, A.C. and Blouin, J.S., 2014. Vestibulocollic reflexes in the absence of head postural control. Journal of neurophysiology, 112(7), pp.1692-1702.

Gehre, C., Gades, H., Wernicke, P., 2009. Objective Rating of Signals Using Test and Simulation Responses. Int. Tech. Conf. Enhanc. Saf. Veh. doi:09-0407

Jakobsson, L. Putra, I.P.A., Levallois, I., Keller, A., Johansen, T., Salters, E., Genzel, J., Leledakis, A., Svensson, M.Y., Recko, P., Muser, M., Högberg, L., Wenäll, J., El-Mobader, S., Iraeus, J., Kovalik, M., Tummler, L., Linder, A., Wågström, L., John, J. (2022) Virtual Testing, Occupant Protection in Future Vehicles, Deliverable D3.2 of the H2020 project VIRTUAL.

Hill, A.V., 1938. The heat of shortening and the dynamic constants of muscle. Proceedings of the Royal Society of London. Series B-Biological Sciences, 126(843), pp.136-195.

Ivancic, P.C., Pearson, A.M., Panjabi, M.M. and Ito, S., 2004. Injury of the anterior longitudinal ligament during whiplash simulation. European spine journal, 13(1), pp.61-68.

Berecki-Gisolf, J., Collie, A., McClure, R., 2013. Work disability after road traffic injury in a mixed population with and without hospitalisation. Accid. Anal. Prev. 51, 129–134. doi:10.1016/j.aap.2012.11.010

Grauer, J.N., Panjabi, M.M., Cholewicki, J., Nibu, K., Dvorak, J., 1997. Whiplash Produces an S-Shaped Curvature of the Neck With Hyperextension at Lower Levels. Spine (Phila. Pa. 1976). 22 21 .

Gray, H., Standring, S., 2008. Gray's anatomy: the anatomical basis of clinical practice. Churchill Livingstone.

Günther, M., Schmitt, S., and Wank, V. 2007. High-frequency oscillations as a consequence of neglected serial damping in Hill-type muscle models. Biol. Cybern. 97, 63–79. doi: 10.1007/s00422-007-0160-6.

Happee R, de Bruijn E, Forbes PA, van der Helm F. 2017. Dynamic head-neck stabilization and modulation with perturbation bandwidth investigated using a multisegment neuromuscular model. JBiomech. 58:203–211.

Hayes KC, Hatze H 1977 Passive visco-elastic properties of the structures spanning the human elbow joint. Eur J Appl Physiol Occup Physiol 37:265–274. https://doi.org/10.1007/BF00430956

Hedenstierna, S., and Halldin, P. 2008. How does a three-dimensional continuum muscle model affect the kinematics and muscle strains of a finite element neck model compared to a discrete muscle model in rear-end, frontal, and lateral impacts. Spine (Phila. Pa. 1976). 33, E236-45. doi: 10.1097/BRS.0b013e31816b8812.

Heitplatz, F., Sferco, R., Fay, P., Reim, J., Kim, A. and Prasad, P., 2003, May. An evaluation of existing and proposed injury criteria with various dummies to determine their ability to predict the levels of soft tissue neck injury seen in real world accidents. In Proc. 18th ESV Conf.

Hessel, A. L., Lindstedt, S. L., and Nishikawa, K. C. 2017. Physiological Mechanisms of Eccentric Contraction and Its Applications: A Role for the Giant Titin Protein. Front. Physiol. 8. doi: 10.3389/fphys.2017.00070.

Iwamoto, M., Nakahira, Y., 2015. Development and Validation of the Total HUman Model for Safety (THUMS) Version 5 Containing Multiple 1D Muscles for Estimating Occupant Motions with Muscle Activation During Side Impacts. Stapp Car Crash J. 59 November , 53–90.

John, J., Klug, C., Kranjec, M., Svenning, E. and Iraeus, J., 2022. Hello, world! VIVA+: A human body model lineup to evaluate sex-differences in crash protection. Frontiers in bioengineering and biotechnology, 10.

John, J., Putra, I.P.A, Iraeus,J., 2022b. Finite Element Human Body Models to Study Sex-Differences in Whiplash: Validation Of VIVA+ Passive Responses in Rear-Impact. IRCOBI Conference 2022. In press

Jörg, J. and Menger, H., 1998. Das Halswirbelsäulen-und Halsmarktrauma. Deutsches Arzteblatt-Koln-, 95, pp.1048-1054.

Kang, Y.S., Moorhouse, K., Icke, K., Stricklin, J., Herriott, R. and Bolte IV, J., 2015. Rear impact head and cervical spine kinematics of BioRID II and PMHS in production seats. In IRCOBI Conference Proceedings (No. IRC-15-38).

Kaneoka, K., Ono, K., Inami, S. and Hayashi, K., 1999. Motion analysis of cervical vertebrae during whiplash loading. Spine, 24(8), pp.763-769.

Keshner EA 2003 Head-Trunk Coordination During Linear Anterior-Posterior Translations. J Neurophysiol 89:1891–1901. https://doi.org/10.1152/jn.00836.2001

Kleinbach C, Martynenko O, Promies J, et al 2017 Implementation and validation of the extended Hill-type muscle model with robust routing capabilities in LS-DYNA for active human body models. Biomed Eng Online 16:1–28. https://doi.org/10.1186/s12938-017-0399-7

Kleinbach, C.G., 2019. Simulation of Occupant Kinematics Using Active Human Body Models, Schriften aus dem Institut für Technische und Numerische Mechanik der Universität Stuttgart. Shaker.

Insurance Development Institute of Korea. Facts and analyses of auto insurance. Seoul, Korea: Insurance Development Institute of Korea; 2002.

Kullgren, A., Krafft, M., Tingvall, C., and Lie, A. 2003. Combining crash recorder and paired comparison technique: Injury risk functions in frontal and rear impacts with special reference to neck injuries. Proc. 18th Int. Tech. Conf. Enhanc. Saf. Veh. (ESV), DOT HS 809 543, May 2003, 1–8.

Krafft, M., Kullgren, A., Ydenius, A., Tingvall, C., 2002. Influence of crash pulse characteristics on whiplash associated disorders in rear impacts-crash recording in real life crashes. Traffic Inj. Prev. 3 2 , 141–149. doi:10.1080/15389580212001

Kullgren, A., Stigson, H., Krafft, M., 2013. Development of Whiplash Associated Disorders for Male and Female Car Occupants in Cars Launched Since the 80s in Different Impact Directions. Traffic Inj. Prev. 46 0 , 51–62.

Larsson E, Iraeus J, Fice J, et al 2019. Active human body model predictions compared to volunteer response in experiments with braking, lane change, and combined manoeuvres. Conf Proc Int Res Counc Biomech Inj IRCOBI 349–369

Lee S, Ott K a, Guenther.,2006. Response of Neck Muscles to Rear Impact in the Presence of Bracing and Engineering Conference. 776–790. https://doi.org/10.4271/2006-01-2369

Lee, K.E., Thinnes, J.H., Gokhin, D.S. and Winkelstein, B.A., 2004. A novel rodent neck pain model of facet-mediated behavioral hypersensitivity: implications for persistent pain and whiplash injury. Journal of neuroscience methods, 137(2), pp.151-159.

Linder, A., Svensson, M. Y., Davidsson, J., Flogård, A., Lövsund, P., Håland, Y., et al., 2002. Design and validation of the neck for a rear impact dummy (BioRID I). Traffic Inj. Prev. 3, 167–174.

Linder, A., 2001. Neck injuries in rear impacts : dummy neck development, dummy evaluation and test condition specifications.

Liu J-X, Thornell L-E, Pedrosa-Domellöf F 2003. Muscle Spindles in the Deep Muscles of the Human Neck: A Morphological and Immunocytochemical Study

LSTC. LS-PrePost Online Documentation. 2012. http://www.lstc.com/lspp/.

LSTC 2016. LS-DYNA manual volume I keyword. Available at: http:// www.lstc.com.

LST 2021. LS-DYNA manual volume 2 keyword. Available at: http:// www.dynasupport.com

Lu, Y., Chen, C., Kallakuri, S., Patwardhan, A. and Cavanaugh, J.M., 2005. Neurophysiological and biomechanical characterization of goat cervical facet joint capsules. Journal of Orthopaedic Research, 23(4), pp.779-787.

Luan, F., Yang, K.H., Deng, B., Begeman, P.C., Tashman, S. and King, A.I., 2000. Qualitative analysis of neck kinematics during low-speed rear-end impact. Clinical Biomechanics, 15(9), pp.649-657.

Mang DWH, Siegmund GP, Brown HJ, et al (2015) Loud preimpact tones reduce the cervical multifidus muscle response during rear-end collisions: A potential method for reducing whiplash injuries. Spine J 15:153–161. https://doi.org/10.1016/j.spinee.2014.08.002

Manschot, J. F., and Brakkee, A. J. 1986. The measurement and modelling of the mechanical properties of human skin in vivo--II. The model. J Biomech 19, 517–521. doi:10.1016/0021-9290(86)90125-9.

Martin, J.L., Pérez, K., Marí-Dell'Olmo, M., Chiron, M., 2008. Whiplash risk estimation based on linked hospital-police road crash data from France and Spain. Inj. Prev. 14 3 , 185–190. doi:10.1136/ip.2007.016600

McClune, T., Burton, A.K., Waddell, G., 2002. Whiplash associated disorders: A review of the literature to guide patient information and advice. Emerg. Med. J. 19 6 , 499–506. doi:10.1136/emj.19.6.499

Mörl F, Siebert T, Häufle D. 2016. Contraction dynamics and function of the muscle-tendon complex depend on the muscle fibre-tendon length ratio: a simulation study. Biomech Model Mechanobiol. 2016;15(1):245–58. doi:10.1007/s10237-015-0688-7.

Naseri, H. 2022. Calibration of Adipose tissue material properties in LS-DYNA. Chalmers University of Technology.

Nightingale, R.W., Winkelstein, B.A., Knaub, K.E., Richardson, W.J., Luck, J.F., Myers, B.S., 2002. Comparative strengths and structural properties of the upper and lower cervical spine in flexion and extension, Journal of Biomechanics.

Nowakowski, K., Carvalho, P., Six, J.B., Maillet, Y., Nguyen, A.T., Seghiri, I., M'pemba, L., Marcille, T., Ngo, S.T. and Dao, T.T., 2021. Human locomotion with reinforcement learning using bioinspired reward reshaping strategies. Medical & biological engineering & computing, 59(1), pp.243-256.

Oka, H., Matsudaira, K., Fujii, T., Tanaka, S., Kitagawa, T., 2017. Epidemiology and psychological factors of whiplash associated disorders in Japanese population. J. Phys. Ther. Sci. 29 9 , 1510–1513. doi:10.1589/jpts.29.1510

Ólafsdóttir, J.M., Brolin, K., Blouin, J.S., Siegmund, G.P., 2015. Dynamic spatial tuning of cervical muscle reflexes to multidirectional seated perturbations. Spine (Phila. Pa. 1976). 40 4 , E211–E219. doi:10.1097/BRS.0000000000000721

Ólafsdóttir, J.M., Chalmers tekniska högskola. Department of Mechanics and Maritime Sciences., Chalmers tekniska högskola, 2017. Muscle responses in dynamic events : volunteer experiments and numerical modelling for the advancement of human body models for vehicle safety assessment. Chalmers University of Technology.

Ólafsdóttir, J.M., Östh, J., Brolin, K., 2019. Modelling Reflex Recruitment of Neck Muscles in a Finite Element Human Body Model for Simulating Omnidirectional Head Kinematics Jóna M. Ólafsdóttir, Jonas Östh, Karin Brolin. Ircobi 308–323.

Ono, K., Ejima, S., Suzuki, Y., Kaneoka, K., Fukushima, M., and Ujihashi, S. 2006. Prediction of Neck Injury Risk Based on the Analysis of Localized Cervical Vertebral Motion of Human Volunteers During Low-Speed Rear Impacts. IRCOBI Conf. Proc., 103–113.

Ono, K., Ejima, S., Yamazaki, K., Sato, F., Pramudita, J. A., Kaneoka, K., et al., 2009. Evaluation criteria for the reduction of minor neck injuries during rear-end impacts based on human volunteer experiments and accident reconstruction using human FE model simulations. Int. Res. Counc. Biomech. Inj. - 2009 Int. IRCOBI Conf. Biomech. Inj. Proc., 381–398.

Ono, K., Kaneoka, K., Wittek, A., and Kajzer, J. 1997. Cervical Injury Mechanism Based on the Analysis of Human Cervical Vertebral Motion and Head-Neck-Torso Kinematics During Low Speed Rear Impacts. in doi: 10.4271/973340.

Östh, J., Brolin, K., Ólafsdóttir, J.M., Davidsson, J., Pipkorn, B., Jakobsson, L., Törnvall, F. and Lindkvist, M., 2015, June. Muscle activation strategies in human body models for the development of integrated safety. In Proceedings of the 24th International Techical Conference on the Enhanced Safety of Vehicles (ESV), Gothenburg, Sweden (pp. 8-11)

Östh J, Mendoza-Vazquez M, Linder A, Svensson MY, B.K., 2017. The VIVA OpenHBM Finite Element 50th Percentile Female Occupant Model: Whole Body Model Development and Kinematic Validation, in: Proc.IRCOBI Conf. 2017. Antwerp, pp. 443–466.

Östh, J., Brolin, K., Bråse, D., 2014a. A Human Body Model With Active Muscles for Simulation of Pretensioned Restraints in Autonomous Braking Interventions. Traffic Inj. Prev. 16 3 , 304–313. doi:10.1080/15389588.2014.931949

Östh, J., Brolin, K., Happee, R., 2012. Active muscle response using feedback control of a finite element human arm model. Comput. Methods Biomech. Biomed. Engin. 15 4 , 347–361. doi:10.1080/10255842.2010.535523

Östh, J., Brolin, K., Ólafsdóttir, J.M., Davidsson, J., Pipkorn, B., Jakobsson, L., Törnvall, F., Lindkvist, M., 2015. Muscle activation strategies in human body models for the development of integrated safety, in: Proceedings of the 24th International Techical Conference on the Enhanced Safety of Vehicles (ESV), Gothenburg, Sweden. pp. 8–11.

Östh, J., Brolin, K., Svensson, M.Y., Linder, A., 2016. A Female Ligamentous Cervical Spine Finite Element Model Validated for Physiological Loads. J. Biomech. Eng. 138 6 , 061005. doi:10.1115/1.4032966

Östh, J., Eliasson, E., Happee, R., Brolin, K., 2014b. A method to model anticipatory postural control in driver braking events. Gait Posture 40 4 , 664–669. doi:10.1016/j.gaitpost.2014.07.021

Östh, J., Mendoza-Vazquez, M., Sato, F., Svensson, M.Y., Linder, A., Brolin, K., 2017. A female head–neck model for rear impact simulations. J. Biomech. 51, 49–56. doi:10.1016/j.jbiomech.2016.11.066

Örtengren, T., Hansson, H.A., Lövsund, P., Svensson, M.Y., Suneson, A. and Säljö, A., 1996. Membrane leakage in spinal ganglion nerve cells induced by experimental whiplash extension motion: a study in pigs. Journal of neurotrauma, 13(3), pp.171-180.

Park, J., Ebert, S. M., Reed, M. P., and Hallman, J. J. 2016. Statistical Models for Predicting Automobile Driving Postures for Men and Women Including Effects of Age. Hum. Factors 58, 261–278. doi: 10.1177/0018720815610249.

Panjabi, M.M., Chen, N.C., Shin, E.K., Wang, J.L., 2001. The cortical shell architecture of human cervical vertebral bodies. Spine (Phila. Pa. 1976). 26 22 , 2478–2484. doi:10.1097/00007632-200111150-00016

Panjabi, M.M., Ito, S., Pearson, A.M. and Ivancic, P.C., 2004. Injury mechanisms of the cervical intervertebral disc during simulated whiplash. Spine, 29(11), pp.1217-1225

Partheni, M., Constantoyannis, C., Ferrari, R., Nikiforidis, G., Voulgaris, S., Papadakis, N., 2000. A prospective cohort study of the outcome of acute whiplash injury in Greece. Clin. Exp. Rheumatol. 18 1 , 67–70.

Pearson, A.M., Ivancic, P.C., Ito, S. and Panjabi, M.M., 2004. Facet joint kinematics and injury mechanisms during simulated whiplash. Spine, 29(4), pp.390-397

Peterson, B.W., Goldberg, J.E.F.I.M., Bilotto, G.E.R.A.R.D. and Fuller, J.H., 1985. Cervicocollic reflex: its dynamic properties and interaction with vestibular reflexes. Journal of Neurophysiology, 54(1), pp.90-109.

Quinlan, K.P., Annest, J.L., Myers, B., Ryan, G. and Hill, H., 2004. Neck strains and sprains among motor vehicle occupants—United States, 2000. Accident Analysis & Prevention, 36(1), pp.21-27.

Quinn, K.P., Lee, K.E., Ahaghotu, C.C. and Winkelstein, B.A., 2007. Structural changes in the cervical facet capsular ligament: potential contributions to pain following subfailure loading. Departmental Papers (BE), p.105.

Reed, M.P. and Ebert, S.M., 2013. The seated soldier study: posture and body shape in vehicle seats. University of Michigan, Ann Arbor, Transportation Research Institute.

Sato, F., Nakajima, T., Ono, K., Svensson, M., 2014. Dynamic Cervical Vertebral Motion of Female and Male Volunteers and Analysis of its Interaction with Head/Neck/Torso Behavior during Low-Speed Rear. Ircobi.Org 227–249.

Sato, F., Odani, M., Miyazaki, Y., Nakajima, T., Antona-Makoshi, J., Yamazaki, K., Ono, K., Svensson, M., Östh, J., Morikawa, S., Schick, S., Ferrero Perez, A., 2016. Investigation of Whole Spine Alignment Patterns in Automotive Seated Posture Using Upright Open MRI Systems.

Schmitt, K.U., Muser, M.H., Walz, F.H. and Niederer, P.F., 2002. N km--a proposal for a neck protection criterion for low-speed rear-end impacts. Traffic injury prevention, 3(2), pp.117-126.

Siebert T, Rode C, Herzog W, Till O, Blickhan R. 2008. Nonlinearities make a difference: comparison of two common Hill- type models with real muscle. Biol Cybern. 2008;98(2):133–43. doi:10.1007/s00422-007-0197-6.

Siegmund, G.P., Sanderson, D.J., Myers, B.S., Timothy Inglis, J., 2003. Rapid neck muscle adaptation alters the head kinematics of aware and unaware subjects undergoing multiple whiplash-like perturbations. J. Biomech. 36 4 , 473–482. doi:10.1016/s0021-9290(02)00458-x

Siegmund, G.P., 2011. What occupant kinematics and neuromuscular responses tell us about whiplash injury. Spine (Phila. Pa. 1976). 36 25 , S175–S179. doi:10.1097/BRS.0b013e3182387d71

Siegmund, G.P., Winkelstein, B.A., Ivancic, P.C., Svensson, M.Y., Vasavada, A., 2009. The Anatomy and biomechanics of acute and chronic whiplash injury. Traffic Inj. Prev. 10 2 , 101–112. doi:10.1080/15389580802593269

Stander, N., Roux, W., Basudhar, A., Eggleston, T., Goel, T., Craig, K., 2015. LS-OPT ® User's Manual - A Design Optimization and Probabilistic Analysis Tool.

Standring S. 2008. Gray's Anatomy: The Anatomical Basis of Clinical Practice. 40th Ed. Philadelphia, PA: Elsevier Saunders.

Sterling, M., 2011. Does knowledge of predictors of recovery and nonrecovery assist outcomes after whiplash injury? Spine (Phila. Pa. 1976). 36 25 , S257–S262. doi:10.1097/BRS.0b013e31823881bc

Sterner, Y., Gerdle, B., 2004. Acute and chronic whiplash disorders - A review. J. Rehabil. Med. 36 5 , 193–210. doi:10.1080/16501970410030742

Stigson, H., Gustafsson, M., Sunnevång, C., Krafft, M., Kullgren, A., 2015. Differences in Long-Term Medical Consequences Depending on Impact Direction Involving Passenger Cars. Traffic Inj. Prev. 16 June , 133–139. doi:10.1080/15389588.2015.1014999

Styrke, J., Stålnacke, B.M., Bylund, P.O., Sojka, P., Björnstig, U., 2012. A 10-year incidence of acute whiplash injuries after road traffic crashes in a defined population in Northern Sweden. PM R 4 10 , 739–747. doi:10.1016/j.pmrj.2012.05.010

Svensson, M. Y., Aldman, B., Boström, O., Davidsson, J., Hansson, H. A., Lövsund, P., et al., 1998. [Nerve cell damages in whiplash injuries. Animal experimental studies]. Orthopade 27, 820–826.

Svensson, M. Y., Aldman, B., Hansson, H. a, Lövsund, P., Seeman, T., Suneson, a, et al., 1993. Pressure Effects in the Spinal Canal during Whiplash Extension Motion: A Possible Cause of Injury to the Cervical Spinal Ganglia. Int. IRCOBI Conf. Biomech. Impacts, 189–200.

Trummler, L., Keller A., Muser M. 2022, Test case of WP3 (rear-impact scenario) implemented, Milestone 1.4 of the H2020 project VIRTUAL.

Viano, D.C. and Davidsson, J., 2002. Neck displacements of volunteers, BioRID P3 and Hybrid III in rear impacts: implications to whiplash assessment by a neck displacement criterion (NDC). Traffic injury prevention, 3(2), pp.105-116.

Wittek, A., Kajzer, J., and Haug, E. (2000). Hill-type muscle model for analysis of mechanical effect of muscle tension on the human body response in a car collision using an explicit finite element

Yadla, S., Ratliff, J.K., Harrop, J.S., 2008. Whiplash: Diagnosis, treatment, and associated injuries. Curr. Rev. Musculoskelet. Med. 1 1 , 65–68. doi:10.1007/s12178-007-9008-x

Yang, K.H., Begeman, P.C., Muser, M., Niederer, P. and Walz, F., 1997. On the role of cervical facet joints in rear end impact neck injury mechanisms (No. 970497). SAE Technical Paper.

Yang, K.H. and King, A.L., 2003. Neck kinematics in rear-end impacts. Pain research and management, 8(2), pp.79-85.

Yao, H. D., Svensson, M. Y., and Nilsson, H. 2016. Transient pressure changes in the vertebral canal during whiplash motion – A hydrodynamic modeling approach. J. Biomech. 49, 416–422. doi: 10.1016/J.JBIOMECH.2016.01.005.

Yoganandan, N., FA, P., Kumaresan, S., Elhagediab, A., 1998. Biomechanical assessment of human cervical spine ligaments. SAE Int. 983159 724 , 1–10

Yoganandan, N., Pintar, F. A., Stemper, B. D., Schlick, M. B., Philippens, M., and Wismans, J. 2000. Biomechanics of human occupants in simulated rear crashes: documentation of neck injuries and comparison of injury criteria. Stapp Car Crash J 44, 189–204. doi: 2000-01-SC14 [pii].

Yoganandan, N., Kumaresan, S., and Pintar, F. A. 2001. Biomechanics of the cervical spine. Part 2. Cervical spine soft tissue responses and biomechanical modeling. Clin. Biomech. 16, 1–27. doi: 10.1016/S0268-0033(00)00074-7.

Yoganandan, N., Pintar, F. A., and Cusick, J. F. 2002. Biomechanical analyses of whiplash injuries using an experimental model. Accid. Anal. Prev. 34, 663–671. doi: 10.1016/S0001-4575(01)00066-